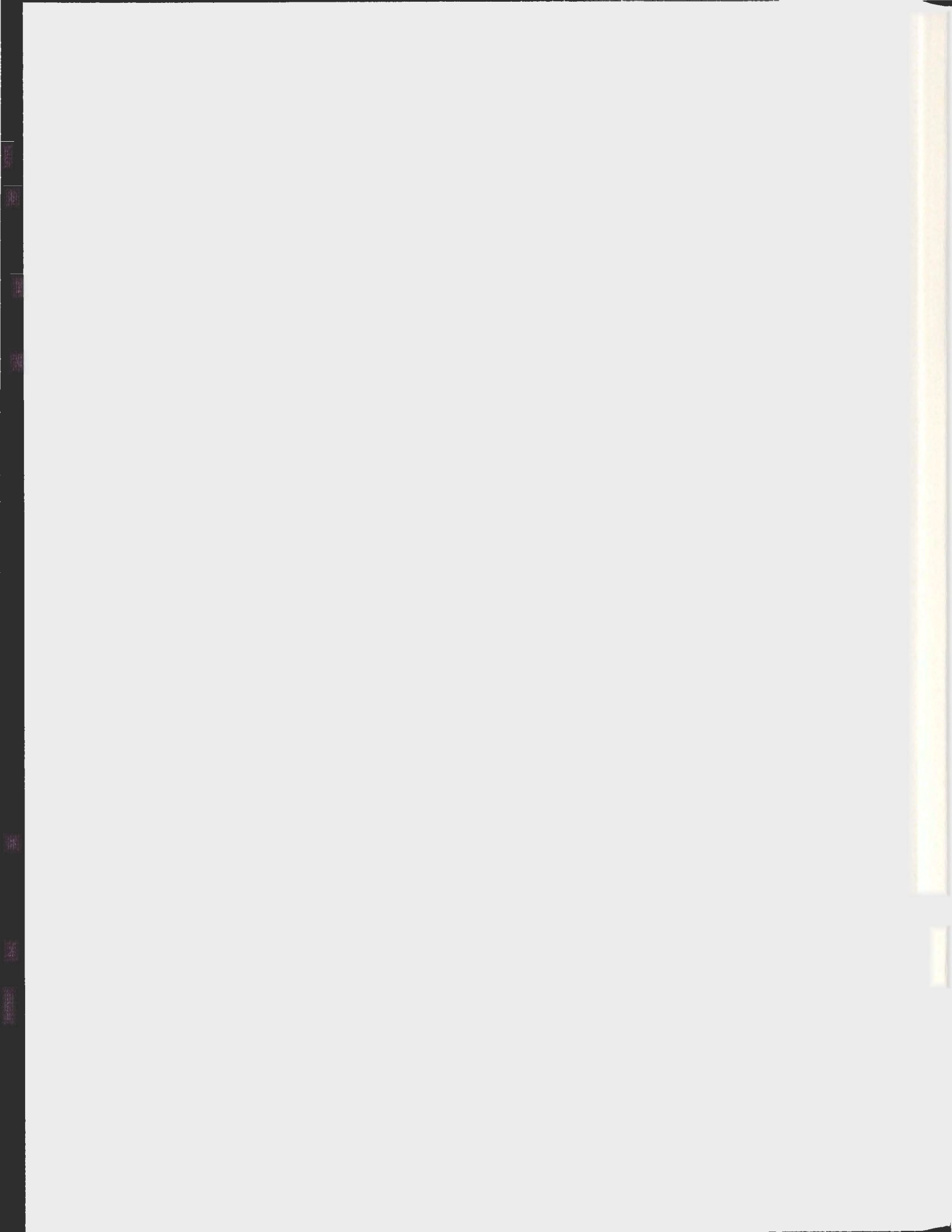


ASSOCIATIONS OF T_H17 CELLS WITH HLA-DR
ALLOTYPES AND OUTCOMES IN BREAST CARCINOMA

LISA LESHANE



**Associations of T_H17 Cells with HLA-DR Allotypes and Outcomes in Breast
Carcinoma**

By

©Lisa LeShane

A thesis submitted to the

School of Graduate Studies

In partial fulfillment of the requirements for the degree of

Master in Science

Faculty of Medicine

Memorial University of Newfoundland and Labrador

February 2013

ABSTRACT

A previous study in the Drover laboratory found that IL-6 and HLA-DR52 were associated with increased breast tumor size and decreased recurrence free survival (RFS). Since IL-6, along with TGF- β , is required for the differentiation of naïve T cells into T_H17 cells, we hypothesized that the number of T_H17 cells would be increased in HLA-DR52⁺ tumors and statistically associate with both larger tumors and decreased RFS.

Following polymerase chain reaction (PCR) analysis of retinoic acid receptor-related orphan receptor C2 (RORc2) and IL-17 transcripts, we developed a T_H17 cell profile. Statistical analysis did not reveal associations between T_H17^{hi}, IL-6^{hi} or HLA-DR52⁺ tumors. Both IL-17^{hi} and T_H17^{hi} correlated with younger age of diagnosis. Further analysis revealed that T_H17^{hi}/HLA-DR52⁺ tumors had the youngest age of diagnosis. There were no significant associations with decreased RFS or overall survival (OS). Yet, both IL-17^{hi} and T_H17^{hi} trended with decreased OS. Future studies should expand on the sample size and determine if these associations and trends remain in a larger sample.

ACKNOWLEDGEMENTS

There are many individuals to whom I am deeply indebted for their varying contributions to this project. I am grateful to my supervisor Dr. Sheila Drover for her generosity, support, guidance, instruction and patience with this project. I would like to acknowledge Diane Codner for her expertise, kindness and patience as well. Further, Dr. Sharon Oldford completed numerous experiments and her conclusions gave way to my master's project.

My supervisory committee, Dr. Thomas Michalak and Dr. Mani Larijani, were incredibly supportive and offered helpful suggestions in developing aspects of the projects.

I would like to thank Ali Atoom, Patricia Cousins and Dr. Rodney Russell for sharing their PCR expertise.

Special thanks are also directed towards Ahmed Mostafa, Christopher Corkum, Tracey Dyer and Christa Dwyer. As lab mates, they shared great moments of triumph and offered encouragement on moments of despair.

Thanks to my fellow master's students for helping me through challenging classes and presentations. A special acknowledgement to the tripod unit and our cooperatively learning styles.

I would like to acknowledge Canadian Institute of Health Research and Memorial University of Newfoundland and Labrador's Graduate Studies for financial support.

Finally, my sincere appreciation, gratitude and respect for my family and friends, who have supported me through my degrees.

TABLE OF CONTENTS

Abstract	ii
Acknowledgements	iii
Table of Contents	iv
List of Figures	ix
List of Tables	xi
List of Abbreviations	xiii
CHAPTER 1. INTRODUCTION	1
1.1. Preface	1
1.2. Breast Carcinoma	2
<i>1.2.1. Epidemiology of Breast Carcinoma</i>	<i>4</i>
<i>1.2.2. Classification and Treatment of Breast Carcinoma</i>	<i>7</i>
1.3. Immune Responses and Profiling	9
<i>1.3.1. Major Histocompatibility Complex Class II</i>	<i>10</i>
<i>1.3.2. HLA Expression and Association with Disease</i>	<i>14</i>
<i>1.3.3. Effector and Regulatory CD4⁺ T cell Subsets in Humans</i>	<i>16</i>
<i>1.3.4. Differentiation of Naïve T Cells into T_H17 Cells</i>	<i>18</i>
1.3.4.1. Interaction of T _H 17 Cells with Other CD4 ⁺ T Cell Subsets	<i>20</i>
<i>1.3.5. T_H17 Cytokine Profile and the Biological Function of T_H17 cells</i>	<i>21</i>
1.4. Immune Response and Cancer	23
<i>1.4.1. Antitumor Immune Responses</i>	<i>23</i>

1.4.2. <i>Protumor Immune Responses</i>	24
1.5. Studies of T_H17 Cells within Tumor Microenvironments	27
1.5.1. <i>T_H17 Cells in Cancers Associated with Chronic Inflammation</i>	29
1.5.1.1. T _H 17 Cells in Gastric Cancer	29
1.5.1.2. T _H 17 Cells in Hepatocellular Cancer	31
1.5.1.3. T _H 17 Cells in Colorectal Cancer	32
1.5.1.4. T _H 17 Cells in Uterine Cervical Carcinoma	33
1.5.1.5. T _H 17 Cells in Lung Cancer	34
1.5.1.6. Summary of T _H 17 Cells in Cancers with Associated Chronic Inflammation	35
1.5.2. <i>T_H17 Cells in Cancers Influenced by Hormones</i>	36
1.5.2.1. T _H 17 Cells in Ovarian Cancer	36
1.5.2.2. T _H 17 cells in Prostate Cancer Patients	38
1.5.2.3. T _H 17 cells in Breast Carcinoma Patients	38
1.5.2.4 Summary of T _H 17 Cells in Cancers Influenced by Hormones	40
1.6. Hypothesis and Objectives	40
 CHAPTER 2. METHODS AND MATERIALS	 43
2.1. Breast Tumor Samples	43
2.2. Cell Lines	44
2.3. RNA Extraction and Determination of RNA Integrity	44
2.4. Standard Reverse Transcriptase Polymerase Chain Reaction	48

2.5. Real Time Polymerase Chain Reaction	51
2.6. Immunohistochemistry	53
<i>2.6.1. Preparation of IHC slides</i>	54
<i>2.6.2. Antigen Retrieval</i>	54
<i>2.6.3. Antibody Staining</i>	55
<i>2.6.4. Dehydration and Mounting</i>	56
<i>2.6.5. Breast tumor sample IHC</i>	56
2.7. Statistical Analysis	57
 CHAPTER 3: RESULTS	 58
3.1. Optimization of RT-PCR Conditions	58
<i>3.1.1. Optimal RT-PCR Annealing Temperatures</i>	58
<i>3.1.2. Optimal RT-PCR Amplification Cycle Number</i>	59
3.1.2.1. Determination of Optimal RT-PCR Amplification Cycle for IL-17	59
3.1.2.2. Determination of Optimal RT-PCR Amplification Cycle for IL-6	62
3.1.2.3. Determination of Optimal RT-PCR Amplification Cycle for TGF- β	62
3.1.2.4. Determination of Optimal RT-PCR Amplification Cycle for FOXP3	67
3.1.2.5. Summary of RT-PCR Cycle Number Optimization	67
3.2. RT-PCR Analysis on Breast Cancer Cell Lines	71
3.3. RNA Integrity Values for Breast Tumor RNA	76

3.4. Analysis of Cytokine Transcripts in Breast Cancer Tissues by Conventional RT-PCR	77
3.5. Optimization of Real-time PCR Conditions	81
3.6. Real-time PCR Analysis of Breast Cancer Cell Lines	89
3.7. Analysis of IL-17 and RORc2 transcripts in Breast Cancer cDNA by Real-Time PCR	89
<i>3.7.1. Derivation of a T_H17 Profile for the Breast Tumor Samples</i>	<i>94</i>
<i>3.7.2. Associations between T_H17 and Tumor Infiltrating Immune Leukocytes</i>	<i>95</i>
<i>3.7.3. Associations between T_H17 Profiles and HLA-DR Allotypes</i>	<i>97</i>
<i>3.7.4. Associations between T_H17 Profiles and Prognostic Indicators</i>	<i>99</i>
<i>3.7.5. Analysis of HLA-DR52 stratified by IL-17 and T_H17 Profiles on Age at Diagnosis</i>	<i>103</i>
<i>3.7.6. Associations between T_H17 Profiles and Overall Survival</i>	<i>106</i>
3.8. Immunohistochemistry Results	113
<i>3.8.1. Positive and Negative Controls</i>	<i>113</i>
<i>3.8.2. IL-17 Immunohistochemistry Results</i>	<i>115</i>
<i>3.8.3. RORc Immunohistochemistry Results</i>	<i>115</i>
CHAPTER 4. DISCUSSION	117

4.1. Summary of Research	117
4.2. Breast Cancer Cell Line Preliminary Research	118
4.3. PCR Analysis of Breast Tumor Samples	120
4.4. The Relationships between IL-6 and the T_H17 Profile within the Breast Tumor Samples	122
4.5. T_H17 Profile and Associations with HLA-DR	123
4.6. T_H17 Profile Associations with Prognostic Indicators	124
4.7. T_H17 Profile Associations with Survival	126
4.8 Concluding Remarks and Future Studies	127
CHAPTER 5. REFERENCES	129
APPENDICES	142

LIST OF FIGURES

Figure 1.1. Normal structure of a breast	3
Figure 1.2. MHC class II:Antigenic peptide interaction	12
Figure 1.3. HLA-DR alleles	13
Figure 1.4. Differentiation of naïve CD4 ⁺ T cell into different effector subsets	17
Figure 1.5. Antitumor effects of T _H 17 cell	26
Figure 1.6. Protumor effects of T _H 17 cells	28
Figure 3.1. Determination of the optimal annealing temperature for IL-17	60
Figure 3.2A-B. Determination of the optimal PCR amplification cycle for IL-17 transcripts	61
Figure 3.3A-B. IL-17 amplification of log-fold diluted cDNA.	63
Figure 3.4A-B. Determination of the optimal PCR amplification cycle for IL-6 transcripts	64
Figure 3.5A-B. IL-6 amplification of log-fold diluted cDNA	65
Figure 3.6A-B Determination of the optimal PCR amplification cycle for TGF- β transcript	66
Figure 3.7A-B. TGF- β amplification of log-fold diluted cDNA	68
Figure 3.8 A-B. Determination of the optimal PCR amplification cycle for FOXP3 transcripts	69
Figure 3.9A-B. FOXP3 amplification of log-fold diluted cDNA	70
Figure 3.10. IL-17 was not detected in BCCL	72
Figure 3.11. BCCL expression of IL-6	73
Figure 3.12. BCCL expression of TGF- β	74
Figure 3.13. BCCL expression of FOXP3	75
Figure 3.14A-B. IL-6 transcript expression in BCT samples	79
Figure 3.15A-B. IL-17 transcript expression in BCT samples	82
Figure 3.16A-B. Determining the optimal dilution of cDNA for real-time assays	84
Figure 3.17A-B. Standard curve of the threshold cycles (C _t)	87

Figure 3.18. BCCL expression of IL-17 and RORc2 as determined by real-time PCR	90
Figure 3.19. Real-time IL-17 transcript expression in BCT samples	91
Figure 3.20A-B. Real-time RORc2 transcript expression in BCT samples	92
Figure 3.21A. ANOVA analysis of HLA-DR52 stratified by IL-17 profiles on age at diagnosis	104
Figure 3.21B. ANOVA analysis of HLA-DR52 stratified by T _H 17 profiles on age at diagnosis.	105
Figure 3.22A-B. Kaplan-Meier analysis of IL-17 profiles with RFS and OS in breast cancer patient	107
Figure 3.23A-B. Kaplan-Meier analysis of RORc2 profiles with RFS and OS in breast cancer patients	109
Figure 3.24A-B. Kaplan-Meier analysis of T _H 17 profiles with RFS and OS in breast cancer patient	111
Figure 3.25. Dual IHC staining of sections from breast cancer lesions using antibodies to FOXP3 and CD3	114

LIST OF TABLES

Table 2.1A. Comparison of the distribution of clinical and pathological features between the T _H 17 subset and the original set.	44
Table 2.1B. Comparison of the distribution of HLA haplotypes between the T _H 17 subset and the original set	45
Table 2.1C. Comparison of the distribution of leukocyte infiltrates between the T _H 17 subset and the original set	45
Table 2.2. Breast Cancer Cell Lines	46
Table 2.3A. Primer sequences for RT – PCR	49
Table 2.3B. NCBI Reference Sequences for RT – PCR primers	49
Table 2.4: Real time PCR RORc2 primer sequences	51
Table 2.5: Real time PCR amplification conditions	52
Table 2.6: Primary antibody application conditions	55
Table 3.1. Annealing temperatures and times of RT-PCR Primers	59
Table 3.2. Optimal cycle numbers	71
Table 3.4. RIN Values for Breast Cancer RNA Samples	77
Table 3.5. Descriptive statistics of RT-PCR transcript levels of IL-6	78
Table 3.6. Descriptive statistics of RT-PCR transcript levels of IL-17	78
Table 3.7. Spearman’s correlation coefficients for RT-PCR relative transcripts of IL-6 and IL-17.	81
Table 3.8. R ² values and efficiencies for real-time PCR standard curves	86
Table 3.9. Transcript specific cDNA amounts for real-time PCR assays	86
Table 3.10. Spearman’s correlation coefficients between IL-17 real-time, IL-17 RT-PCR, RORc2 and IL-6 (N=49)	94
Table 3.11A. Chi Square analysis for associations of IL-17 with T cell markers in breast tumor samples	96
Table 3.11B. Chi Square analysis for associations of RORc2 with T cell markers in breast tumor samples	96

Table 3.11C. Chi Square analysis for associations of T _H 17 with T cell markers in breast tumor samples	97
Table 3.12A Chi Square analysis for associations of IL-17 with HLA-DR allotypes	98
Table 3.12B. Chi Square analysis for associations of RORc2 with HLA-DR allotypes	98
Table 3.12C. Chi Square analysis for associations of T _H 17 with HLA-DR allotypes	99
Table 3.13A Chi Square analysis for associations of IL-17 with prognostic indicators	100
Table 3.13B. Chi Square analysis for associations of RORc2 with prognostic indicators	101
Table 3.13C Chi Square analysis for associations of T _H 17 with prognostic indicators	102
Table 3.13D. Associations of IL-17, RORc2 and T _H 17 with age of diagnosis	102

LIST OF ABBREVIATIONS

ANOVA	analysis of variance
APCs	antigen presenting cells
ATCC	American Type Culture Collection
BCCLs	breast cancer cell lines
BCR	B cell receptor
BRCA1	breast cancer 1 gene
BRCA2	breast cancer 2 gene
C _t	threshold cycle
CC1	cell conditioning buffer
CCL	CC ligand motif
CCR	CC receptor
cDNA	cloned DNA
CI	confidence interval
CIN	cervical intraepithelial neoplasia
CRC	colorectal carcinoma
CLIP	class II-associated invariant chain peptide
CTL	cytolytic T lymphocytes
CTLA	cytolytic T lymphocyte antigen
CXCL	CXC chemokine ligand
CXCR	CXC chemokine receptor
DAB	diaminobenzidine
DAMPs	damage associated molecular pattern molecules
DCs	dendritic cells
DCIS	ductal carcinoma in situ
DNA	deoxyribonucleic acid
DX	diagnosis
EAE	experimental autoimmune encephalomyelitis
ED	extended stage disease
ER	estrogen receptor
FFPE	formalin fixed and paraffin embedded
FOXP3	forkhead box P3
GAPDH	glyceraldehyde 3-phosphate dehydrogenase
G-CSF	granulocyte colony stimulating factor
HCC	heptacellular carcinoma
HBV	hepatitis B
HCV	hepatitis C
HPV	human papillomavirus
HER2/neu	human epidermal growth factor receptor 2
HLA	human leukocyte antigen
HMGB	high mobility group box
HPV	human papillomavirus

IBC	inflammatory breast carcinoma
ICAMs	inter-cellular adhesion molecule
IDC	invasive ductal carcinoma
IFN	interferon
IHC	immunohistochemistry
Ii	invariant chain
IL	interleukin
ILC	invasive lobular carcinoma
iNK	invariant natural killer
LCIS	lobular carcinoma in situ
LD	limited stage disease
MBTB	Manitoba Breast Tumor Bank
MHC	major histocompatibility complex
MIIC	MHC class II loading compartment
MGB	minor groove binder
mRNA	messenger ribonucleic acid
NC	negative control
NCBI	National Center for Biotechnology Information
NHS	normal horse serum
NK	natural killer
OS	overall survival
PBLs	peripheral blood lymphocytes
PBMCs	peripheral mononuclear cells
PBS	phosphate buffered saline
PHA	phytohemmagglutinin
PILs	prostate infiltrating lymphocytes
PMA	phorbol 12-myristate 13-acetate
PR	progesterone receptor
qPCR	real-time PCR
UCC	uterine cervical cancer
UV	ultraviolet
RIN	RNA integrity number
RFS	recurrence free survival
RORc2/ROR γ t	retinoic orphan receptor
RT-PCR	reverse transcriptase polymerase chain reaction
SCLC	small cell lung cancer
SDF-1	stromal cell derived factor 1
SE	standard error
SEM	standard error of the mean
SNP	single nucleotide polymorphisms
STAT	single transducer and activators of transcription factor
T-bet	T box transcription factor
T1D	type 1 diabetes mellitus
T _H 1	type 1 T helper cell
T _H 2	type 2 T helper cell

T _H 17	type 17 T helper cell
T _{reg}	regulatory T cell
TAMs	tumor associated macrophages
TBE	Tris/Borate/EDTA
TCR	T cell receptor
TGF	transforming growth factor
TILs	tumor infiltrating lymphocytes
TLR	toll like receptor
TNF	tumor necrosis factor
TNM	tumor, node, metastases
UCC	uterine cervical carcinoma
VAD	Ventana antibody diluent
VEGF	vascular endothelial growth factor

Chapter 1: Introduction

1.1. Preface

Previous work in the Drover laboratory focused on CD4⁺ T cells, and the correlation of tumoral lymphocytes with human leukocyte antigen (HLA)-DR phenotypes, prognosis and survival. In total, 85 breast tumors were examined by both immunohistochemistry (IHC) for immune infiltrates and reverse transcriptase polymerase chain reaction (RT-PCR) for the presence of various cytokine messenger ribonucleic acid (mRNA) transcripts. IHC provided characterization of the numbers and pattern of inflammatory cell infiltration and RT-PCR allowed relative levels of intratumoral cytokine or transcription factor mRNA to be quantified. A type 1 helper T (T_{H1}) cell profile was identified by high levels (greater than the 75 percentile) of T_{H1} type cytokines: interferon (IFN)- γ , interleukin (IL)-2 and IL-12. A type 2 helper T (T_{H2}) cell profile was identified by high levels of IL-4 and IL-10 transcripts. Forkhead box P3 (FOXP3) positive regulatory T (T_{reg}) cell profile was defined by high levels of FOXP3 transcripts. Inflammatory T cell profiles were identified by IL-6 and IL-1 β transcripts. Dual staining IHC was also used to determine the presence of FOXP3 (nucleus) and CD4 or CD25 (cytoplasm) in paraffin embedded breast tumors samples in a later study. Although most of the mRNA transcripts were analyzed by RT-PCR, and ideally should be confirmed by real time PCR, the data revealed several important trends. High levels of IFN- γ transcripts, detected by both RT-PCR and qPCR, correlated with increased survival of patients, whereas high IL-6 levels and HLA-DR52 were associated with large tumors and decreased survival (Oldford et al, 2006). As IL-6 is required for the commitment and differentiation of a naïve T cell into a T_{H17} cell (Bettelli et al., 2008), we first questioned

if T_H17 cells were present in tumors with high IL-6. Secondly, if T_H17 cells were present, we predicted these cells would be increased in HLA-DR52⁺ patients and associate with decreased survival. We also intended to expand on this work by analyzing markers associated with T_H17 cells and their association with prognostic indicators. Thus, the following chapter is divided into sections that provide a brief overview of breast carcinoma and a more detailed description of T_H17 cells and immune responses in cancer.

1.2. Breast Carcinoma

Breast carcinoma normally originates in breast tissue of the ducts or the lobules (Figure 1.1). Ductal carcinoma begins in ducts that facilitate the movement of milk from the breast to nipple. Generally, ductal cancer is more common than lobular breast cancer, which originates in the area of the breast that produces milk, the lobules. Further, both ductal and lobular breast cancer can be defined as either non-invasive/*in situ*, meaning the cancer is confined to the layer of cells where it began or invasive, meaning the cancer has grown beyond the originating cell layer. Ductal carcinoma in situ (DCIS) is the most common non-invasive breast cancer. Nearly 1/5 of new breast cancer cases are DCIS and the prognosis for these patients is favorable because early DCIS diagnoses are associated with high survival (Ernster, et al., 2002).

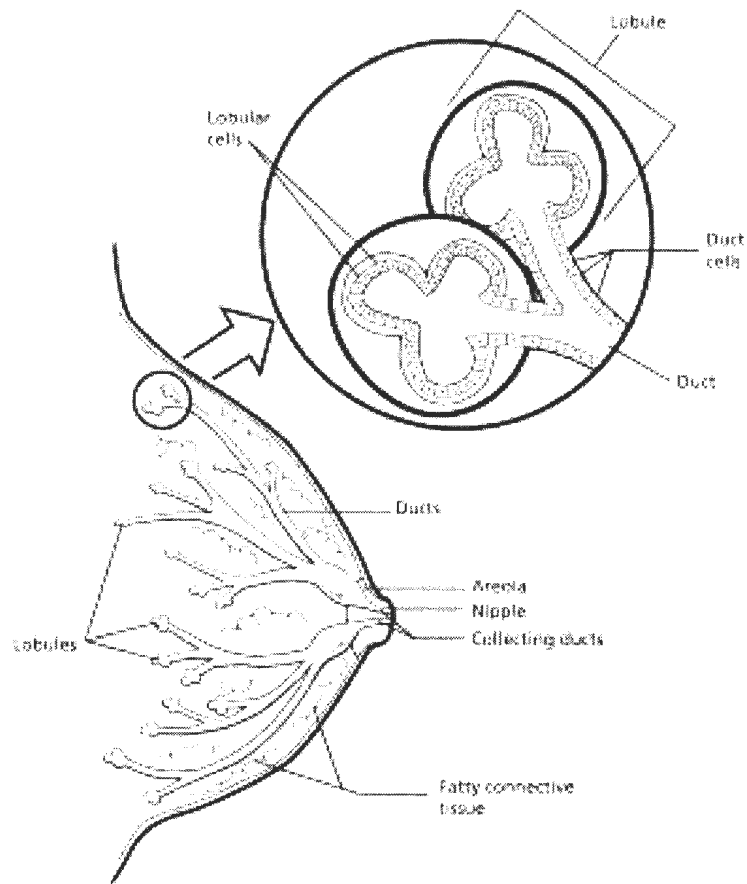


Figure 1.1. *Normal structure of a breast.* The most common tissues where breast cancer develops are the ducts and the lobules. The ducts supply milk to the nipple and the lobules produce the milk. Typically, breast carcinoma will arise in either the lobules or the ducts. Both the lobules and the ducts are illustrated above.

Lobular carcinoma in situ (LCIS) is less common than DCIS. Invasive ductal carcinoma (IDC) is the most common type of breast cancer. IDC begins in the milk duct and cancerous cells break through the wall of the duct and these cells proliferate in the fatty tissue of the breast. The cancer cells can then metastasize to other areas of the body through the lymphatic system and blood stream. Roughly eighty percent of invasive cancers are IDC (Carlson et al., 2009, McPherson et al., 2000). Invasive lobular cancer (ILC) begins in the lobules and can spread to other parts of the body (Carlson et al., 2009, McPherson et al., 2000).

Breast cancers originating in tissues other than ducts and lobules are uncommon. Of these, inflammatory breast cancer (IBC) accounts for 1 – 6% of these diagnoses (Wingo et al., 2004). IBC occurs when cancer cells block lymph vessels in the skin and is not characterized by a lump and therefore, is difficult to detect (Wingo et al., 2004). Medullary, mucinous, tubular and metaplastic carcinomas are examples of rare types of invasive breast cancers. Paget's disease of the nipple is a type of breast cancer that initiates in the ducts and spreads to the nipple and the areola. Paget's disease of the nipple is extremely rare, accounting for only 1% of diagnoses and is often associated with DCIS. With each different kind of breast carcinoma, unique treatment plans must be developed (Allred, D.C., 2008).

1.2.1. Epidemiology of Breast Cancer

In 2012, an estimated 22,700 Canadian women and 200 Canadian men will be diagnosed with breast cancer. Despite the high number of new cases, the survival rates

are encouraging. It is estimated that 87% of the women and 84% of the men diagnosed will survive at least 5 years post diagnoses (Canadian Cancer Statistics, 2012).

The incidence of developing breast cancer is influenced by many factors. Men with breast cancer comprise less than 1% of new breast cancer cases. Women, in comparison, are almost 100 times more likely to develop the disease than men. Further, as individuals age, the risk of developing breast cancer rises. Among the 22,700 women diagnosed in 2012, approximately 80% of the cases occurred in women over 50 (Canadian Cancer Statistics, 2012).

Women who had an early menarche (before 12 years) or a late menopause (after 55 years) were more likely to have increased incidences of breast cancer than those who had neither an early menarche or late menopause (Carlson et al., 2009, McPherson et al., 2000). Following menarche, the ovaries secrete estrogen, estradiol and progesterone in a cyclic pattern based upon the menstrual cycle. The secretions of these hormones tend to fluctuate as a woman approaches menopause and the ovaries ultimately cease production of estradiol, estrogen and progesterone at the end of menopause (Burger, 1994). Earlier menarche and later menopause means a prolonged production of estrogen in the body and there is reliable evidence to suggest that elevated estrogen levels increase the risk of developing breast cancer (Yager and Davidson, 2006)

Studies have found links and potential mechanisms between estrogen and development of cancer in various tissues including the kidneys, liver, uterus and breast. After estrogen (or estradiol) binds to an estrogen receptor (ER), the estrogen is internalized and the cell will commence a series of reactions to eliminate the estrogen. In the case of expression of metabolizing carcinogenic estrogens, the reactions can produce

oxygen radicals. Oxygen radicals can be damaging to DNA. The damaged deoxyribonucleic acid (DNA) can result in mutations, leading to the promotion of cancer (Yager and Davidson, 2006). Furthermore, breast cancer is frequently hormone dependent and cancer cells express receptors for hormones. Therefore, hormones, such as estrogen and progesterone can stimulate cancer cells to grow. Conversely, proliferative cancer cells can be down-regulated by anti-hormones. As a result, tamoxifen, an antagonist of the ER, is the preferred treatment for ER⁺ breast cancer (Bai and Gust, 2009).

Family history and genetics are also indicators for the likelihood of developing breast cancer. Generally, a family history of breast, uterine, ovarian or colon cancer increases an individual's risk of developing breast cancer (Wooster et al, 1994; Rastelli et al, 2011). Furthermore, genetic defects, particularly in breast cancer 1 (BRCA1) and breast cancer 2 (BRCA2) genes, increase an individual's chance of developing breast cancer. BRCA1 and BRCA2 are tumor suppressor proteins; the former is involved in DNA repair and the latter in chromosomal repair (Wooster et al, 1994; Rastelli et al, 2011). Women with defects in these genes, leading to improper production of the protective proteins, have an 80% chance of developing breast cancer (Carlson, 2009; Gage, 2012). However, these genetic defects account for a minority of breast cancer cases (between 5 – 10%) (Gage, 2012).

In addition to the aforementioned factors, external and environmental factors play a role in breast cancer development. Such external risk factors can be the frequency of consumption of alcohol, smoking, age of first childbirth (hormonal link) and incidence of radiation exposure or hormone replacement therapies (Carlson et al., 2009).

1.2.2. Classification and Treatment of Breast Carcinoma

Breast cancer is classified and staged on the basis of several clinicopathologic factors. The stage is determined using the tumor, node, metastases (TNM) classification of malignant tumors (Irvin and Carey, 2008). The letter T is followed by a number, either 0 to 4 and describes the size of the tumor. A category of T0 means that there is no evidence of a primary tumor, T1 indicates that the tumor is less than 2 cm in diameter, T2 indicates the tumor is between 2 and 5 cm in diameter, T3 indicates a tumor greater than 5 cm in diameter, and T4 is representative of a tumor of any size growing into the chest wall or skin and is typical of inflammatory breast cancer. The letter N, for node, is followed by a number between 0 and 3 and indicates whether the cancer has spread to nearby lymph nodes. As the numbers increase, the number and severity of lymph nodes invaded by cancer cells increases. Lastly, the letter M is followed by either a 0 or 1 and indicates whether or not the cancer has metastasized to distant organs. Taking the TNM categories into consideration the breast cancer is then staged between stage I (least advanced breast cancer) and stage IV (most advanced breast cancer). Appendix A provides characterization of breast cancer stages according to TNM (Irvin and Carey, 2008; Michaud et al., 2008).

Tumor grade is also used to classify breast tumors. Most classification schemes for tumor differentiation are based on the scheme proposed by Bloom and Richardson (Bloom and Richardson, 1957). Tumors are assigned qualitative scores between 1 – 3 for tubule formation, nuclear pleiomorphism and mitotic rate. The three scores are then combined to assign a tumor a grade from 3 – 9. Tumors are then further divided into low (Grade I, scores 3-5), intermediate (Grade II, scores 6-7) and high (Grade III, scores 8-9).

Patients with Grade I tumors show improved 5, 10, and 15 year survival in comparison to patients who have Grade II/III tumors (Bloom and Richardson, 1957). A common modification of this system, Nottingham System, uses a semi-quantitative assessment of the three factors mentioned by Bloom and Richardson for a more objective system for histological grade. Tumors are classified as well-differentiated (Grade I, scores 3-5), moderately differentiated (Grade II, scores 6-7), and poorly differentiated (Grade III, scores 8-9). Similar to the Bloom and Richardson system (1957), patients with lower tumor grades have improved disease free survival (Elston and Ellis, 1991).

In addition to the TNM system, there are other clinicopathologic factors, which can serve as prognostic indicators and aid in the determination of an appropriate treatment. Breast cancer cells may express ER and progesterone receptors (PR) (frequently analyzed together), and the human epidermal growth factor receptor 2 (HER2) (Irvin and Carey, 2008). Estrogen or progesterone binding to their respected receptor can lead to the proliferation and growth of breast cancer cells. Therefore, an appropriate treatment of ER⁺/PR⁺ breast cancer would be to block the receptor (Irvin and Carey, 2008). For example, ER can be blocked using tamoxifen, which is the standard drug for treating hormone receptor positive breast tumors (Delozier, 2010). Tamoxifen is an antagonist of the ER in breast tissue and will competitively bind to ER on tumors. Tamoxifen, therefore, decreases deoxyribonucleic acid (DNA) synthesis and inhibits the pro-tumor effects of estrogen (Jordan, 1993; Ali et al., 2011)

HER2 is a membrane bound receptor tyrosine kinase and is encoded by the proto-oncogene HER2/neu. It is involved in signal pathways leading to cell growth and differentiation (Coussens et al., 1985). HER2/neu is expressed in 20 – 30 % of invasive

breast cancer (Hudis, 2007). Overexpression of this receptor is generally associated with disease recurrence and a poor prognosis. Treatment of HER2⁺ tumors includes administering the humanized monoclonal antibody trastuzmaub (Ye et al., 1999). Trastuzmaub binds to the extracellular juxtamembrane HER2 domain and inhibits proliferation. As a result, HER2⁺ tumors regress (Hudis, 2007).

Triple negative breast cancers have very low levels or no ER, PR or HER2/neu present on the tumor cells. It has a poor prognosis and requires more aggressive treatments, such as chemotherapy, radiation or surgery (Irvin and Carey, 2008).

1.3. Immune Responses and Immune Profiling

Transformed cells have the potential to proliferate and develop into a tumor. If a tumor is benign, the transformed cells are molecularly and functionally similar to normal cells (Lodish, et al. 2000). In contrast, malignant cells express some proteins characteristic of the normal cell, but these cells tend to grow and divide more rapidly. Malignant cells have the ability avoid detection by immune cells through altering immune recognition and manipulating immunosurveillance mechanisms (Lodish et al., 2000; Mincheff, M, 2009). If the transformed cells develop into a tumor, the immunogenic phenotype of the tumor can either facilitate tumor progression or regression. Clinical data suggest that immune profiles of patients with malignancies can be distinguished from immune profiles of healthy individuals. For example, a patient with a malignant tumor can have impaired T cell function and have activated suppressor cells and T_{reg} cells found within circulation, the lymphoid organs and neoplastic tissues. These regulatory cells

have the potential to disable the tumor-killing cytotoxic T cells (CTLs) (Hrubisko et al., 2010).

An immune response mounted against a foreign element or antigen is initially broad and involves the innate immune system, which is followed by a more specific adaptive immune response. The innate immune response occurs rapidly upon exposure to the foreign antigen with phagocytic cells and inflammatory processes being activated. The adaptive immune response is slower and involves activation of T and B cells, which express unique antigen specific receptors. For example, the T cell receptor (TCR) recognizes antigens in the context of the major histocompatibility complex (MHC) bound to an antigenic peptide. MHC class I molecules are recognized by CD8⁺ T cells and MHC class II molecules are recognized by CD4⁺ T cells (Mesquita et al., 2010). As the focus of this thesis is on CD4⁺ T_H17 cells, the next section will review antigen presentation by MHC class II molecules and antigen recognition by T cells.

1.3.1. Major Histocompatibility Complex Class II

MHC class II molecules, called HLA class II molecules in humans, are found on antigen presenting cells (APCs). Due to the enormous number of antigens an individual encounters, HLA genes evolved to be highly polymorphic. HLA class II molecules (HLA-DR, -DP, or -DQ) are synthesized in the endoplasmic reticulum and are heterodimers, consisting of two peptide chains; α and β . During synthesis of HLA class II molecules, the α and β chains complex with the invariant chain (Ii). Ii blocks the peptide binding groove of the HLA molecule to prevent premature peptide binding. The Ii also facilitates the export of the MHC class II molecules into the golgi and in the MHC class II

loading compartment (MIIC). Once in the golgi, Ii chain is cleaved into a truncated form known as class II-associated invariant chain peptide (CLIP). The MHC class II compartment (MIIC), containing the MHC class II molecule:CLIP complex, fuses with an endosome containing endocytosed and degraded antigens. CLIP is removed by a MHC class II-like structure, HLA-DM, which allows antigenic peptides to bind to the MHC class II molecule. The MHC Class II:peptide complex transits to the cell surface where the MHC molecule can interact with CD4⁺ T cells (Figure 1.2).

The HLA class II region is very complex due to polygenic and polymorphic nature of the HLA. The immunogenetics (IMGT)/HLA database has identified 7 DRA, 1,150 DRB (1,051 DRB1, 1 DRB2, 57 DRB3, 15 DRB4, 19 DRB5, 3 DRB6, 2 DRB7, 1 DRB8 and 1 DRB9), 46 DQA1, 160 DQB1, 33 DPA1 and 150 DPB1 alleles (HLA Nomenclature, 2012). The genes that encode the α and β chains are designated A and B, respectively

The polygenic nature of the MHC facilitates the binding of a range of peptides. The polymorphism refers to the variants of the genes within populations. In particular, the HLA-DRB1 locus is extremely variable with 1,051 variants known to date. Generally the HLA-DRB1 variations are linked with additional structural HLA-DRB genes. For example, HLA-DRB1*15 and 16 alleles associate with HLA-DRB5 alleles (old nomenclature: HLA-DR51 allele); HLA-DRB1*04, 07 and 09 associate with HLA-DRB4 (HLA-DR53); HLA-DRB1*03, 11, 12, 13 and 14 associate with HLA-DRB3 (HLA-DR52); while HLA-DRB1*01, 10 and 08 are not associated with other HLA-DRB genes (Figure 1.3) (Campbell and Trowsdale, 1993). Therefore, due to the linkage of the DRB genes and co-dominant expression of HLA, an individual can express up to four different

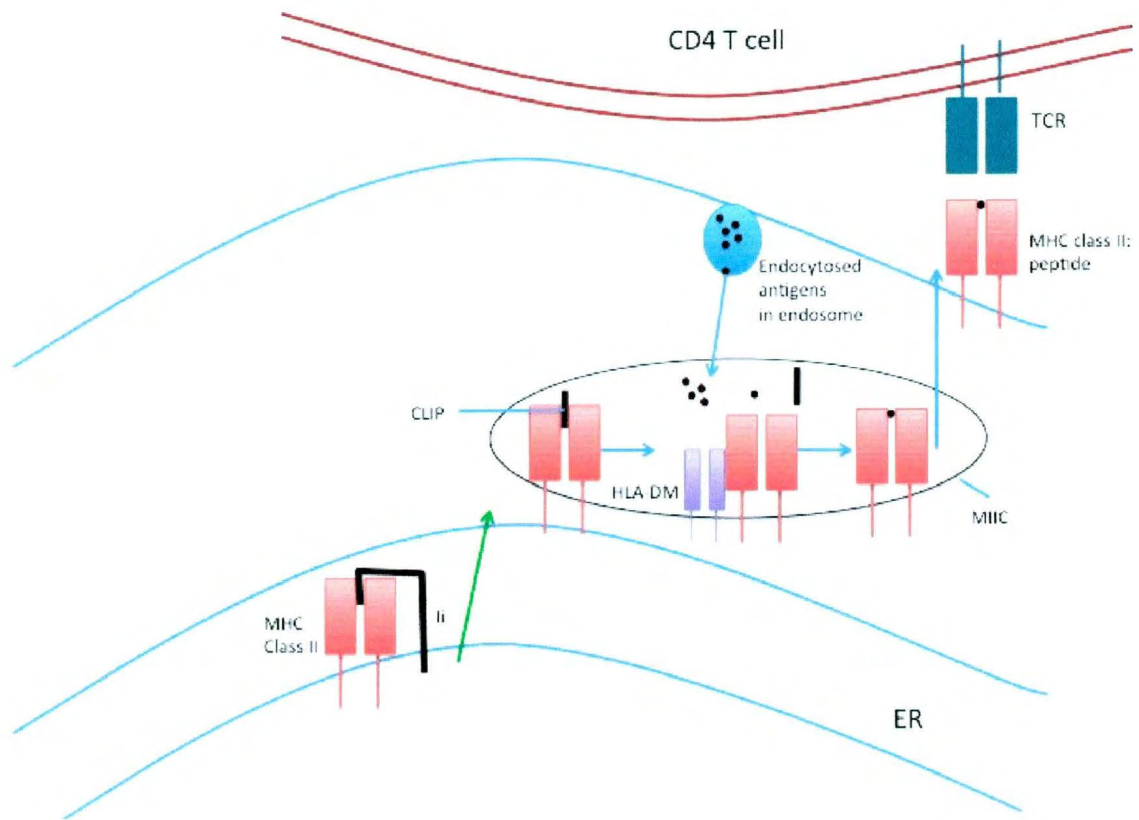
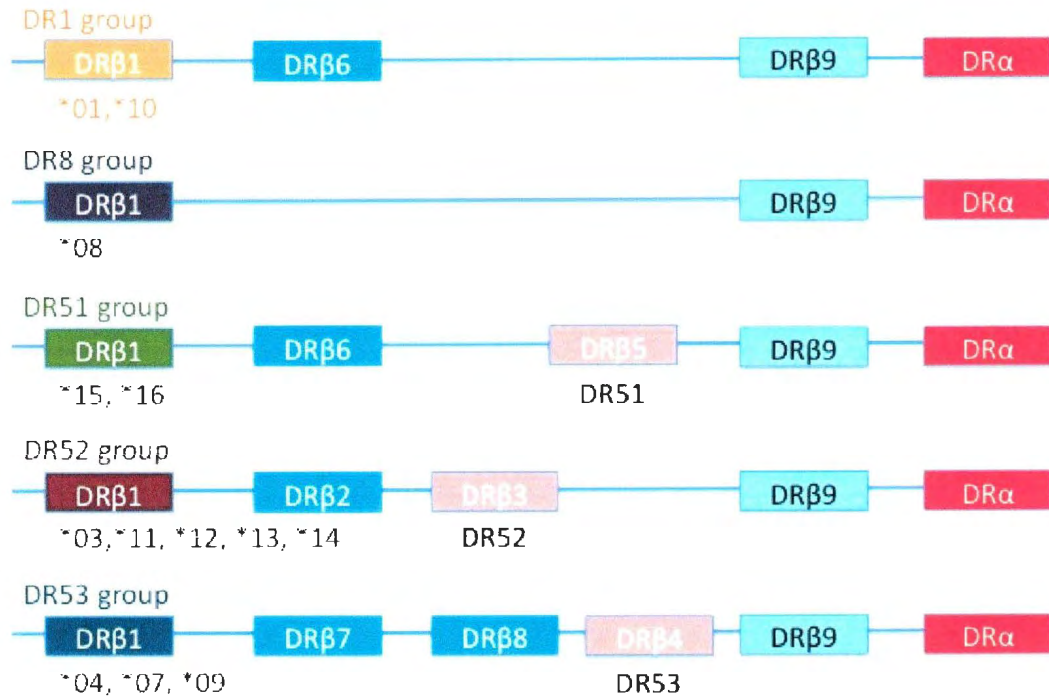


Figure 1.2. *MHC class II:Antigenic peptide interaction.* Antigen is endocytosed and degraded into peptides by the proteolytic environment in endosomes. The endosome, containing antigenic peptides, fuses with the MIIC. This compartment contains a MHC class II molecule (red) with a truncated form of the Ii, CLIP, bound to the binding groove. HLA-DM (purple) facilitates the removal of CLIP and the loading an antigenic peptide when the MIIC fuses with the endosome containing the antigenic peptides. The HLA class II molecules:peptide complex then moves towards the cell surface to present the antigen to a CD4 T cell (green).



Adapted from Campbell and Trowsdale, 1993

Figure 1.3. *HLA-DR alleles.* HLA-DR alleles grouped into 5 groups based upon the DRB/DRβ genes. Pseudogenes are indicated by the colored boxes (light blue) (Campbell and Trowsdale, 1993).

HLA-DR allotypes . In addition to HLA-DR – HLA-DR associations, HLA-DR and HLA-DQ also have associated linkages.

1.3.2. HLA Expression and Association with Disease

As mentioned, HLA alleles are highly polymorphic and possess polymorphic peptide binding pockets that allow them to preferentially bind some peptides and present the peptides to T cells to elicit a T cell response (Mesquita et al., 2010). Therefore, depending on the HLA haplotypes an individual carries, an individual may differ in their response to pathogens. These differences in peptide binding due to allelic variants may predispose an individual to developing an autoimmune disease or carcinomas.

Evidence from various studies suggests associations between carriage of particular HLA alleles and prominence of certain diseases or susceptibility to cancer. Type 1 diabetes mellitus (T1D) has been intensely studied for relationships with HLA molecules (Nerup et al., 1974; Platz et al., 1981). Initial studies in Caucasians found links between increased susceptibility to T1D and HLA-B8, HLA-B15 (HLA-B62) and HLA-B18 (Platz et al., 1981). Later studies revealed associations with HLA-DRB1*0301 (HLA-DR3), HLA-DRB1*04, HLA-DQ*0201, HLA-DQ*0302 in patients with T1D (Hirschhorn, 2003; Eisenbarth, 2003). Certain HLA alleles seem to associate with a genetic predisposition to other autoimmune diseases as well. For example, greater than 90% of ankylosing spondylitis patients carry HLA-B27, suggesting that this allele may be necessary for the development of the disease. Alleles HLA-DQA1*0102 and DQB*0602 (DQ6) associate with a susceptibility to multiple sclerosis and narcolepsy, but seem to confer protection against T1D. Rheumatoid arthritis also associates with several HLA-DR4

alleles (Thorsby and Lie, 2005). Recalling that MHC molecules are specific for particular peptides and T cell selection, an association between HLA allele presence and prominence of an autoimmune disease could indicate that tolerance to self-peptides is lost more frequently when that allele is present. This could suggest that HLA alleles interact with T cells in such a way that a self-peptide could be recognized as a foreign and an immune response would be mounted against the self. It could also mean that there is an association with another gene that is in linked disequilibrium with the particular HLA allele.

In addition to association with autoimmune diseases, studies have found that certain HLA alleles associate with development of various types cancers. This is particularly true for virally associated cancers such as human papillomavirus (HPV) (cervical cancer) and hepatitis B or C virus (hepatocellular carcinoma) (Wallboomers et al., 1999; Alison, et al. 2011). A study of 52 ovarian cancer patients and 239 healthy female controls found a significant increase in the frequencies of the haplotypes HLA-DRB1*0301, HLA-DQA1*0501, HLA-DQB1*0201; and HLADRB*1001, HLA-DQA1*0101, HLA-DQB1*0501 in cancer patients (Kubler et al., 2006). A study by *Chaudhuri et al.* (2000) analyzed HLA associations in patients with early onset breast carcinoma as compared to healthy age-matched controls in an American population in the Boston area. They reported that HLA-DQB*03032 and HLA-DRB1*11 may be protective alleles against early onset breast cancer as these alleles were increased in healthy controls and decreased in patients with early onset breast cancer (Chaudhuri et al., 2000). They also found that HLA-DRB3*02, a DR52 subtype, was increased in patients compared to healthy controls, suggesting that DRB3*02 can increase an individual's

susceptibility to breast cancer (Chaudhuri et al., 2000). A more recent study analyzing HLA associations between early onset Iranian breast cancer patients, compared to healthy age matched controls revealed that HLA-DQA1*0301 and HLA-DRB1*1303 were associated with higher incidences of breast cancer, whereas the alleles HLA-DQA1*0505 and HLA-DRB1*1301 were increased in healthy controls and decreased among breast cancer patients (Mahmoodi et al, 2011). Therefore, associations have been found to support the role of HLA haplotypes and risk for developing cancer and protection against cancer. However, not all CD4⁺ T cell responses are protective. Some studies have shown that CD4⁺ T_{reg} cells associate with the suppression of the immune system, therefore conferring an advantage to the virus or cancer (Wraith et al., 2004). This concept will be discussed further in section 1.3.3.

1.3.3. Effector and Regulatory CD4⁺ T cell Subsets in Humans

As mentioned in section 1.3.1., MHC molecules are crucial for an adaptive immune response because MHC molecules present antigens to T cells. The presentation of foreign antigens leads to their subsequent activation and differentiation. Following antigen recognition, CD4⁺ naïve T cells differentiate into several effector cells, as summarized in Figure 1.4. Significant evidence indicates the existence of functionally unique CD4⁺ T cells based on expression of certain transcription factors and their profile of cytokine secretion. CD4⁺ T_{H1} cells require the T box transcription factor (T-bet) and secrete the cytokines IFN- γ , tumor necrosis factor (TNF)- α and IL-2. These cytokines promote cell-mediated immunity, phagocyte-dependent protective responses, increase antigen processing and up regulate expression of MHC class I and II molecules

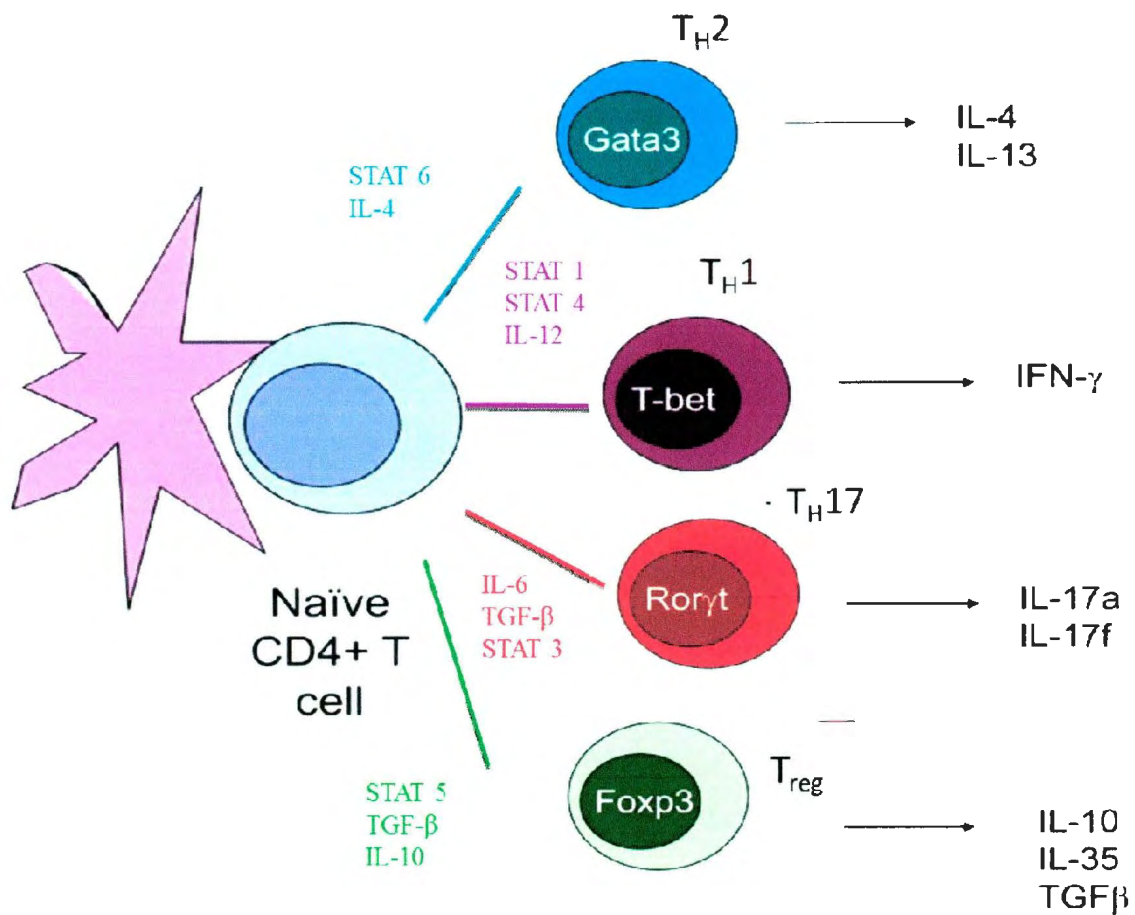


Figure 1.4. Differentiation of naïve CD4⁺ T cell into different effector subsets. A naïve CD4⁺ which has encountered an antigen in the context of a MHC Class II molecule may differentiate into several effector cells depending on the cytokine milieu present. TH2 cells require IL-4, STAT6 and GATA3 to differentiate. TH1 cells require STAT1, STAT4, IL-12 and T-bet for differentiation. TH17 cells require IL-6, TGF- β , STAT3 and RORc2/ γ t for differentiation. T_{reg} cells require STAT5, TGF- β , IL-10 and FOXP3 for differentiation. Items that are listed in the cell are transcription factors (ie: Gata3, T-bet), items that are colored and precede the T cell are required for the differentiation of the cell, and the items that are black and indicated by an arrow pointing right, in relation to the T cell, are cytokines produced by the cell (O'Shea and Paul, 2010).

(Romagnani, 2000). CD4⁺ T_H2 cells require the transcription factor GATA3 and secrete cytokines such as IL-4, IL-5, IL-6, IL-9, IL-10 and IL-13. Generally, T_H2 associated cytokines cause T_H1 cell anergy and limit CTL proliferation but enhance humoral immunity, promote mast cell and eosinophil growth (Romagnani., 2000). CD4⁺ T_{reg} cells dampen the immune response through secretion of IL-10 and transforming growth factor (TGF)- β . T_{reg} cells inhibit T cell growth and macrophage activation. Recently, T_H17 cells have been identified as another CD4⁺ effector T cell. These cells produce IL-17 (A-F), IL-6, IL-22 and IL-21 (Murugaiyan et al., 2009; Weaver et al., 2006; Bettelli et al., 2008). As T_H17 cells are a major focus of this study, the function of T_H17 cells will be reviewed in detail in the upcoming sections.

1.3.4. Differentiation of Naïve T Cells into T_H17 Cells

For a naïve T cell to differentiate into an effector T_H17 cells, the cytokines IL-6 and TGF- β are required. IL-6 preferentially activates single transducer and activators of transcription factor 3 (STAT3) (Bettelli et al., 2008). STAT3 leads to the expression of retinoic orphan receptor C2/ γ t (RORc2/ROR γ t) (Bettelli et al., 2008). RORc2 binds to the promoters of IL-17 and IL-21, leading to their transcription and translation (Bettelli et al., 2008). IL-6 and IL-21 act in an autocrine manner and lead to the expression of STAT3 in naïve T cells. This favors further T_H17 differentiation as described. In addition to IL-6 and TGF- β , IL-23 is required for the commitment and stability of the T_H17 cell (Bettelli et al., 2008). Once differentiated, a T_H17 cell, expresses IL-23R and IL-23 stabilizes the T_H17 phenotype (Murugaiyan et al., 2009). IL-1 β is also reported to cause expansion of memory T_H17 cells in patients with psoriasis (Kryczek et al., 2009).

In terms of tissue homing molecules, T_H17 cells have been reported to express high levels of CXC chemokine receptor 4 (CXCR4), CC-chemokine receptor 6 (CCR6), several CD49 and the C type lectin receptor CD161 (Zou and Restifo, 2010, Yamazaki et al., 2008; Boisvert et al., 2010). CXCR4 is specific for the stromal cell-derived factor 1 (SDF-1) or CXC chemokine ligand 12 (CXCL12) and $CD4^+$ T cells migrate towards this ligand. Generally, CXCL12 is found in bone marrow and tumors (Kryczek et al., 2007) and as a result, $CD4^+$ T cells home towards bone marrow and tumors. The presence of CCR6 results in migration towards CC-motif ligand 20 (CCL20), which is expressed by tissues (i.e. liver, appendix, lymph node and Peyer's patch) and cells (peripheral blood mononuclear cells (PBMCs), epithelial cells) (Ito et al., 2011). The role of CD161 on T_H17 cells is currently unknown (Kesselring et al., 2011). The absence of markers of lymphoid migration, CCR7 and CD62L, suggest that T_H17 cells do not migrate to lymphoid tissues.

With respect to other cell markers, conventional T cell molecules have not been detected on T_H17 cells. For example, HLA-DR, found on $CD4^+$ T_H1 , T_H2 and T_{reg} cells, is not expressed by T_H17 cells. CD25, a surface molecule found on activated T cells is not present on T_H17 cells. Granzyme B, located in the granules of CTL and NKT cells, is not found in T_H17 cells. Immunosuppression markers, such as programmed cell death 1 (PD-1), expressed on activated T cells, and FOXP3 are not present on T_H17 cells either. Therefore, it would appear that T_H17 cells are distinct from the other T cell subsets (Zou and Restifo, 2010).

1.3.4.1. Interaction of T_H17 Cells with Other CD4⁺ T Cell Subsets

As described in section 1.3.4. and presented in Figure 1.4., TGF- β is required for the differentiation of FOXP3⁺CD4⁺ T_{reg} cell and T_H17 cells (O'Shea and Paul, 2010). It has been suggested that although TGF- β supports T_{reg} cell differentiation, simultaneous stimulation of naïve T cells with IL-6 and TGF- β promotes T_H17 cell differentiation and suppresses T_{reg} differentiation (Bettelli et al., 2006; Pan et al., 2011). This is further supported by the identification of T cells, in both mice and humans, which express both RORc2 and FOXP3, the transcriptional regulators for T_H17 cells and T_{reg} cells, respectively (Zhou et al., 2009; Yang et al., 2008). Depending on the cytokine milieu present, it appears that one transcription factor will dominate the other. For example, higher levels of TGF- β favor FOXP3 expression and repress IL-23R expression, which is required for T_H17 cell maintenance (Zhou et al., 2009; Yang et al., 2008). Once expressed, FOXP3 can also bind to RORc2 and antagonize the T_H17 transcription factor. On the other hand, if pro-inflammatory cytokines are present, such as IL-21 and IL-6, these cytokines will activate STAT3 and overcome the FOXP3 mediated inhibition of RORc2 (Zhou et al., 2009; Yang et al., 2008). The pro-inflammatory environment will favor T_H17 cell differentiation (Zhou et al., 2009; Yang et al., 2008).

Studies have also been conducted to determine if T_H17 cells interact with T_H1/T_H2 subsets. Although, some IL-17 producing CD4⁺ T cells in humans were found to secrete small amounts of IFN- γ (Kryczek et al., 2009). IFN- γ , tends to inhibit the induction of IL-17. Further a member of the IL-12 cytokine family, IL-27, promotes expression of the T_H1 transcription factor, T-bet, but inhibits T_H17 cell differentiation in a STAT1 dependent manner (Zhou et al., 2009; Dong, 2011). In experiments conducted in mice,

in vitro generated T_H17 cells can convert to T_H1 cells in lymphopenic environments (Lee et al., 2009; Martin-Orozco et al., 2009), suggesting plasticity exists between these two helper T cell groups. Similarly, IL-4, a cytokine required for the differentiation of GATA3 T_H2 cells activates growth factor independent 1 (GFI-1), which is reported to inhibit both T_H17 and T_{reg} cell differentiation (Zhou et al., 2009).

1.3.5. T_H17 Cytokine Profile and the Biological Function of T_H17 cells.

In the years following the identification and classification of CD4⁺ T_H17 cells, an abundance of research concerning their biological function has been conducted. T_H17 cells were originally defined by their production of IL-17 cytokines, previously termed CTLA (cytolytic T lymphocyte antigen)-8 cytokines (Harrington et al., 2006). There are 6 types of IL-17: IL-17 A-F. T_H17 cells primarily produce IL-17A and IL-17F, which are functionally similar because they induce the production of proinflammatory cytokines, chemokines and metalloproteases by cells and tissues that express IL-17R (Bettelli et al., 2008). IL-17A is generally produced 4 – 8 hours following a microbial infection and enhances neutrophil chemotaxis, granulocyte colony stimulating factor (G-CSF) and CXCL8 (Happel et al., 2005; Cua and Tato, 2010). However, it was previously thought that T_H17 cells were the sole producers of IL-17. Yet, recent research suggests that $\gamma\delta$ T cells, invariant natural killer (iNK) T cells, NK cells, neutrophils, macrophages, eosinophils and some myeloid cells can produce IL-17 cytokines (Cua and Tato, 2010; DeNardo and Coussens, 2007).

Along with the secretion of IL-17, T_H17 cells have been shown to secrete IL-22, which is a member of the IL-10 family of cytokines and is a mediator of cellular

inflammatory responses. IL-22 initiates innate immune responses against bacterial pathogens, especially in epithelial cells. IL-22 can also induce β -defensins in epithelial cells and promote psoriasis (Zheng et al., 2007; Liang et al., 2006). Differentiated T_H17 cells also secrete IL-21, which acts in an autocrine manner by activating STAT3 and leading to the amplification of T_H17 cells as previously described in Section 1.3. IL-21 further supports B cell differentiation and antibody class switching (Spolski et al., 2008).

Together, IL-17 and IL-21 promote inflammation. Therefore, it is not a surprise that T_H17 cells have a role in autoimmune disease. Overexpression of IL-17 is associated with a variety of inflammatory diseases, such as rheumatoid arthritis, systemic lupus erythematosus and asthma (Bettelli et al., 2008). A key study that illustrated the role of T_H17 cells in autoimmunity was performed on mice deficient in IL-12p40 subunit, part of the IL-23R (Bettelli et al., 2008). As IL-23 is required for the maintenance of the T_H17 phenotype, without a functioning receptor for IL-23, there would be no functioning T_H17 cells. Mice that had this deficiency were found to have lower levels of T_H17 and were protected from experimental autoimmune encephalomyelitis (EAE) and collagen induced arthritis. It was therefore concluded that T_H17 cells could induce autoimmunity through tissue inflammation and activation of the innate immune system (Bettelli et al., 2008; Dong et al., 2008). The association between T_H17 cytokines and autoimmunity has been studied more in depth than the association between these cytokines and promotion or protection from cancer.

1.4. Immune Response and Cancer

The immune system plays a dual role in cancer. Through destroying cancer cells or inhibiting their growth, the immune system can suppress tumor growth. However, through recruiting certain cells, such as T_{reg} cells, and establishing a particular microenvironment, the immune system may facilitate and promote tumor growth. This section will explore the immune system's ability to act in a pro-tumor and anti-tumor manner (Schreiber et al., 2011).

1.4.1. Anti-tumor Immune Responses

An anti-tumor immune response can involve both components of the innate and adaptive immune system. Type 1 IFNs, components of the innate immune system, may be present within a tumor environment, potentially produced from $CD11c^+$ dendritic cells (Diamond et al., 2011). Type 1 IFNs activate other dendritic cells, which engulf tumor antigens to promote an anti-tumor immune response (Matzinger, 1994; Schreiber et al., 2011). Type 1 IFNs also increase NK cell activity and subsequently increase CTL killing of tumor cells. Type 1 IFNs also have the ability to induce growth inhibition and death of cancer cells (Trinchieri, 2010). Damage-associated molecular pattern molecules (DAMPs) can be released from dying tumor cells. In particular, high mobility group box (HMGB) 1, a DAMP, may be recognized by toll like receptor (TLR) 4 on dendritic cells and facilitate an anti-tumor response (Sims, 2010)

Although these elements of the innate immune system assist in protection against tumor development, an adaptive immune response is needed to protect the host against a developing tumor. Most tumors cells are positive for MHC class I. $CD8^+$ T cells or CTLs

may recognize tumor antigens presented in the context of MHC class I and induce tumor killing (Yu and Fu, 2006). The ability of CD8⁺ T cells to act as effectors against tumors is further supported by clinical data. A recent study conducted by *Mahmoud et al.* (2011) on 1334 breast tumors analyzed the infiltrating CD8⁺ T cell populations by immunohistochemistry. This study found significant correlations between the total number of CD8⁺ T cells and the number of distant stromal CD8⁺ T cells and increased patient survival (Mahmoud et al., 2011).

CD4⁺ T_H1 cells also assist in the activation of CTLs. T_H1 cells interact with APCs and cause APCs to express inter-cellular adhesion molecule (ICAM) 1, CD80 and CD86 or promote IL-12 secretion from the APCs. These factors are essential for more efficient CTL activation (Yu and Fu, 2006). T_H1 cells also secrete cytokines, such as IFN- γ , which promote up-regulation of MHC molecules. This can improve tumor associated antigen presentation (Yu and Fu, 2006).

Whether or not T_H17 cells have a pro-tumor or anti-tumor role is debatable. T_H17 cells may recruit dendritic cells to tumor sites and promote activation of tumor specific CTL (Bronte, 2008). A model which suggests that T_H17 cells promote an anti-tumor response within a tumor microenvironment, is based on the ability of IL-17, in the presence of IFN- γ , to promote the secretion of CXCL9 and CXCL10 from tumor cells. Both CXCL9 and CXCL10 are ligands that attract CXCR3⁺ NK cells and CTLs. Therefore, the production of both CXCL9 and CXCL10 can lead to the migration of NK cells and CTLs to the tumor microenvironment and lead to cytolytic killing of tumor cells (Figure 1.5.) (Maniati et al., 2010). CCL20, secreted by T_H17 cells, can attract dendritic cells to the tumor microenvironment due to the presence of CCR6 on dendritic cells. The

dendritic cells can engulf tumor antigens and present these antigens to CD4⁺ or CD8⁺ T cells, leading to a specific immune response against the tumor (Figure 1.5.) (Maniati, et al.,2010).

1.4.2. Pro-tumor Immune Responses

Section 1.4.1. detailed potential anti-tumor roles of the adaptive immune system. However, there is evidence to suggest that elements of the adaptive immune system promote tumor growth. For example, T_H2 cells facilitate antibody production and can sway immunity away from beneficial cellular mediated responses. T_H2 cells, through secretion of IL-4, can enhance pro-metastatic EGF receptor signaling profiles in malignant cells, therefore promoting tumor growth (DeNardo et al., 2009). CD4⁺CD25⁺FOXP3⁺ T cells (T_{reg} cells), enriched with CTLA-4 and glucocorticoid induced tumor necrosis factor receptor family related gene, are considered to suppress anti-tumor behavior from cells such as T_H1 cells (Watanabe et al., 2010; Ostrand-Rosenberg, 2008). There are several studies that support the concept that T_{reg} cells suppress anti-tumor behaviors of other cells. For example, Liu *et al.* (2011) examined 1270 invasive breast carcinomas by IHC for infiltrating T_{reg} cells. They found high densities of T_{reg} cells associated with poor prognostic indicators such as ER and PR negative tumors, high histological grades and HER2 overexpression. Further, high T_{reg} cell populations correlated with decreased overall survival and recurrence free survival (RFS) (Liu et al., 2011)

The anti-tumor effects of T_H17 cells were previously discussed in Section 1.4.1. However, models and studies exist to support the hypothesis that T_H17 cells support

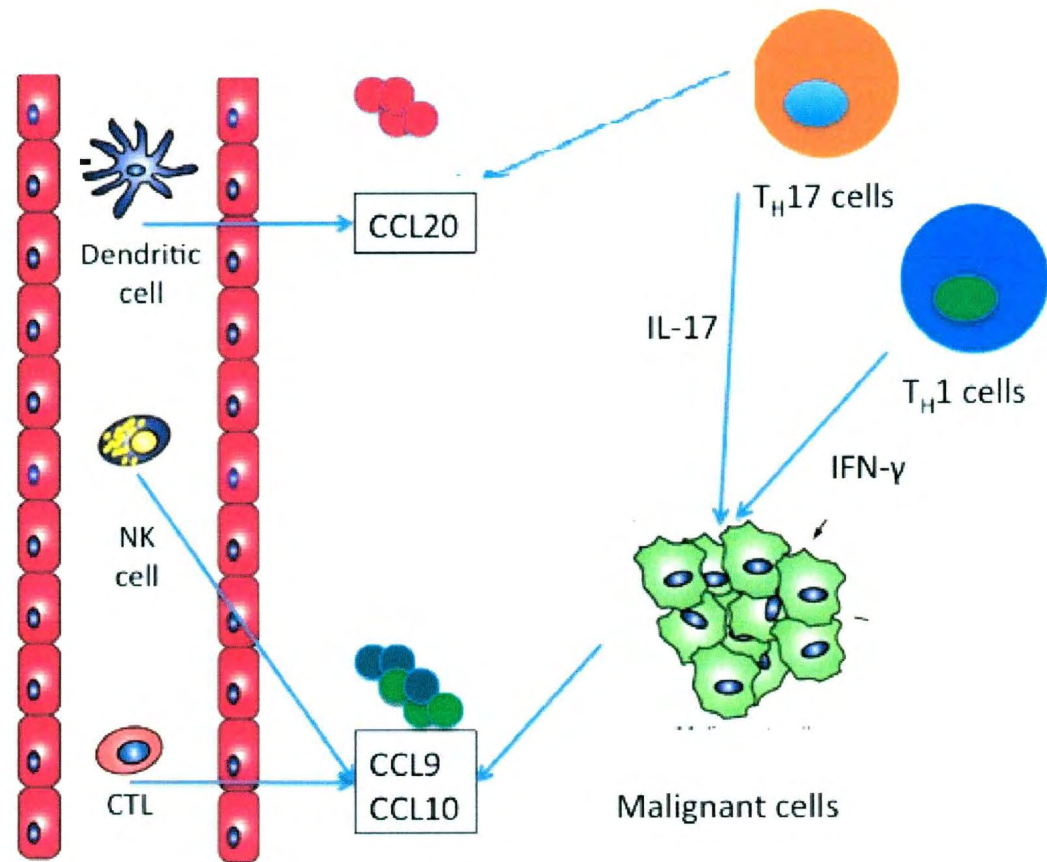


Figure 1.5. *Anti-tumor effects of T_H17 cells.* IL-17 and IFN- γ work together and stimulate tumor cells to release the chemokines CXCL9 and CXCL10, which recruit NK cells and CTLs to the tumor environment. This can lead to cytolytic killing of the tumor cells. T_H17 cells also release CCL20, a chemoattractant for dendritic cells. Dendritic cells take up tumor antigens and lead to an immune response against the tumor antigen. Adapted from Maniati et al 2010 (Maniati et al., 2010).

tumor growth as well. The exact mechanism by which inflammation promotes metastasis is unclear, but it is likely through the production of IL-17. IL-17 induces vascular endothelial growth factor (VEGF) secretion from endothelial, stromal and tumor cells. VEGF acts in an autocrine manner to promote secretion of TGF- β and IL-6. The combination of TGF- β and IL-6 forms a positive feedback loop, leading to more T_H17 cell differentiation. This could promote chronic inflammation leading to metastasis (Murugaiyan et al., 2009). IL-17 can support the production of several chemokines, CXCL1/CXCL2 and these chemokines recruit neutrophils. In the presence of IL-17, neutrophils secrete inflammatory proteinases, thereby contributing to promotion of inflammation in the tumor microenvironment. Furthermore, IL-17 promotes CXCL-8 production from stromal and epithelial cells. CXCL-8 promotes angiogenesis, which is the process of growing new blood vessels from existing blood vessels. By creating new blood vessels, angiogenesis allows nutrients and oxygen to reach a tumor mass, thereby facilitating growth (DeNardo et al., 2007; Maniati et al., 2010). Figure 1.6. summarizes the pro-tumor role of T_H17 cells. As the role of T_H17 cells as either mediators of tumor growth or suppression is controversial, the next section will summarize results from several clinical studies.

1.5. Studies of T_H17 Cells Within Tumor Microenvironments

The following Sections 1.5.1-1.5.2. review studies that have analyzed tumor infiltrating and peripheral populations of T_H17 cells in cancers that are associated with chronic inflammation (Section 1.5.1.) and hormones (Section 1.5.2.). Several cancers have been linked to chronic inflammation and understanding if T_H17 cells have a role in

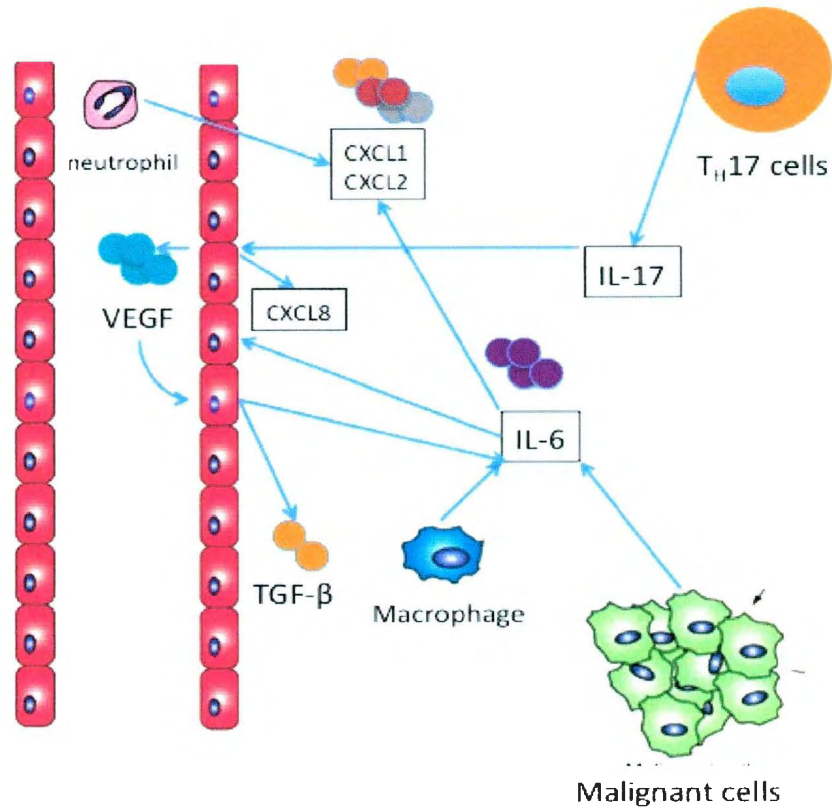


Figure 1.6. Pro-tumor effects of T_H17 cells. IL-17 can have direct effects on angiogenesis by acting upon endothelial cells and causing the secretion of VEGF. VEGF leads to the production of TGF- β and IL-6 from endothelial cells, which can act together to cause the differentiation of more naïve T cells into T_H17 cells. Malignant cells and tumor associated macrophages also secrete IL-6. IL-17 also promotes the secretion of CXCL1 and CXCL2 from the endothelial cells and these recruit neutrophils. Due to the IL-17 present in the tumor microenvironment, the neutrophils will produce inflammatory proteinases. This could produce a state of chronic inflammation and promote metastases of the tumor cells. Endothelial cells also secrete CXCL8 in the presence of IL-17 and CXCL8 can promote angiogenesis. Adapted from Maniati et al. 2010

such inflammatory cancers could provide new therapies. Furthermore, as breast cancer progression and treatment is strongly influenced by the hormones estrogen and progesterone, it is beneficial to analyze the role of T_H17 cells in other cancers influenced by steroid hormones.

1.5.1. T_H17 Cells in Cancers Associated with Chronic Inflammation

A substantial number of studies have supported the notion that chronic inflammation can predispose an individual to cancer. For example, there is association between chronic inflammatory bowel diseases and the increased risk of colon carcinoma (Ullman, et al. 2011). Gastric (Zhang et al., 2008; Maruyama et al., 2010), hepatocellular, (Zhang et al., 2006), colorectal (Liu et al., 2011), uterine cervical (Zhang et al., 2011) and lung cancers (Provinciali et al., 2011) have associations with chronic inflammation and studies have been conducted on these cancers to determine if associations with T_H17 cells and patient outcome exist.

1.5.1.1. T_H17 Cells in Gastric Cancer

Helicobacter pylori infection leads to the induction of chronic inflammation in the gastric mucosa. Changes in the gastric mucosa can lead to changes in gastric hormone release and disruption of neural pathways that contribute to the secretion of gastric acid. If gastric acid secretion is impaired or increased, the phenotype of gastritis may change. If the corpus atrophies, the secretion of essential substances, such as hydrochloric acid and pepsin, is impaired. When such atrophy occurs, these patients carry the highest risk for developing gastric cancer (Marteau et al., 2011). *Zhang et al.* (2008) analyzed

PBMCs, tumor draining lymph nodes and tumor tissue from 53 gastric cancer patients. Thirteen of the 53 patients had stage I gastric cancer, while the other 40 patients had more advanced stages. The *Zhang et al.* (2003) study observed an increase in PBMC population of T_H17 cells with disease progression. The population of T_H17 cells in the tumor draining lymph nodes also increased with disease progression. Although the number of patients in this study was small, they observed a positive correlation between the number of T_H17 cells in circulation and in tumor draining lymph nodes, and progression of gastric cancer, suggesting a potential pro-tumor role of T_H17 cells (Zhang et al., 2008).

A later study analyzed populations of tumor infiltrating lymphocytes (TILs) and PBMCs in 55 gastric cancer patients (Maruyama et al., 2010). Twenty-seven patients had stage I disease and 28 had advanced stage disease. Flow cytometric methods were employed to analyze the peripheral blood lymphocytes (PBLs) and IHC methods were used to analyze paraffin embedded tissue. Flow cytometry revealed that PBMC T_H17 cell frequency (identified by IL-17 positive/CD4 positive cells) was lower in advanced staged cancer than in comparable healthy donor PBMC. Upon stimulating isolated T_H17 cells from gastric cancer with anti-CD3 and anti-CD28, the cytokines IL-17, IL-21 and IL-23 were produced. IHC staining of tumor lesions revealed that T_H17 cells significantly decreased with progressing stages. This study further noted that the ratio of T_H17/T_{reg} cells was significantly higher in earlier stage disease and decreased with progressing stages. This study, in contrast to *Zhang et al* (2003), suggests that T_H17 cells did not have a pro-tumor role in gastric cancer as the populations decreased with advancing cancer (Maruyama et al., 2010). Since these two studies produced conflicting results and in both

studies only small numbers of patients were investigated, it is unclear whether T_H17 cells are beneficial or not to gastric cancer patients.

1.5.1.2. T_H17 Cells in Hepatocellular Carcinoma

Hepatocellular carcinoma (HCC) frequently develops in livers of patients infected with hepatotropic viruses (Hepatitis B virus (HBV) and Hepatitis C virus (HCV)), high levels of toxins (alcohol bi-products), or metabolic liver diseases. All of these conditions promote chronic inflammation within the liver (Alison et al., 2011). Zhang *et al.* (2006) characterized IL-17 producing cells in HCC and determined if the presence of these cells had prognostic value. To study the distribution of IL-17 producing cells, PBLs and TILs were collected and levels of IL-17 producing cells were determined by flow cytometry. TILs had the highest population of IL-17 producing cells. They also observed that 20-40% of tumor and non-tumor (from healthy donors) IL-17 producing cells were not CD4⁺ cells, suggesting another cell was producing IL-17. Next, Zhang *et al.* (2006) characterized tumor infiltrating T_H17 cells and observed that almost half of these cells could produce IFN- γ and IL-17 together. IL-17 producing cells in the PBLs population did not produce IFN- γ simultaneously with IL-17. This is suggestive of a functional or development relationship between T_H1 and T_H17 cells within hepatocellular tumor environments. IHC and confocal microscopy were used to visualize IL-17 producing cells within tumor environments. They observed that not all IL-17 producing cells were CD4⁺ cells, therefore confirming the flow cytometry data. The Zhang *et al.* (2006) also reported that CD4⁺ producing IL-17 cells expressed CD45RO, CCR4 and CCR6 but not CD62L or CCR7. These results are similar to the study by Kryczek *et al.* (2009) on

ovarian cancer, described in Section 1.5.2.1 (Kryczek et al., 2009). With regards to overall survival, patients with increased intratumoral levels of IL-17 had shorter overall survival (OS) and RFS. Based on the observations of this study, higher levels of T_H17/IL-17 producing cells appear to be a poor prognostic indicator for hepatocellular cancer patients (Zhang et al., 2009).

1.5.1.3. T_H17 Cells in Colorectal Cancer

As with the case of gastric cancer, chronic inflammation is also linked to the development of colorectal cancer (CRC). *Liu et al.* (2011) studied 52 patients with CRC stage III. CRC sections were stained for IL-17 using IHC techniques. Although non-tumor adenoma had positive IL-17 staining, the peritumor, and more so in the intratumor region, had more concentrated staining. Dual staining confocal microscopy showed that both CD4 cells (T_H17 cells) and CD68 (macrophages) cells were producing IL-17. IL-17 was found to be an independent predictor of overall survival, as high IL-17 levels had statistically significant lower 5-year survival and decreased RFS. Based on this study, it would appear that IL-17 negatively impacts patients with CRC (*Liu et al.*, 2011).

Another study by *Tosolini et al.* (2011) analyzed the balance between cytotoxic T cells and different subsets of helper T cells in 125 frozen colorectal tumor specimens. T_H17 cells were analyzed by mRNA levels of ROR γ c and IL-17A. Through real-time PCR, this study identified increased IL-17A in colorectal cancer tissues when compared to adjacent normal mucosa. Furthermore, upon defining three T_H17 categories (low,

heterogenous and high based on mRNA IL-17A and RORc levels), the T_H17^{hi} category corresponded to a poor overall survival. In particular, when analyzing T_H17 categories in relation to profiles developed for T_H1 , the T_H17^{hi}/T_H1^{lo} combination had the worst disease free survival determined by Kaplan-Meier ($p=0.005$). This study would suggest that T_H17 cells within a colorectal tumor environment have a negative impact on the patient, similar to the results found by *Liu et al. (2011)* and *Tosolini et al. (2011)*.

1.5.1.4. T_H17 Cells in Uterine Cervical Cancer

HPV is the most important etiological agent of cervical cancer. A report in 1999, cited as high as 93% of invasive cervical cancers contain replicating HPV (Walboomers et al., 1999). When a host is infected with HPV, the inflammatory response can promote lesion progression and affect potential tumor development by involving inflammatory channels and cells (Boccardo, 2010). *Zhang et al. (2011)* examined the expression of IL-17, FOXP3 and IL-10 in uterine cervical cancer (UCC), cervical intraepithelial neoplasia (CIN) and healthy donors PBL using flow cytometry and enzyme linked immunosorbent assays. IL-17 producing $CD4^+$ T cells were classified as T_H17 cells and $CD4^+CD25^+FOXP3^+$ cells were classified as T_{reg} cells. Levels of peripheral blood T_H17 cells were significantly increased in UCC and CIN patients as compared to healthy controls. T_H17 cell frequency also positively correlated with lymph node metastases and vaso-invasion. Similarly, T_{reg} cells were increased in untreated UCC patients as compared to CIN patients and healthy donors. This increase in T_{reg} cells was not observed in CIN or healthy donor peripheral blood. Up-regulation of both T_{reg} and T_H17 cells in UCC suggests that both cell types may be involved in the progression or

development of the disease. Moreover, the link between T_{H17} cells and metastases would suggest that T_{H17} are not beneficial to cervical cancer patients (Zhang et al., 2011).

1.5.1.5. T_{H17} Cells in Lung Cancer

Inhaling cigarette smoke, as well as chimney smoke and forest fire smoke, irritates the lung tissue and leads to an inflammatory response to eliminate the foreign toxin/chemical. If this response is repetitive, as in the case of addicted cigarette smokers, chronic inflammation develops within the lungs. The link between smoking cigarettes and cancer has been well established, but whether or not inflammatory cells, such as T_{H17} cells have a role in the promotion of cancer is less clear (Provinciali et al., 2011). *Koyama et al.* (2008) analyzed peripheral blood T cell populations in 35 small cell lung cancer (SCLC) patients, 8 long term survivors of SCLC and 19 healthy donors. Those patients that lacked detectable distant metastases and had tumors confined to hemithorax (half of the thorax) and mediastinum (non-delineated structures in the thorax) were defined as limited stage disease (LD) SCLC and those patients that had prominent distant metastases were referred to as extended stage disease ED- SCLC. Flow cytometric methods were used to isolate and analyze PBMCs. The overall percentages of $CD4^+$ T cells did not differ among healthy donors, LD-SCLC and ED-SCLC. However, $CD62L^{high}CD4^+$ T_{reg} cells were increased in ED-SCLC, as compared to healthy donors. $CD4^+$ T cells were sorted by flow cytometry and stimulated with anti-CD3 and cytokine production was analyzed. The study found that $CD62L^{low}CD4^+$ cells produced T_{H1} , T_{H2} and T_{H17} cytokines. Furthermore, IL-17A production was significantly up-regulated in LD-SCLC as compared to healthy donors and ED-SCLC. Based on these observations, IL-17

producing cells were increased in LD-SCLC and seemed to be beneficial to the patient (Koyama et al., 2008).

1.5.1.6. Summary of T_H17 Cells in Cancers with Associated Chronic Inflammation

The link between prevalence of inflammation and development of cancers in tissues is still being studied. However, based on the studies summarized in Section 1.5.1., increased frequency of T_H17 cells/IL-17 producing cells is often associated with decreased RFS, OS and poor prognostic indicators. The two gastric studies mentioned yielded conflicting results: the most recent by *Maruyama et al.* (2010), suggests that T_H17 cells slow cancer development and progression, whereas the *Zhang et al.* study (2008) suggested T_H17 cells have a pro-tumor role. In both HCC and CRC, increased levels of IL-17 correlate with decreased RFS and OS. Increased levels of T_H17 cells in UCC patients were associated with disease progression. However, in the case of small cell lung cancer, higher levels IL-17 producing cells in the peripheral blood seemed to associate with limited stage disease, a better prognosis than extended stage disease. It should be noted that a caveat of these studies is the small number of patients and studies examined. Furthermore, some studies focused on circulating T_H17 cells, rather than tumor infiltrating T_H17 cells, which may provide inaccurate representations of the tumor milieu. Yet, overall, there seems to be a trend for higher IL-17 levels or T_H17 cells to promote tumor growth in tissues that are frequently inflamed.

1.5.2. T_H17 Cells in Cancers Influenced by Hormones

As the development of cancer is influenced by inflammation, exposure to hormones, such as estrogen, progesterone and testosterone, may influence the growth of tumors. As ovarian, breast and prostate cancer cells frequently express hormone receptors, these cancer cells may proliferate due to exposure to hormones.

1.5.2.1 T_H17 Cells in Ovarian Cancer

As discussed in Section 1.2.1., breast cancer cells expressing ER and PR proliferate when exposed to either steroid hormone. Ovarian cancer cells multiply as a result of ER/PR as well (Ahmad and Kumar, 2011). In 2008, *Miyahara et al.* analyzed peripheral blood, ascitic fluid and tumor specimens from ovarian cancer patients for T_H17 type cytokines. The tumor environment contained the cytokine milieu necessary for the differentiation and expansion of T_H17 cells. Further, this study determined that T_H17 cell populations were increased in ovarian cancer tissue as compared to peripheral blood populations (Miyahara et al., 2008). Another study on ovarian cancer, conducted by *Kryczek et al.* (2009), analyzed the presence of T_H17 cells and their clinical significance in 201 ovarian cancer patients. This study focused on the characterization and evaluation of the distribution and phenotype of T_H17 cells in tumor environments. Similar levels of T_H17 cells were found in tumor draining lymph nodes of cancer patients, cancer patient peripheral blood and health donor peripheral blood. Evaluation of the phenotype revealed that tumor infiltrating T_H17 cells expressed CD4, CXCR4, CCR6, CD61, CD49c, CD49d and CD49e which suggest that T_H17 cells could migrate and be retained within a tumor microenvironment. HLA-DR, CD25, CCR2, CCR5 and CCR7 were not expressed by the

tumor infiltrating T_H17 cells. With respect to the cytokine profile of the tumor infiltrating T_H17 cells, significant amounts of IL-17, IFN- γ , TNF- α and IL-2 were found. This cytokine profile was observed in five other types of cancer studied: colon cancer, HCC, pancreatic cancer, melanoma and renal cancer (Kryczek et al., 2009). The Kryczek et al. study (2009) investigated the mechanism of induction of T_H17 cells within the ovarian cancer tumors. It was found that plasmacytoid dendritic cells (DCs) had minimal effect on T_H17 induction but tumor-associated macrophages (TAMs) and myeloid DCs could stimulate the induction of T_H17 cells from memory T cells, but not naïve T cells. The mechanism behind the induction of T_H17 cells by TAMs was thought to be through the production of IL-1 β , which is reported to play a role in expanding memory T cell populations into T_H17 (Kryczek et al., 2009). Further analysis revealed a correlation between higher levels of IL-17, CXCL9 and CXCL10 in ovarian cancer ascites. Both CXCL9 and CXCL10 are involved in T_H1 cell recruitment, suggesting T_H17 cells support an anti-tumor response. Lastly, Kryczek et al. (2009) found a significant relationship between improved patient outcome and T_H17 cells, which suggests that T_H17 cells are antagonizing the tumor, favoring the theory that T_H17 cells have an anti-tumor role (Kryczek et al., 2009).

A more recent study in 2012 investigated peripheral blood and epithelial ovarian cancer specimens from 44 patients undergoing cytoreductive surgery in Prague (Fialova et al., 2012). T_H17 lymphocytes (determined through flow cytometry, based on presence of IL-17A) were detected in 100% of the ovarian tumor samples and the proportion of T_H17 cells within the CD4⁺ T cell subset was higher in patients with limited stage disease. The frequency of T_H17 cells within the peripheral blood was not predictive of the number

of T_H17 cells within the tumor (Fialova et al., 2012). Therefore, this recent study seems to support the findings of *Kryczek et al.* (2009): that T_H17 cells may have an anti-tumor role in ovarian cancer.

1.5.2.2. T_H17 cells in Prostate Cancer Patients

Sfanos et al. (2008) studied prostate infiltrating lymphocytes (PIL) in 20 patients with prostate cancer. CD4⁺ T cells were isolated from the PILs and analyzed by flow cytometry to determine the frequencies of T cell subsets present. Upon stimulation of CD4⁺ T cells with phorbol 12-myristate 13-acetate (PMA) and ionomycin, a significant skewing towards T_H17 cells (IL-17 producing/CD4⁺ T cells) in the PIL population was observed. They suggest the frequency of T_H17 cells in the PIL may be due to the presence of both TGF- β and IL-6 in the tumor. *Sfanos et al.* (2008) also noted that there was an inverse relationship among T_{reg} and T_H17 cells, ie. when T_H17 cells were present in higher relative amounts, there were less T_{reg} cells present. With respect to T_H17 cell population and prognostic indicators, there was an inverse relationship between T_H17 cells skewing and Gleason tumor grade, suggesting a potential anti-tumor role for T_H17 cells (*Sfanos et al.*, 2008).

1.5.2.3. T_H17 cells in Breast Carcinoma Patients

The effect of estrogen and progesterone on breast cancer cells has been previously discussed in Section 1.2.1. *Horlock et al.* (2009) studied the effects of trastuzumab on T_H17 cell and T_{reg} cell populations in the peripheral blood of 34 breast cancer patients, 27 of which were HER2⁺. Peripheral blood from healthy donors was used as a control.

Patients with HER2⁺ breast cancer were treated with trastuzumab and samples were taken before, during and after treatment. T_{reg} cells, identified by FOXP3 and CD25, were significantly higher in breast cancer patients, regardless of HER2 status in comparison to healthy controls. There was no significant difference in T_{reg} frequency between HER2⁺ and HER2^{neg} patients. Following treatment of HER2⁺ patients with trastuzumab, the T_{reg} population in the peripheral blood decreased. This observation suggests that T_{reg} cells aid in tumor progression as treatment reduces their numbers. With respect to T_H17 cells, healthy donors and HER^{neg} patients had similar numbers of T_H17 cells. However, HER2⁺ patients had increased peripheral T_H17 cells in comparison to HER2^{neg} and healthy donors. Following treatment of HER2⁺ patients with trastuzumab, the levels of T_H17 cells increased. Furthermore, analyze of the ratio of T_{reg}:T_H17 cells in peripheral blood revealed that HER2⁺ patients had a significantly higher ratio than HER2^{neg} patients and healthy controls. There was no significant difference in the ratio between HER2^{neg} patients and healthy controls. This study suggests an anti-tumor role for T_H17 cells and supports the concept that T_H17 cells and T_{reg} cells are inversely related (Horlock, et al. 2009).

In 2012, *Yang et al.* (2012) studied 30 breast cancer patients. In particular, they analyzed the TIL population for T_H17 cells. It was found that there were increased IL-17 positive cells in cancerous tissue as compared to normal breast tissue (both evaluated by flow cytometry and IHC methods). The frequency of T_H17 cells was also proportional to the amount of IL-6, TGF- β and IL-1 β in the tumor sample. When *Yang et al.* (2012) compared the frequency of T_H17 cells to prognostic indicators, there were negative associations between TNM stage, blood vessel invasion and increased numbers of

metastatic lymph nodes. However, there was no correlation with the frequency of T_{reg} cells. Therefore, Yang's study supports the notion that T_H17 cells have an anti-tumor role (Yang et al., 2012).

1.5.2.4. Summary of T_H17 Cells in Cancers Influenced by Hormones

In each of the hormonal cancers discussed, T_H17 cells were associated with improved outcomes and prognoses, suggesting T_H17 cells have an anti-tumor role in these hormonally influenced cancers.

The previous Sections 1.5.1 and 1.5.2, chronicled studies of T_H17 cells within tumor microenvironments. However, due to the outcomes of these studies, it is difficult to deduce the role of T_H17 cells within tumor microenvironments. It is quite possible that T_H17 cells cannot be generalized as either pro-tumor or anti-tumor but the role of T_H17 cells is dependent upon the cancer type, location, stage of cancer and whether or not chronic inflammation or hormones influence the cancer.

1.6. Hypothesis and Objectives

A previous study in Dr. Drover's laboratory reported that high levels of IFN- γ transcripts in breast tumor tissues associated with increased survival in patients (Oldford et al., 2006), whereas high IL-6 levels and carriage of HLA-DR52 were associated with large tumors and decreased survival (Oldford, unpublished data). Since IL-6 is a proinflammatory cytokine that is required for the differentiation of naïve $CD4^+$ T cells into proinflammatory T_H17 cells, we hypothesized an association between high intratumoral IL-6 and HLA-DR52 haplotypes with increased $CD4^+$ T_H17 cells. We further

hypothesized that if a T_H17 profile significantly associated with IL-6 and HLA-DR52, it would also associate with a poor prognosis and outcome.

Stemming from this hypothesis, we developed the following objectives:

Objectives:

1. The first objective was to analyze a panel of breast cancer cell lines (BCCLs) for expression of T_H17 associated markers (IL-17 and RORc2) as well as IL-6 and TGF- β and FOXP3. FOXP3 and TGF- β had previously been reported in established BCCLs (Karanikas et al., 2008). If BCCLs expressed T_H17 associated transcripts, it would suggest the possibility that tumor cells in the breast cancer tissues also produce T_H17 associated transcripts, and raise serious concerns that a T_H17 profile based on IL-17 and RORc2 transcripts could produce false positive results.
2. The second objective was to determine the levels of T_H17 associated transcripts (IL-17 and RORc2) by real time RT-PCR and/or by immunohistochemistry in the breast cancer tissues and to use these values to derive a T_H17 profile. Since T_H17 cells are derived primarily from CD4⁺ T cells, we expected that a meaningful T_H17 marker should be positively associated with increased numbers of infiltrating CD4⁺ T cells.
3. The third objective was to statistically analyze whether a derived T_H17 profile or associated markers: i) correlated with levels of IL-6 transcripts; ii) associated with HLA-DR52 haplotypes; and iii) associated with poor prognosis, increased recurrence and decreased survival. With respect to prognostic indicators, I was to determine if transcript level of IL-17 and RORc2 corresponded to ER/PR status, HER2/neu status, tumor grade, lymph node positive patients and age at diagnoses. As these are

prognostic indicators, an association between T_H17 cell markers and these indicators may shed light on new potential therapies for breast cancer.

Chapter 2: Materials and Methods

2.1. Breast Tumor Samples

Breast cancer tissue samples were obtained from the Manitoba Breast Tumor Band (MBTB) (Winnipeg, Manitoba, Canada), with approval from the local Human Investigation Committee. Information on tumor levels or ER and PR, age at diagnosis, clinicopathological parameters and follow-up information were provided by the MBTB. In the initial study (Oldford et al., 2006), frozen-tissue sections from 99 primary tumors were analyzed by IHC for tumor cell expression of HLA-DR, HLA-DM and Ii; T cell infiltrates (CD3, CD4 and CD8); B cell infiltrates (CD20) and infiltrating macrophages/dendritic cells (CD68). Eighty-nine tissues were further analyzed by IHC for over expression of HER2/neu. Cytokine profiling (IFN- γ , IL-1 β , IL-2, IL-4, IL-6, IL-10, TGF- β and TNF- α transcripts) and FOXP3 transcripts were done on cloned DNA (cDNA) prepared from RNA extracted from frozen tissue sections and stored at -80°C. Detailed results of this study are available in Dr. Oldford's doctoral thesis (2006) and have been published in part (Oldford et al, 2006). As part of the ongoing investigation formalin-fixed paraffin-embedded tissues from 40 patients were analyzed by IHC for dual-stained CD25⁺FOXP3⁺ T_{reg} cells (Oldford, unpublished data).

Sixty-five of the original RNA samples (from 65 patients), stored at -80°C, were available for this study, which focuses on T_H17 profiling as described in Section 1.3.5. Table 2.1A provides a numerical breakdown of the samples with respect to clinicopathologic factors, ER and PR status and age at diagnosis and leukocyte infiltrates. Table 2.1B contains a comparison of the distribution of HLA haplotypes. Table 2.1C

provides a comparison of the leukocyte cell surface markers. To ensure that the 65 samples were representative of the initial 99 samples, we compared the distribution of the relevant parameters in the original set to those in the subset of samples used in this study, the T_H17 subset (Table 2.1A, Table 2.1B and Table 2.1C).

Table 2.1A. Comparison of the distribution of clinical and pathological features between the T_H17 subset and the original set.

Prognostic Factor	Original Set		T _H 17 Subset		P-value ^a
	Count	%	Count	%	
<i>Tumor Size</i>					
≤ 2 cm	24	25	14	25.9	NS
> 2 cm	72	75	40	74.1	
<i>Tumor Type</i>					
IDC	80	83.3	46	85.2	NS
Others	16	16.7	8	14.8	
<i>Histological grade</i>					
Grade IV – V	12	13.2	6	11.5	NS
Grade VI – VII	44	48.4	27	51.9	
Grade VIII - IX	35	38.5	19	36.5	
<i>Clinical Node Status</i>					
Negative	45	45.9	23	42.6	NS
Positive	53	54.1	31	57.4	
<i>Estrogen Receptor^b</i>					
ER ^{-ve}	43	43.4	18	32.7	0.016*
ER ^{+ve}	56	56.6	37	67.3	
<i>Progesterone Receptor^b</i>					
PR ^{-ve}	34	34.3	15	27.3	NS
PR ^{+ve}	65	65.7	40	72.7	
<i>HER2/Neu</i>					
Codes 0-2	70	78.7	39	81.3	NS
Code 3	19	21.3	9	18.8	
<i>Age of Diagnosis</i>					
Mean	58.76		59.98		NS
Median	60		62		NS

*There was a significant difference between the ER status between the two cohorts.

a. Pearson Chi Square

b. Determined by ligand binding assays. Negative status was defined as ER or PR < 10 fmol/mg. Positive status was defined as ER or PR ≥ 10fmol/mg

Table 2.1B. Comparison of the distribution of HLA haplotypes between the T_H17 subset and the original set

Prognostic Factor	Original Set		T _H 17 Subset		P-value ^a
	Count	%	Count	%	
<i>DR52</i>					
<i>DR52</i> ^{-ve}	50	50.5	25	45.5	NS
<i>DR52</i> ^{+ve}	49	49.5	30	54.5	
<i>DR52DQ2</i>					
<i>DR52DQ2</i> ^{-ve}	84	84.8	46	83.6	NS
<i>DR52DQ2</i> ^{+ve}	15	15.2	9	16.4	
<i>DR52DQ6</i>					
<i>DR52DQ6</i> ^{-ve}	79	79.8	42	76.4	NS
<i>DR52DQ6</i> ^{+ve}	20	20.2	13	23.6	
<i>DR52DQ7</i>					
<i>DR52DQ7</i> ^{-ve}	77	77.8	42	76.4	NS
<i>DR52DQ7</i> ^{+ve}	22	22.2	13	23.6	

a. Pearson Chi Square

Table 2.1C. Comparison of the distribution of leukocyte infiltrates between the T_H17 subset and the original set

Prognostic Factor	Original Set		T _H 17 Subset		P-value ^a
	Count	%	Count	%	
<i>CD3 Infiltrate</i>					
None-Small*	41	41.4	23	41.8	NS
Moderate-Large**	58	56.8	32	56.2	
<i>CD4 Infiltrate</i>					
None-Small*	51	52.6	28	52.8	NS
Moderate-Large**	46	47.4	25	47.2	
<i>CD8 Infiltrate</i>					
None-Small*	55	56.7	33	62.3	NS
Moderate-Large**	42	43.3	20	37.7	
<i>CD68 Infiltrate</i>					
None-Small*	8	8.1	3	5.5	NS
Moderate-Large**	91	91.9	52	94.5	

a. Pearson Chi Square

* Staining was positive for no or few scattered cells with small aggregate staining

** Staining was positive for moderate to large number of cells with several small to large aggregate staining patterns

The only significant difference between the two investigations was that the ER⁺ cases were increased in the T_H17 study in comparison to the original study.

2.2. Cell Lines

Prior to analyzing the cDNA from breast tumor samples, a panel of BCCLs was analyzed by RT-PCR and real time-PCR for mRNA expression of IL-17, TGF- β , IL-6, RORc2, FOXP3, and glyceraldehyde-3-phosphatase dehydrogenase (GAPDH). Eight BCCLs, initially obtained from American Type Culture Collection (ATCC), were analyzed by single nucleotide polymorphism (SNP) assays to ensure these lines were not contaminated by other cells (Allison Edgecombe's thesis, 2002). The cell lines were MDA-MB-435, T-47D, MDA-MB-231, MCF-7, Hs 578T, MDA-MB-468, BT-474 and SK-BR-3. The characteristics of the BCCLs are shown in Table 2.2 (Edgecombe, 2002).

Table 2.2. Breast Cancer Cell Lines

BCCL	ATTC Identification*	Morphology	Description	ER status**	PR status**
MDA-MB-435	HTB-129	Spindle-shape	Ductal carcinoma	-	-
T-47D	HTB-133	Epithelial	Ductal carcinoma	+	+
MDA-MB 231	HTB-26	Epithelial	Adeno-carcinoma	-	-
MCF-7	HTB-22	Epithelial	Adeno-carcinoma	+	+
SK-BR-3	HTB-30	Epithelial	Adeno-carcinoma	-	-
Hs 578T	HTB-126	Epithelial	Ductal carcinoma	-	-
MDA-MB-468	HTB-132	Epithelial	Adeno-carcinoma	-	-
BT-474	HTB-20	Epithelial	Ductal carcinoma	+	+

*American Type Culture Collection (ATCC) (Manassas, VA)

** (Subik, et al., 2010; Lacroix, et al. 2004)

To determine the relative expression of transcripts by the BCCLs and the breast tumor samples, cDNA from control cells, known to express relevant cytokine transcripts,

were chosen. These included C10/MJ for IL-6, TCL-6D for FOXP3, Jurkat for TGF- β and human PBLs for IL-17 and RORc2. C10/MJ (Obtained from Dr. Michael Grant, original source: AIDS Research and Reference Reagent Program, Division of AIDS, NIAID, NIH: C10/MJ from Dr. Dean Mann and Dr. Miklaus Popovi), TCL-6D (provided by Dr. William Marshall) and Jurkat (original source: ATCC TIB-152) were available in the Drover lab. PBLs were isolated from whole blood using the Ficoll-Hypaque method (English and Andersen, 1974) and placed in RPMI 1640 media (Gibco) at a concentration of 2×10^6 cells/mL. The PBLs were subsequently stimulated with phytohemagglutinin (PHA (MP Biomedicals, Soron, Ohio) at a concentration of 5 μ g/ml and incubated for 12-18 hours at 37°C in 10% CO₂. Following the incubation period, the cells were collected, washed and RNA was extracted from the cells (Section 2.3.)

2.3. RNA Extraction and Determination of RNA Integrity

RNA was extracted from the BCCLs and the positive control cells using the Trizol reagent (Gibco BRL, Rockville, MD), followed by treatment with DNase Free reagent (Ambion, Austin, TX) to remove contaminating DNA.

RNA had previously been isolated from the breast tumor tissues by homogenization using Trizol reagent, followed by treatment with DNase Free reagent and stored at -80°C. Prior to cDNA preparation and PCR analyses, RNA quality was analyzed using an Agilent 2100 Bioanalyzer (Agilent Technologies, Ontario, Canada). If the RNA was too degraded, the results obtained from PCR analysis may not be an accurate representation of mRNA expression. Briefly, RNA integrity was tested using RNA Nano kits (Agilent Technologies, Ontario, Canada). The RNA sample undergoes

electrophoresis and an electropherogram is then constructed. A RNA integrity number (RIN) is assigned based upon an algorithm. If the RNA is intact, the RIN value can be as high as 10. Degraded RNA is considered to have RIN value less than 5. Based upon results presented by *Fleige and Pfaffl* (2006), we assigned the threshold of acceptable RIN values to be 5. They noted that variability among real-time PCR assays increased with RNA that was considered degraded (RIN = 1-3) in comparison to RNA that was highly intact (RNA = 8-10) (*Fleige and Pfaffl*, 2006). Therefore, we assigned our cutoff to be 5. We found that 49 of the 65 available RNA samples had RIN values equal to or greater than 5. To avoid additional freezing and thawing of the RNA, cDNA was made for all 65 RNA samples at the same time as the samples were analyzed by the Bioanalyzer.

cDNA was transcribed from the extracted RNA using the first strand cDNA synthesis kit (Fermentas, Thermo Fisher Scientific, Canada), according to the manufacturer's instructions. 1 µg of RNA was transcribed into 20 µL of cDNA, which provided the template for primers in RT-PCR and real-time PCR assays.

2.4. Standard Reverse Transcriptase Polymerase Chain Reaction

RT-PCR was done using a Biometra T Gradient thermocycler (Montreal Biotech Inc., Quebec, Canada). Primers for IL-17 and GAPDH were purchased from Gibco (GIBCO, Invitrogen, California, US) and primers for IL-6, TGF-β and FOXP3 were from Invitrogen (Carlsbad, California, US). Sequences for the primers and expected base pair product size are listed in Table 2.3A. The IL-17 primer was designed using PrimerBlast

(National Center for Biotechnology Institute, Pubmed, US) and the National Center for Biotechnology Information (NCBI) reference sequence numbers are given in Table 2.3B.

Table 2.3A. Primer sequences for RT – PCR

Gene	Forward 5' to 3'	Reverse 5' to 3'	Predicted base pair size of amplicon
IL-17A	GGA ATC TCC ACC GCA ATG AG	ACA CCA GTA TCT TCT CCA GCC	201
GAPDH	TGA CCT TGC CCA CAG CCT TG	CAT CAC CAT CTT CCA GGA GCG	443
IL-6	AGC TCA GCT ATG AAC TCC TTC TC	GTC TCC TCA TTG AAT CCA GAT TGG	338
FOXP3	CAG CTG CCC ACA CTG CCC CTA G	CAT TTG CCA GCA GTG GGT AG	382
TGF- β	GCC CTG GAC ACC AAC TAT TGC	AGG CTC CAA ATG TAG GGG CAG GG	160

Table 2.3B. NCBI Reference Sequences for RT – PCR primers

Primer	Reference Sequence
IL-17A	NM_002190.2
GAPDH	NM_001256799.1
IL-6	NM_000600.3
FOXP3	NM_014009.3
TGF- β	NM_000660.4

All PCR reactions were performed in a volume of 50 μ L with 200mM of dNTPs (Invitrogen, California) and 1 μ L of cDNA. Samples containing ultrapure distilled water (molecular water) (GIBCO) instead of cDNA were included as contamination controls. cDNA from cell lines C10/MJ, Jurkat, TCL-6D and PBLs, from a healthy donor (HLA 04), stimulated with PHA, were used as positive controls as described in Section 2.2. GAPDH was used as the endogenous housekeeping control. Primers were used at concentrations of 20 pM for IL-17 and GAPDH and 10 pM for IL-6 and TGF- β . The optimal primer concentration was determined by running parallel reaction mixtures using

different concentration of primers. If the primer concentration was too high, primer dimers and non-specific binding could occur. Alternatively, if the primer concentration was too low, insufficient specific template binding could occur, thereby lowering the PCR product. The optimal concentration of MgCl₂ (Invitrogen) was determined to be 2.0 mM for all reactions; 0.2 µL of Taq DNA polymerase (Invitrogen) was used for all reactions.

All reaction mixtures were denatured at 94°C for 1 minute. The optimal annealing temperature was determined using a temperature gradient. As noted previously, the melting points of the primers were determined using the program Primer BLAST (Pubmed) and a temperature gradient was chosen based upon the melting temperature. Optimal annealing temperature is normally within 5°C of the melting temperature of the primer (PCR Amplification, 2012). The denaturation and extension steps remained the same during the gradient and the number of cycles was consistent at 35. The extension step of the PCR was 72°C for 1 minute for all the primers, except for GAPDH (3 minutes). The optimal cycle number for each primer set was also determined to avoid over or under amplification of the desired transcript. Section 3.2. provides the results of determining the annealing temperature and cycle number.

Following the amplification cycling, PCR products were loaded on three 1.5% agarose gel (prepared with agarose dissolved in 45 mM Tris-borate 1mM EDTA (TBE) containing ethidium bromide (2 µL) and visualized using UV light in a Kodak Imager. The base pair size of the PCR product was estimated by comparison to a 100 base pair ladder (Fermentis, Thermo Fischer Scientific, Canada). Using Kodak Molecular Imaging Software V.4.0.0. (Kodak, St. Rochester, New York), the density of the bands were determined and the intensity of the bands was expressed as a relative quantity using the

following formula: ((target gene in sample)/(GAPDH in sample)) ÷ ((target gene in positive control)/(GAPDH in positive control)).

2.5. Real Time Polymerase Chain Reaction

Real time PCR was performed using a StepOne Real Time PCR System and Software (Applied Biosystems, Life Technologies, Carlsbad, California).

IL-17, RORc2, and GAPDH transcripts were analyzed in the 65 breast tumor samples (from 65 patients). TaqMAN® Gene Expression Assays for GAPDH (Hs99999905_m1) and IL-17 (HS00174383_m1) were available from Applied Biosystems whereas the RORc2 assay was custom designed (Olivito et al., 2009). The sequences of RORc2 specific primers are given in Table 2.4.

Table 2.4: Real time PCR RORc2 primer sequences

Target transcript	Forward Primer	Reverse Primer	Probe (FAM)
RORc2	5'-GAA GGA CAG GGA GCC AAG GC-3'	5'- CTT GTC CCC ACA GAT TTT GCA-3'	5' – TCA GTC ATG AGA ACA CAA ATT GAA GTG ATC CC -3'

For all assays, the reporter dye was FAM™, a fluorescent dye, at the 5' end of the TaqMAN® minor groove binder (MGB) probe. A nonfluorescent quencher was at the 3' end of the probe. The TaqMAN® MGB probes and primers were premixed in a 20X solution. The concentration of the primers and probes were 18 µM and 5 µM, respectively. TaqMAN Gene Expression Master mix (Applied Biosystems) was for PCR application. The premade master mix contains Amplitaq® Gold DNA Polymerase

Ultra-Pure, Uracil DNA glycosylase, dNTPs, ROX™ Passive Reference and buffer components.

The PCR mixtures were 20 μ L in total. There was 10 μ L of TaqMan Gene Expression Master Mix, 1 μ L of specific primer/probe, 1 μ L of cDNA and 8 μ L of molecular water. The optimal concentration of cDNA added to each reaction was determined through serial dilution assays described in Section 3.5. The conditions of the thermal cooling and heating cycles were uniform for all 4 transcripts analyzed and are given in Table 2.5.

Table 2.5: Real time PCR amplification conditions

Amplification	Time
Step 1: 50°C	2 minutes
Step 2: 95°C	10 minutes
Step 3: 95°C 60°C	15 seconds 1 minute repeat for 40 cycles

Each sample was tested in triplicate to ensure accuracy and real-time analysis of IL-17 was done on two separate occasions. The data were analyzed using the formula $2^{-\Delta\Delta C_t}$ and expressed as a fold-increase. The C_t is the relative measure of the concentration of a target in the PCR reaction. The C_t is also inversely proportional to the amount of target nucleic acid in the sample. The relative quantity of the target gene is expressed in terms of comparative relative quantity. The two separate genes, such as RORc2 or IL-17 and the endogenous control, GAPDH, were amplified in separate tubes. The C_t for each sample was determined by the StepOne program and the C_t for the endogenous control was subtracted from the C_t of the gene of interest (ΔC_t). Each ΔC_t was subtracted from the ΔC_t that was the largest ($\Delta\Delta C_t$). This number is then used as an exponent of 2.

Therefore, the formula used to calculate the relative quantity is $2^{-\Delta\Delta C_t}$. The average and standard deviation was calculated.

2.6. Immunohistochemistry

The prior Sections 2.3 – 2.5 described methods to determine transcript levels in the RNA extracted from bulk tumors obtained from the MBTB. To confirm and validate results obtained by PCR, we planned to assess relevant protein expression using IHC. Sections from 40 tumor blocks (from 40 unique patients), that had been formalin-fixed and paraffin-embedded (FFPE), were obtained from MBTB and we planned to test these tumors blocks by IHC for T_H17 associated markers.

Dual staining methods had been previously carried out to identify CD25⁺FOXP3⁺ T cells on a set of the sections from the same FFPE tissue blocks. The cytoplasm was stained with CD25 antibody (Vector, Burlingame, CA) and the nucleus was stained using FOXP3 antibody (Abcam, Cambridge, MA). A similar procedure was conducted for this work, using antibodies for RORc (Imagnex, San Diego, CA) and FOXP3 to stain the nucleus and antibodies for IL-17 (Santa Cruz, Santa Cruz, CA) or CD3 (Abcam) to stain the cytoplasm. Two antibodies for RORc were optimized (Imagnex, IMG6013A and IMG71896). FOXP3 and CD3 were the nuclear and cytoplasmic positive controls. Additionally, HER2 (Dako, Agilent Technologies) antibody (2 µg/mL) was used as a control to ensure that the secondary antibody, anti-rabbit, was working properly. This antibody had been optimized in our laboratory previously (Drover, unpublished data). Mouse and Rabbit immunoglobulins (Vector) were used for the negative controls using dilutions that matched the primary antibody used. However, there were problems

encountered in the optimization phase and dual staining of the FFPE tissue blocks did not occur. Section 3.8. describes the optimization results.

2.6.1. Preparation of IHC slides

Prior to staining the FFPE sections, antigen retrieval and staining conditions were optimized. Positive control tissues for RORc and IL-17 were thymus and tonsil slides, respectively. Paraffin was removed by soaking the slides in xylene for 10 minutes twice. This was followed by rehydration in 100% ethanol for 30 seconds 3 times, then 95% ethanol for 30 seconds twice and 70% ethanol once. The slides were then placed in deionized water for 5 minutes and the water was circulated using a magnetic stir bar.

2.6.2. Antigen Retrieval

The next step involved antigen retrieval which is necessary because during the fixation process, antigenic epitopes are frequently lost due to cross-linking of proteins by formalin. Sodium citrate buffer, 0.01M solution, was made by dissolving 0.588 grams of sodium citrate (Fisher Scientific Company, New Jersey, USA) in 200 mL of deionized water. The pH of the solution was adjusted to 6 using concentrated hydrochloric acid (Fisher Scientific Company). During antigen retrieval, the slides being prepared for CD3, IL-17 and RORc staining were placed in a canister containing the sodium citrate buffer and steamed in a hot water bath at 100°C. The time required for antigen retrieval of the CD3, IL-17 and RORc epitopes was 20 minutes, 60 minutes and 60 minutes, respectively. Slides being prepared for FOXP3 staining were placed in a canister containing cell conditioning buffer, CC1 (Vector) (pH=8) and steamed in a hot water bath at 100 °C for

60 minutes. The slides were then left to cool for 20 minutes and followed by washing using a 1% phosphate buffered saline (PBS) solution and Tween (Fisher Scientific Company) solution. Each PBS/Tween washing step consisted of three five minute washes in PBS/Tween.

2.6.3. Antibody Staining

Prior to addition of the primary antibody, non-specific binding was prevented by applying two drops of Normal Horse Serum (NHS) (Vector Labs) to the slides for 30 minutes in a humidified environment at room temperature. Following removal of the NHS, the primary antibody was optimally diluted in Ventana Antibody Diluent (VAD) Buffer (Ventana, Tucson, AZ). An optimal concentration range for each antibody was provided from the company to determine the concentration which gave the best signal to background staining. Optimal concentrations of the primary antibodies and conditions are given in Table 2.6.

Table 2.6: Primary antibody application conditions

Antibody	Concentration	Time period	Temperature
RORc (IMG6013A)	15 µg/mL	45 minutes	Room temperature
RORc (IMG71896)	20 µg/mL	60 minutes	Room temperature
FOXP3	5 µg/mL	120 minutes	Room temperature
IL-17	0.5 µg/mL	Overnight	4 °C
CD3	6/100 µL	60 minutes	Room temperature

The primary antibody was removed from the slides using three 0.1M PBS / 0.1% Tween washes. Next, 100 µL of 0.3% hydrogen peroxide was applied to the slides for 10

minutes at room temperature, followed by three PBS/Tween washes. The H₂O₂ blocks endogenous peroxidases within the section to prevent false staining.

The secondary antibody was then added using two drops of anti-mouse (Vector) and anti-rabbit (Vector) for CD3/FOXP3 and IL-17/RORc, respectively. After the 30 minute incubation the antibodies were removed followed by washing three times in PBS/Tween. Vector diaminobenzidine (DAB) or Vector SG Blue were used as the substrate and incubation times varied between 5 – 15 minutes at room temperature, followed by a wash in deionized water.

Dual staining of slides follows the same procedure of antigen retrieval, blocking, addition of the second primary antibody followed by secondary antibody application and staining. Generally for dual staining, SG blue was used for cytoplasmic staining and DAB was used for nuclear staining.

2.6.4. Dehydration and Mounting

After washing the sections were next dehydrated and mounted which consisted of soaking in 70% ethanol for 1 minute, 2 changes of 95% ethanol for 1 minute, 3 changes of 100% ethanol for 1 minute and 2 changes of xylene for 2 minutes. The slides were then mounted, dried and examined using light microscopy.

2.6.5. Breast tumor sample IHC

Although resources were used to optimize the conditions for the IL-17 and RORc IHC antibodies, a high degree of uncertainty remained due to granular staining patterns and high background for both antibodies. We had confidence in our methods as the dual

staining was successful for CD3 and FOXP3. Furthermore, both RORc antibodies were not specific for RORc2 and an antibody designed for just RORc2 did not exist. Therefore, subsequent experimentation on the 40 breast tumors was not carried out. Section 3.8. provides the results of the experiments conducted.

2.7. Statistical Analysis

Analysis was performed using SPSS Version 19 Statistical Software. Contingency tables were analyzed using Person's chi-square. Non-parametric Mann Whitney U or Kruskal-Wallis H test were used to assess statistical significance of continuous variables, with the exception of age at diagnosis, which was normally distributed and assessed by one way analysis of variance (ANOVA).

Survival estimates were calculated using Kaplan-Meier method with log-rank statistic. Ninety-five percent confidence intervals (95% CI) around each estimate were calculated using the standard error (SE) of cumulative survival probability (95% CI = cumulative survival probability \pm 1.96 x SE). Estimates were calculated as time to distant metastasis for distant RFS. No patients were lost to follow up and patients without recurrence were censored at the time of last follow up or at 5 years for 5-year survival. For survival analysis, normalized cytokine and transcript factor units were stratified into high and low categories (the high category refers to values that were greater than the median of the data collected).

Chapter 3: Results

3.1. Optimization of RT-PCR Conditions

Optimal conditions for the RT-PCR amplification with primers used in this study were determined. The following subsections of Section 3.1. describe the optimization procedures and results.

3.1.1. Optimal RT-PCR Annealing Temperatures

The primers are described in Section 2.4. For each primer, an initial RT-PCR experiment was conducted to determine the optimal annealing temperature. The annealing temperature gradient was chosen based on the melting temperatures of the primers. Generally, temperatures $\pm 5^{\circ}\text{C}$ of the melting temperature of the primer were included in the temperature gradient. The conditions for denaturation and extension remained constant for the annealing temperature gradient experiments, i.e. 94°C for 1 minute for denaturation and 72°C for 1 minute for extension. Figure 3.1. shows a representative gel of the annealing temperature gradient for the IL-17 primer set. The PCR products were loaded in a 1.5% agarose gel, viewed under UV light and digitized (see Section 2.4 for a more in depth description). 61.6°C was chosen as the optimal annealing temperature for IL-17 primers based on a comparison of the density of the amplicon bands.

The optimal annealing temperatures for the other primers used in this study were determined using the same method. Table 3.1. shows a list of the primers and the associated annealing temperature.

Table 3.1. Annealing temperatures and times of RT-PCR Primers

Primer	Annealing Temperature (°C)	Annealing time
IL-17	61.6	60 seconds
IL-6	64	60 seconds
TGF- β	65	60 seconds
FOXP3	65	60 seconds

The denaturation and extension temperatures for all primers were 94°C and 72°C, respectively. The time required for denaturation was 60 seconds for all the primers. The extension step was 60 seconds for all the primers, except for GAPDH (180 seconds, previously determined in the Drover laboratory).

3.1.2. Optimal RT-PCR Amplification Cycle Number

If transcripts were under-amplified, the target transcript would appear to be present in lower amounts, leading to false negatives. Conversely, over-amplification would result in cDNA samples appearing to have higher amounts of target transcript and lead to positive results that could not be quantified. We, therefore, performed preliminary experiments to determine the optimal RT-PCR amplification number for each primer pair.

3.1.2.1. Determination of Optimal RT-PCR Amplification Cycle for IL-17

The transcript IL-17 was amplified over even cycles between 22-38. Figure 3.2A shows a representative gel of the amplification of the IL-17 transcript over the cycle range. The bands, from three separate gels, were digitized and the mean band density is plotted in Figure 3.2B. The results of the PCR assay were as expected with amplification occurring over an exponential phase followed by a linear (plateau) phase (Figure 3.2B).

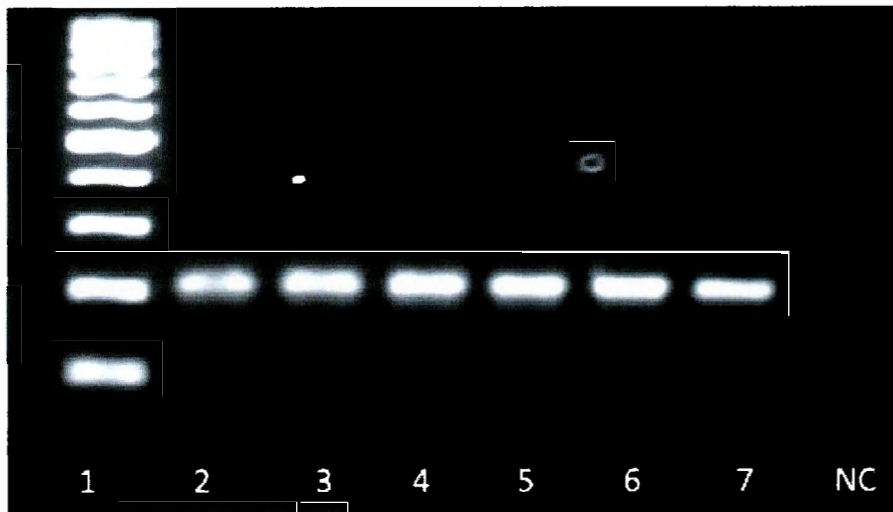
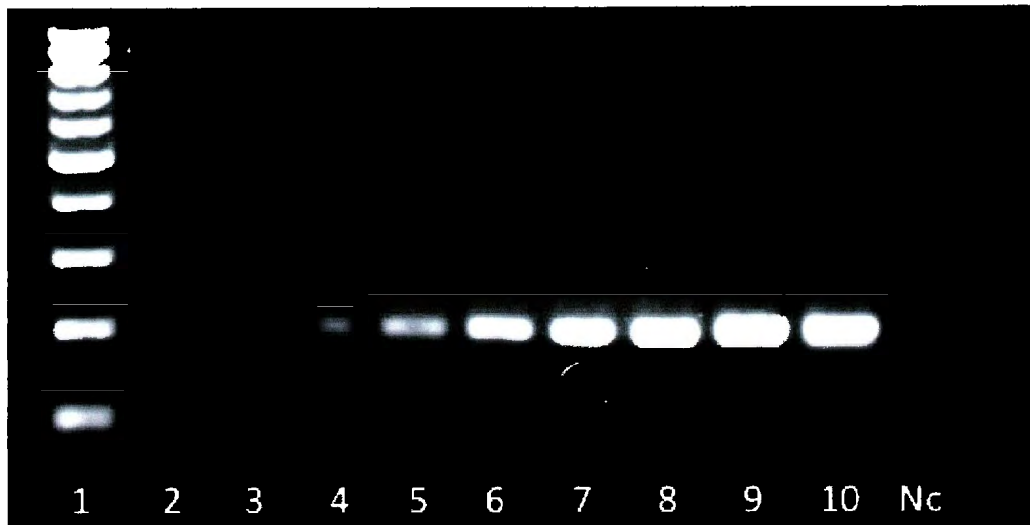


Figure 3.1. *Determination of the optimal annealing temperature for IL-17.* Based on the software program, PRIMER-Blast, the melting temperatures, T_m , of the forward IL-17 primer was 53.93°C and the melting temperature of the reverse IL-17 primer was 53.38°C. A temperature gradient was constructed using annealing temperatures 56°C (lane 2), 58°C (lane 3), 60.4°C (lane 4), 61.6°C (lane 5), 64°C (lane 6) and 66°C (lane 7). Lane 1 contained the 100 base pair ladder. The negative control (NC) is in the last lane.

A)



B)

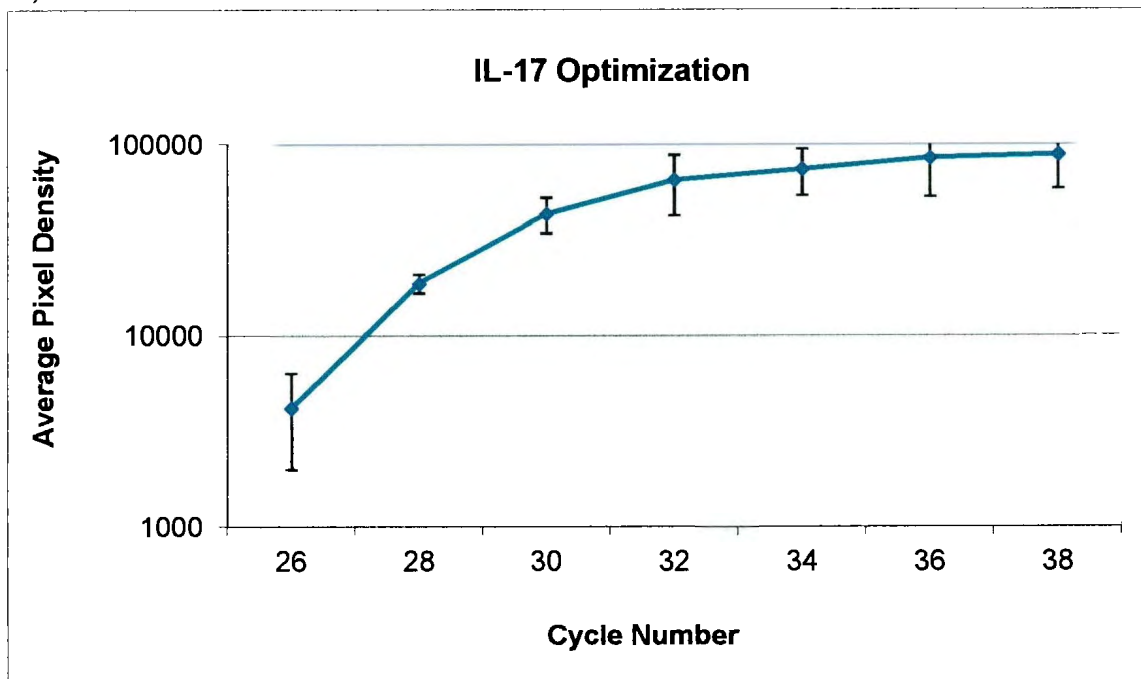


Figure 3.2. Determination of the optimal PCR amplification cycle for IL-17 transcripts. **A)** Representative image showing products for cycle 22 (lane 2), 24 (lane 3), 26 (lane 4), 28 (lane 5), 30 (lane 6), 32 (lane 7), 34 (lane 8), 36 (lane 9) and 38 (lane 10). Lane 1 contained the 100 base pair ladder. The last lane has the no template control. **B)** PCR products were run in three replicate gels, digitized using Kodak Molecular Imaging, and the mean and error bars (representing 1 standard deviation of the mean of the three replicate gels) were graphed.

Analyzing the exponential phase, three cycles were chosen for the subsequent log fold dilution assay; cycles 30, 32, and 34. The PCR products of the log fold dilution are shown in Figure 3.3A and the digitized values were plotted in Figure 3.3B. Theoretically, at the optimal cycle number, the log-fold diluted PCR products should yield a straight line when plotted. Using Figure 3.3B, cycle 32 was chosen as the optimal cycle number for amplification of IL-17 as this produced the most linear line as determined by slope.

3.1.2.2. Determination of Optimal RT-PCR Amplification Cycle for IL-6

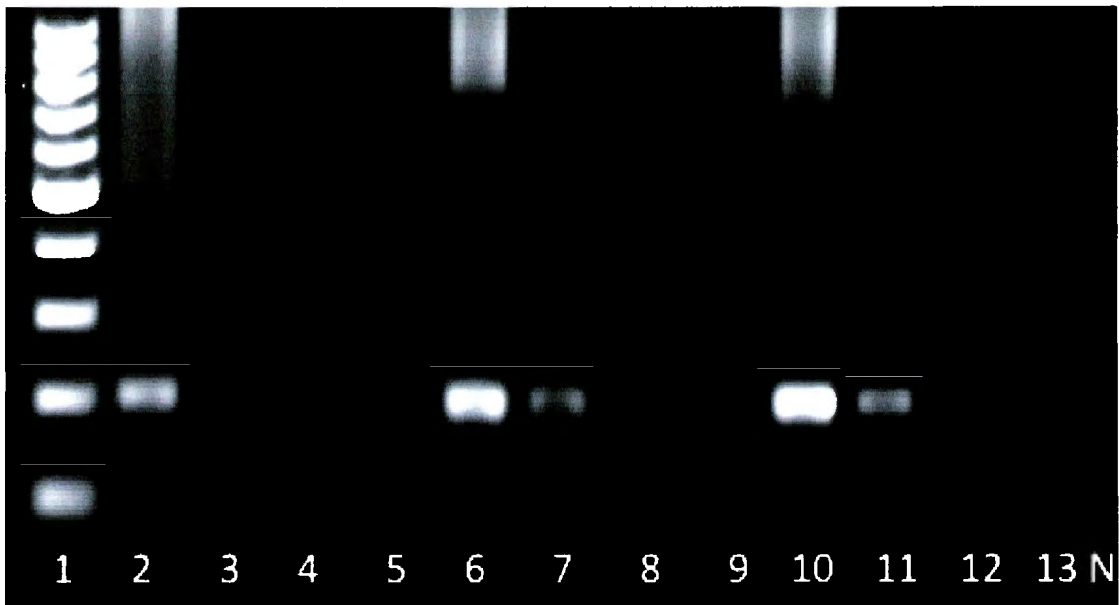
The transcript IL-6 was amplified over the even cycles between 24-38. The PCR products (Figure 3.4A) were digitized and the average number of pixels was graphed (Figure 3.4B), illustrating the amplification over increasing cycle numbers. The results were as expected, showing an exponential phase, followed by the plateau.

Cycles 34 and 35 were chosen from the exponential phase (Figure 3.4B) for the serial dilution assay (Figure 3.5A-B). Following analysis of the graphs in Figure 3.5B, cycle 35 log fold dilution was the most linear and therefore, cycle 35 was chosen as optimal cycle number for amplification of IL-6 transcripts.

3.1.2.3. Determination of Optimal RT-PCR Amplification Cycle for TGF- β

The transcript TGF- β was amplified over the even cycles between 18-40. The PCR products (Figure 3.6A) were digitized and the average number of pixels was graphed (Figure 3.6B), illustrating the amplification over increasing cycle numbers. The results were as expected, showing an exponential phase, followed by the plateau.

A)



B)

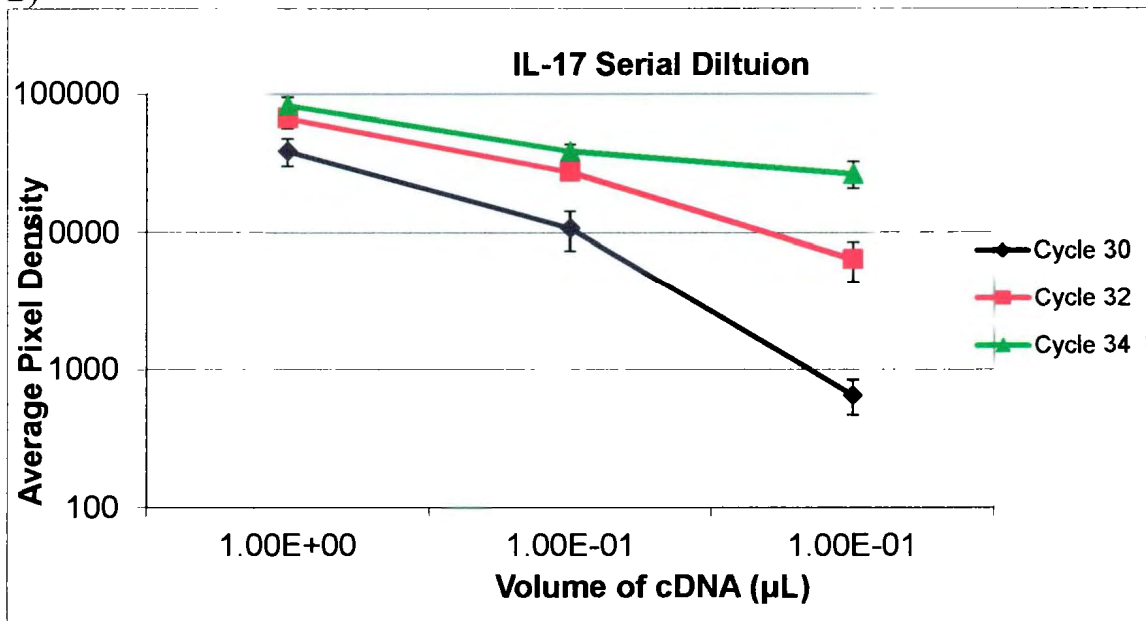


Figure 3.3. *IL-17* amplification of log-fold diluted cDNA. **A)** Representative image showing the PCR products during cycle 30 (lanes 2-4), 32 (lanes 5-7) and 34 (lanes 8-10). Lanes 2, 5 and 8 were PCR mixtures with 1 μ L of cDNA, lanes 3, 6 and 9 contained a 1 fold log dilution of cDNA and lanes 4, 7 and 10 contained 2 fold log dilution of cDNA. Lane 1 contained the 100 base pair ladder. The last lane has the no template control. **B)** PCR products were run in three replicate gels, digitized using Kodak Molecular Imaging, and the mean and error bars (representing 1 standard deviation of the mean) were graphed.

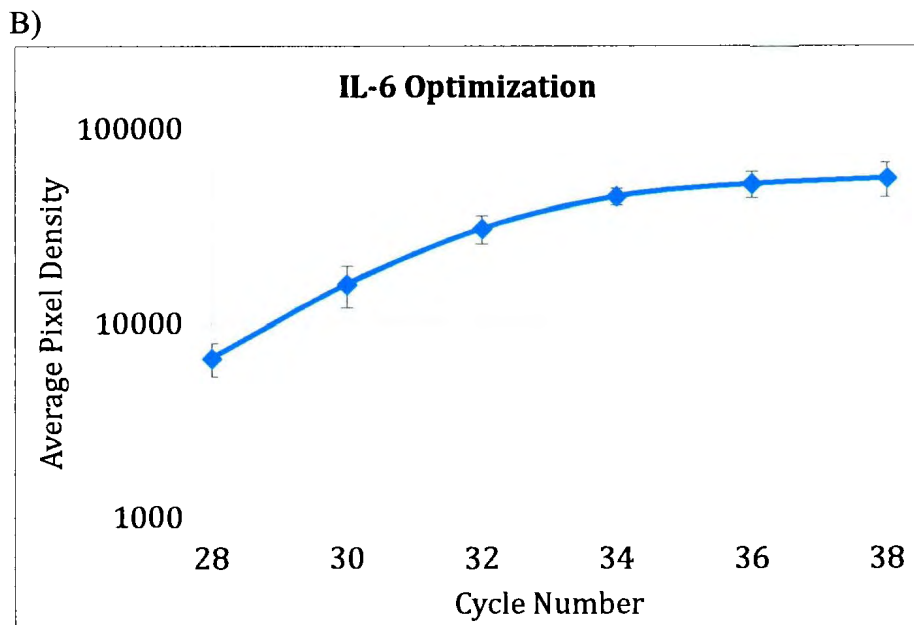


Figure 3.4. Determination of the optimal PCR amplification cycle for IL-6 transcripts **A)** Representative image showing products for cycle 24 (lane 2), 26 (lane 3), 28 (lane 4), 30 (lane 5), 32 (lane 6), 34 (lane 7), 36 (lane 8) and 38 (lane 9). Lane 1 contained the 100 base pair ladder. The last lane has the no template control (NC). **B)** PCR products were run in three replicate gels, digitized using Kodak Molecular Imaging, and the mean and error bars (representing 1 standard deviation of the mean) were graphed.

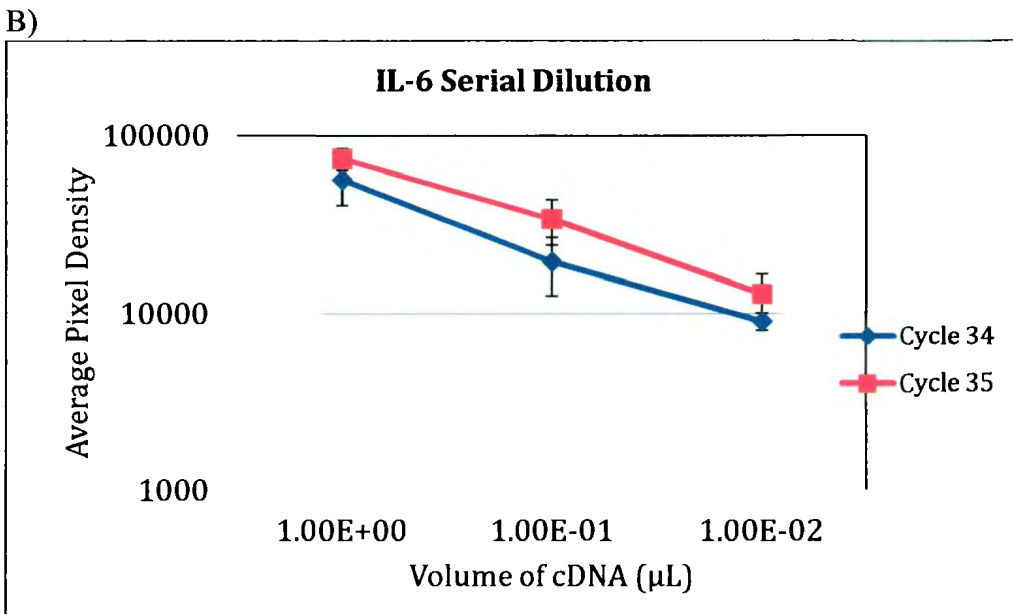
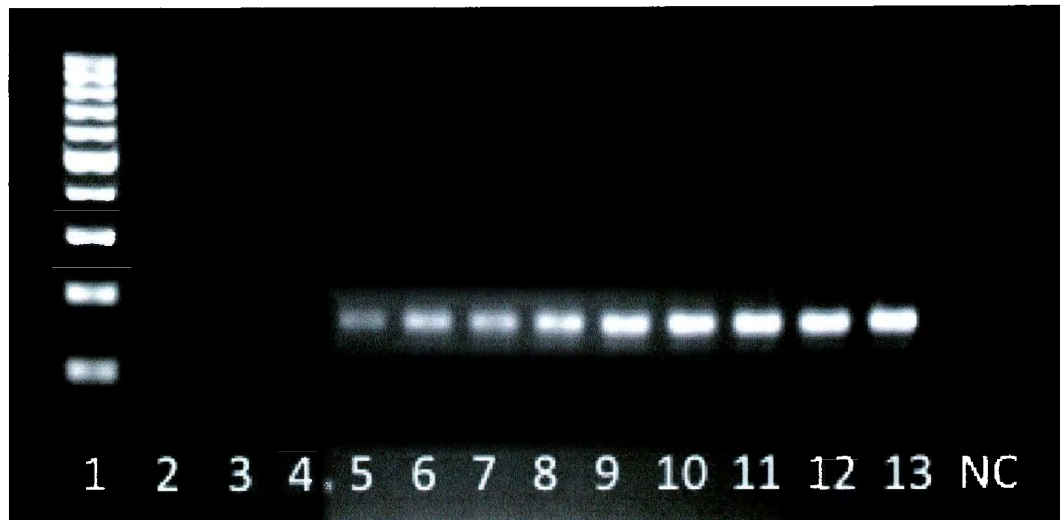


Figure 3.5. *IL-6* amplification of log-fold diluted cDNA. **A)** Representative image showing the PCR products during cycle 34 (lanes 2-4) and 35 (lanes 5-7). Lanes 2 and 5 PCR mixtures with 1 μL of cDNA, lanes 3 and 6 contained a 1 fold log dilution of cDNA and lanes 4 and 7 contained a 2 fold log dilution of cDNA. Lane 1 contained the 100 base pair ladder. The last lane has the no template control (NC). **B)** PCR products were run in three replicate gels, digitized using Kodak Molecular Imaging, and the mean and error bars (representing 1 standard deviation of the mean) were graphed.

A)



B)

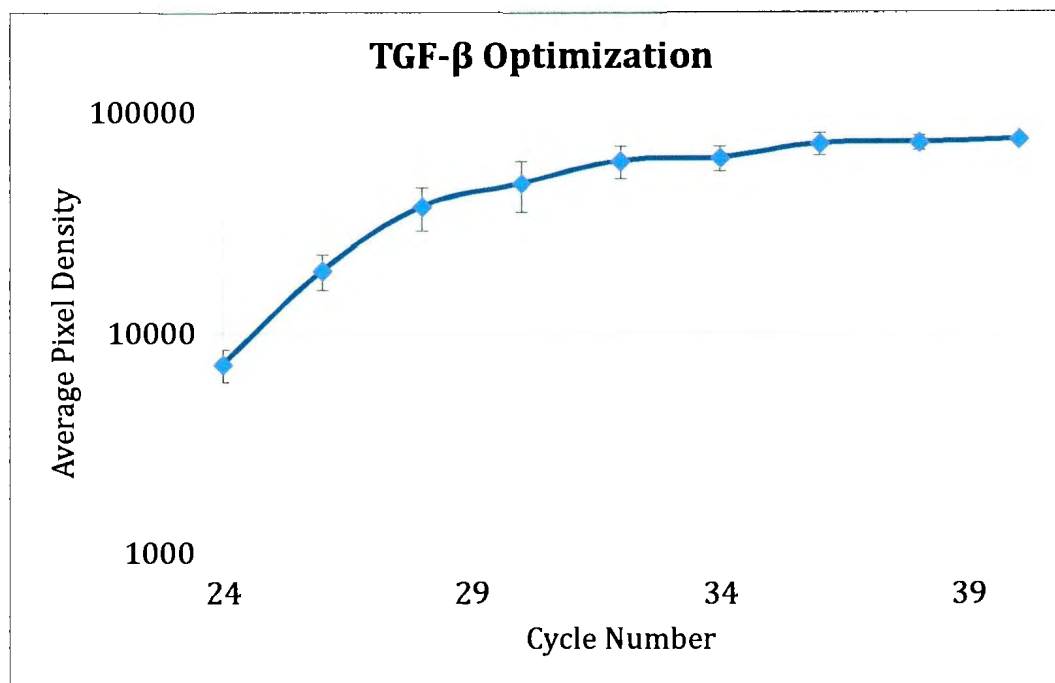


Figure 3.6. Determination of the optimal PCR amplification cycle for TGF-β transcripts
A) Representative image showing products for cycle 18 (lane 2), 20 (lane 3) 22 (lane 4), 24 (lane 5), 26 (lane 6), 28 (lane 7), 30 (lane 8), 32 (lane 9), 34 (lane 10), 36 (lane 11), 38 (lane 12) and 40 (lane 13). Lane 1 contained the 100 base pair ladder. The last lane has the no template control (NC). **B)** PCR products were run in three replicate gels, digitized using Kodak Molecular Imaging, and the mean and error bars (representing 1 standard deviation of the mean) were graphed.

Cycles 31 and 32 were chosen from the exponential phase of Figure 3.7B for the serial dilution assay (Figure 3.7A-B). Following analysis of the graphs in Figure 3.7B, cycle 31 log fold dilution was linear and therefore, cycle 31 was chosen to be the optimal cycle number for TGF- β amplification.

3.1.2.4. Determination of Optimal RT-PCR Amplification Cycle for FOXP3

The transcript FOXP3 was amplified over the even cycles between 28-42. The PCR products (Figure 3.8A) were digitized and the average number of pixels was graphed (Figure 3.8B), illustrating the amplification over increasing cycle numbers. The results were as expected, showing an exponential phase, followed by the plateau.

Cycles 33, 34 and 35 were chosen from the exponential phase of Figure 3.8B for the serial dilution assay (Figure 3.9A-B). Following analysis of the graphs in Figure 3.8B, cycle 33 log fold dilution was linear and therefore, cycle 33 was chosen to be the optimal cycle number for FOXP3 amplification.

3.1.2.5. Summary of RT-PCR Cycle Number Optimization

RT-PCR optimization was successfully completed for IL-17, IL-6, TGF- β and FOXP3. The optimal cycle numbers are listed in Table 3.2. Similar attempts were made to optimize two different RORc2 primer sets. However, despite considerable efforts, we were not successful. Following reconstitution of both primer sets, the specific band would fade gradually and primer dimers became the dominant product. Therefore, we decided to test RORc2 by real-time PCR only.

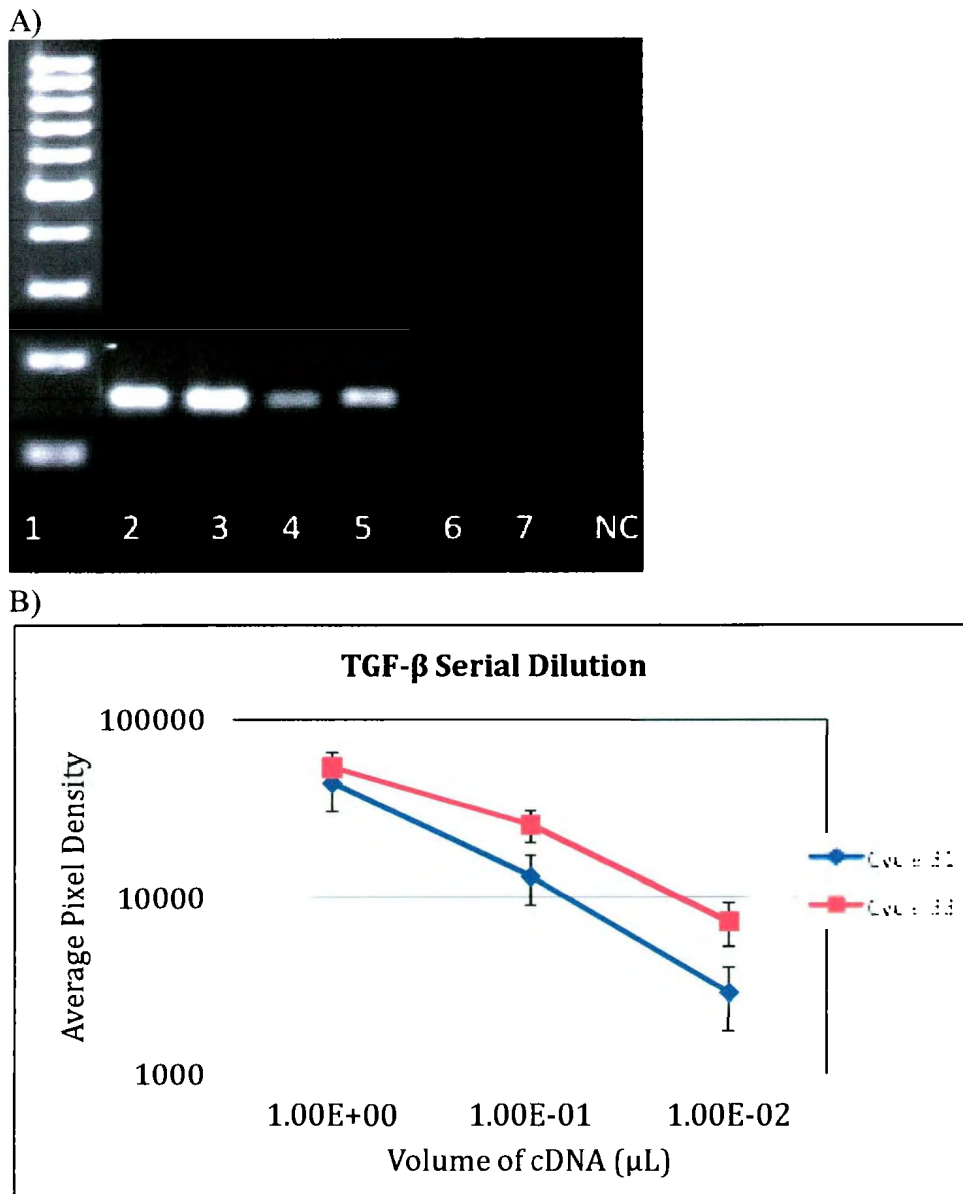


Figure 3.7. *TGF- β amplification of log-fold diluted cDNA.* **A)** Representative image showing the PCR products of cycle 31 (lanes 5-7) and 32 (lanes 2-4). Lanes 2 and 5 PCR mixtures with 1 μ L of cDNA, lanes 3 and 6 contained a 1 fold log dilution of cDNA and lanes 4 and 7 contained a 2 fold log dilution of cDNA. Lane 1 contained the 100 base pair ladder. The last lane has the no template control (NC). **B)** PCR products were run in three replicate gels, digitized using Kodak Molecular Imaging, and the mean and error bars (representing 1 standard deviation of the mean) were graphed.

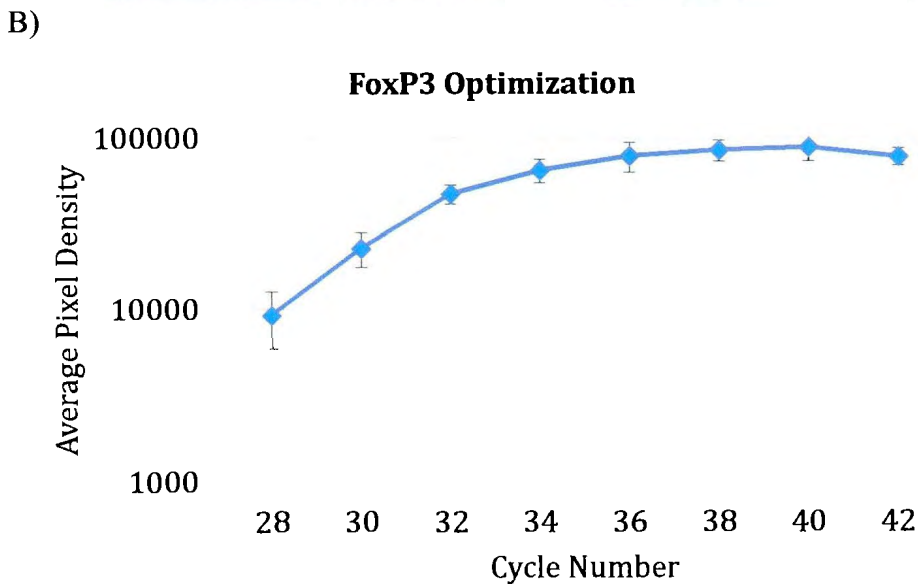
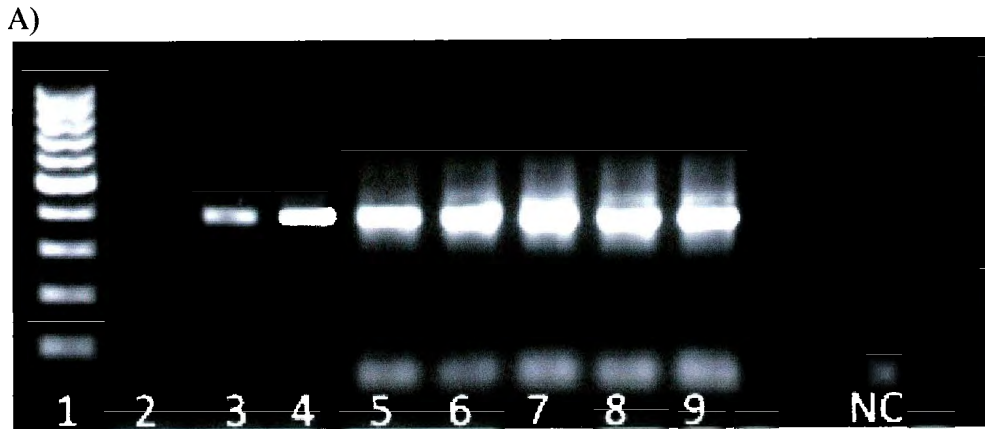


Figure 3.8. *Determination of the optimal PCR amplification cycle for FOXP3 transcripts*
A) Representative image showing products for cycle 28 (lane 2), 30 (lane 3), 32 (lane 4), 34 (lane 5), 36 (lane 6), 38 (lane 7), 40 (lane 8) and 42 (lane 9). Lane 1 contained the 100 base pair ladder. The last lane has the no template control (NC). **B)** PCR products were run in three replicate gels, digitized using Kodak Molecular Imaging, and the mean and error bars (representing 1 standard deviation of the mean) were graphed.

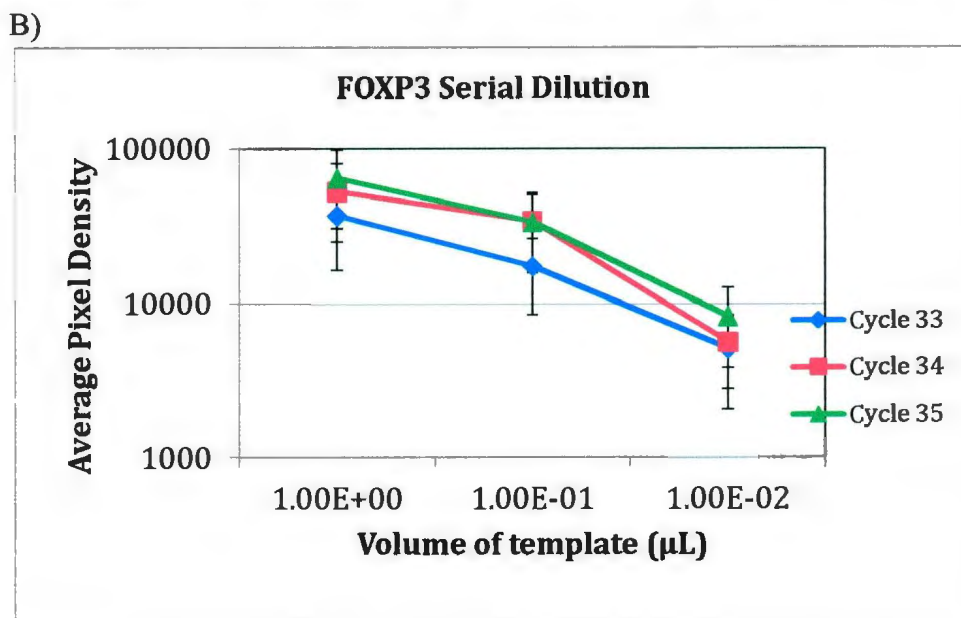
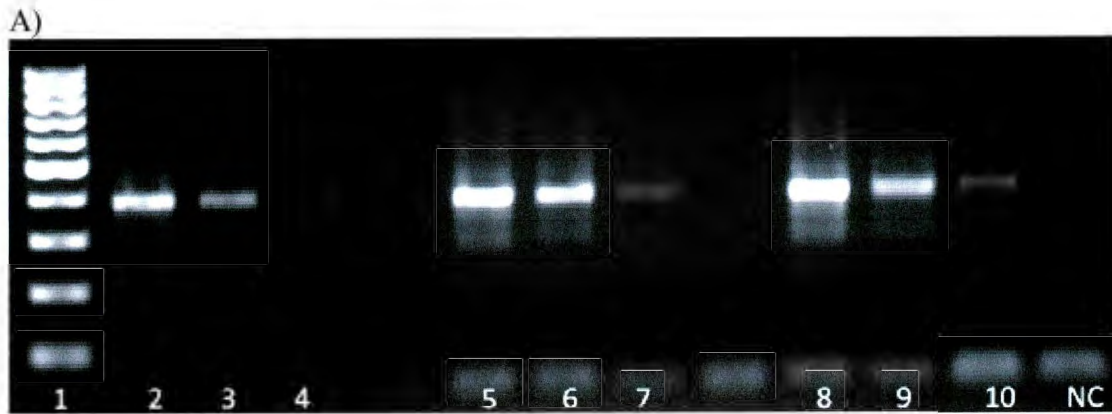


Figure 3.9. *FOXP3* amplification of log-fold diluted cDNA **A)** Representative image showing the PCR products of cycle 33 (lanes 2-4), 34 (lane 5-7) and 35 (lanes 8-10). Lanes 2, 5 and 8 PCR mixtures with 1 µL of cDNA, lanes 3, 6 and 9 contained a 1 fold log dilution of cDNA and lanes 4, 7 and 10 contained a 2 fold log dilution of cDNA. Lane 1 contained the 100 base pair ladder. The last lane has the no template control (NC). **B)** PCR products were run in three replicate gels, digitized using Kodak Molecular Imaging, and the mean and error bars (representing 1 standard deviation of the mean) were graphed.

Table 3.2. Optimal cycle numbers

	IL-17	IL-6	TGF- β	FOXP3
Cycle Number	32	34	31	33

3.2. RT-PCR Analysis of Cytokine and Transcription Factors Transcripts in Breast Cancer Cell Lines

A recent study reported FOXP3 transcripts in several human cancer cell lines, including BCCLs (Karanikas et al., 2008). Therefore, our first objective was to investigate if BCCLs had IL-17 and other cytokine transcripts found within a tumor environment. To test this, a panel of eight BCCLs (as described in Section 2.2.) was analyzed by RT-PCR to determine if IL-17, IL-6, TGF- β and FOXP3 transcripts were present. As shown in Figure 3.10, no IL-17 was detected in any of the eight BCCL suggesting that if transcripts were detected in the cDNA from breast cancer tissues, T cells, or other infiltrating cells, such as macrophages, would produce them. IL-6 was present in higher levels in Hs 578 and MDA-MB-231 (Figure 3.11A-B). By contrast, all cell lines except T-47D, SK-BR-3, BT-474 expressed large amounts of TGF- β transcripts (Figure 3.12A-B), indicating that this marker is not a useful marker for profiling regulatory T cells. FOXP3 was present in all BCCLs in low amounts, which contradicts findings by *Karanikas et al.* (2008) (Figure 3.13A-B). Therefore, it is unclear whether high levels of FOXP3 transcripts detected in breast tumor tissue are produced from only T cells.

Based on the above results and the literature provided in Chapter 1, we decided to analyze both IL-17 and RORc2 by real-time PCR as these are related to T_H17 cells.

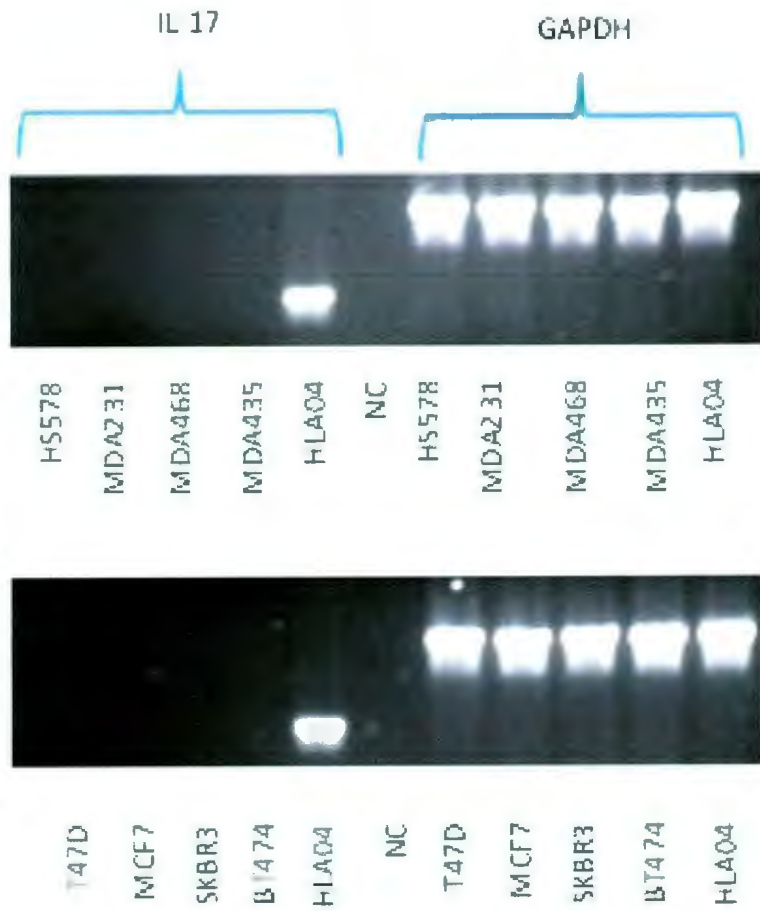


Figure 3.10. *IL-17 was not detected in BCCLs.* Representative image of relative levels of IL-17 in BCCLs. The cell line represented by the PCR product is shown beneath the band; HLA04 (PHA stimulated PBLs), the positive control; NC, no template control.

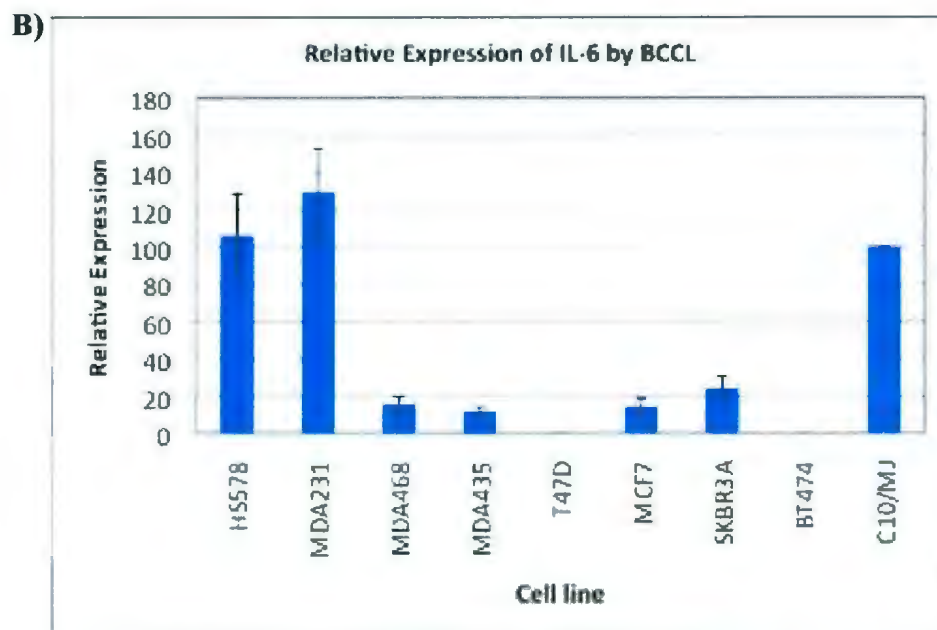
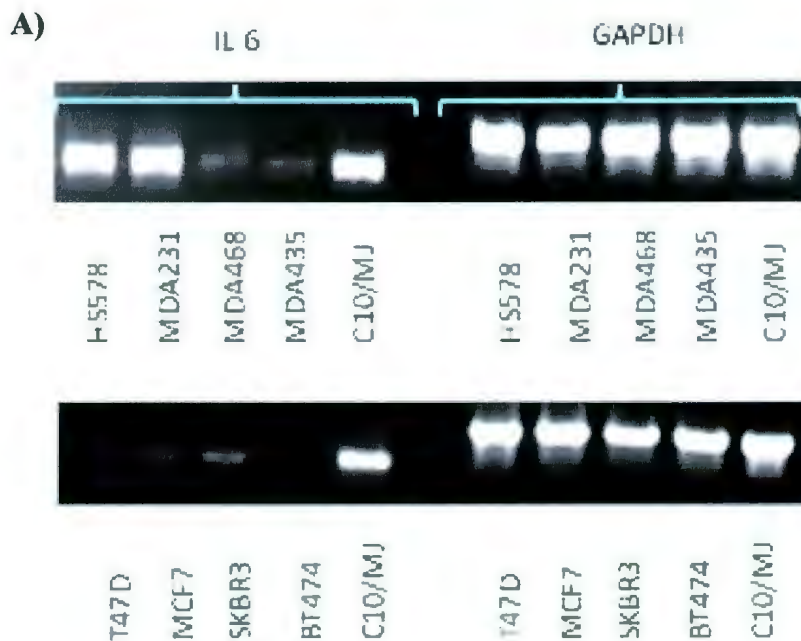


Figure 3.11. BCCL expression of IL-6. **A)** Representative image of relative levels of IL-6 in BCCLs. The cell line represented by the PCR product is shown beneath the band; C10/MJ, the positive control; NC, no template control (NC). **B)** PCR products were run in three replicate gels, digitized using Kodak Molecular Imaging, and the mean and standard deviation were calculated and graphed. The relative expression is defined as $((\text{IL-6 in BCCL})/(\text{GAPDH in BCCL})) \div ((\text{IL-6 in C10/MJ})/(\text{GAPDH in C10/MJ}))$.

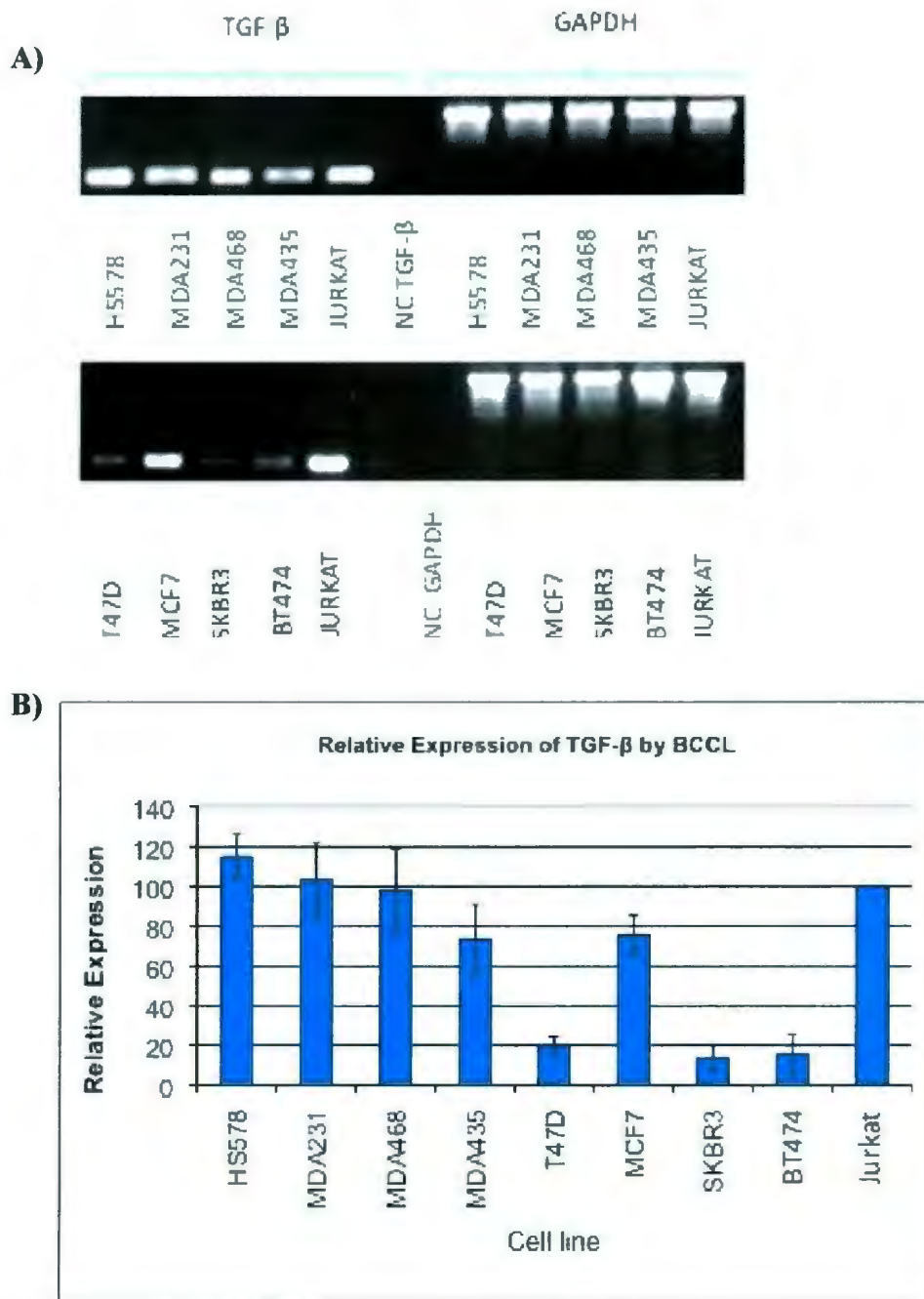


Figure 3.12. BCCL expression of TGF- β . **A)** Representative image of relative levels of TGF- β in BCCLs. The cell line represented by the PCR product is shown beneath the band; Jurkat the positive control; NC, no template control (NC). **B)** PCR products were run in three replicate gels, digitized using Kodak Molecular Imaging, and the mean and standard deviation were calculated and graphed. The relative expression is defined as $((\text{TGF-}\beta \text{ in BCCL})/(\text{GAPDH in BCCL})) \div ((\text{TGF-}\beta \text{ in Jurkat})/(\text{GAPDH in Jurkat}))$

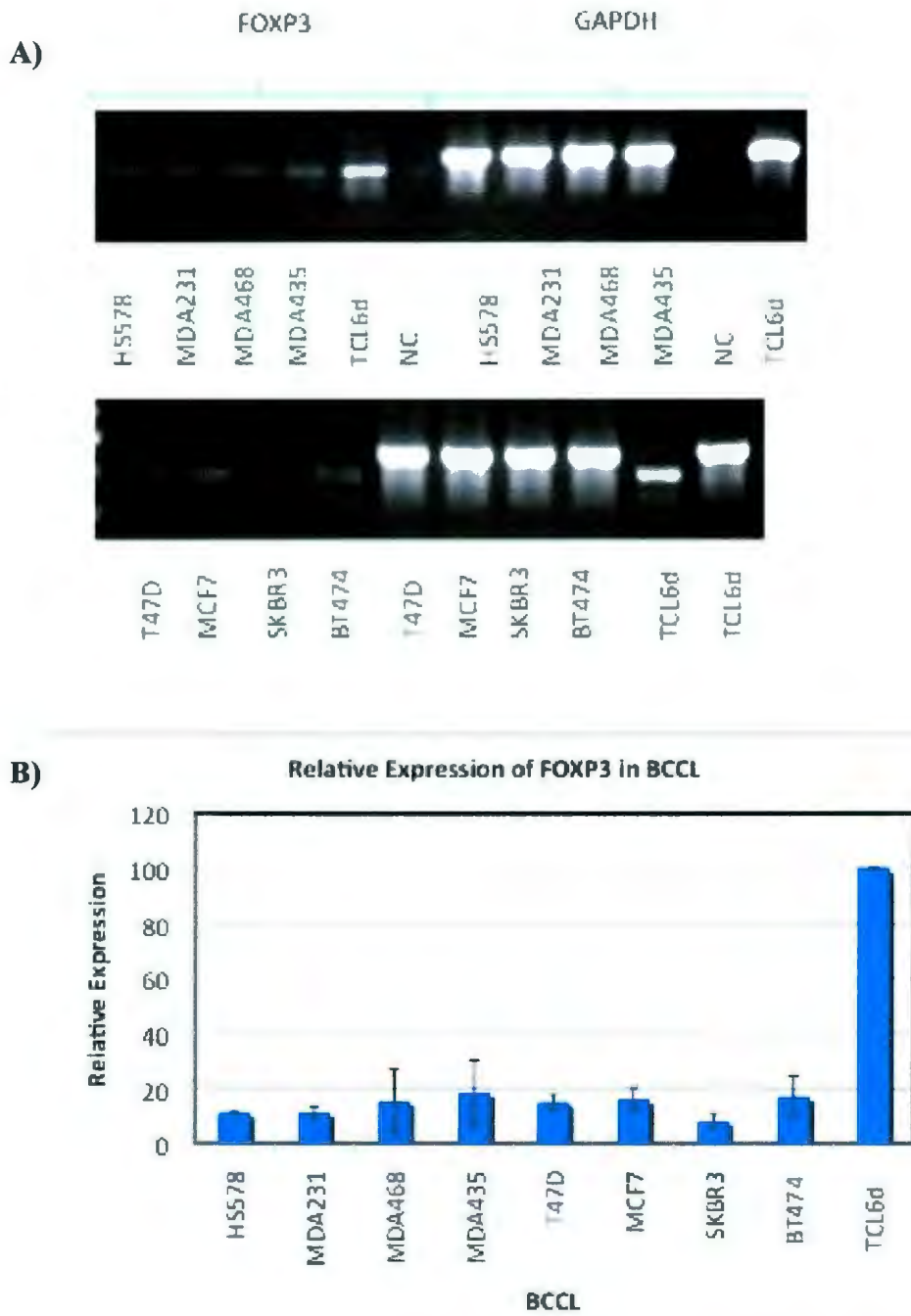


Figure 3.13. *BCCL* expression of *FOXP3*. **A)** Representative image of relative levels of *FOXP3* in BCCLs. The cell line represented by the PCR product is found beneath the band; TCL6D, the positive control; NC, no template control (NC). **B)** PCR products were run in three replicate gels, digitized using Kodak Molecular Imaging, and the mean and standard deviation were calculated and graphed. The relative expression is defined as $((\text{FOXP3 in BCCL})/(\text{GAPDH in BCCL})) \div ((\text{FOXP3 in TCL6d})/(\text{GAPDH in TCL6d}))$

We analyzed both transcripts as both IL-17 and RORc2 are not exclusively produced by T_H17 cells.

3.3. RNA Integrity Values for Breast Tumor RNA

When cDNA was prepared from the 65 breast tumor RNA samples, the RNA integrity was also tested. The RNA samples were stored for 6 years at -80°C and there were some concerns over RNA degradation. If RNA is greatly degraded, the analysis and interpretation of PCR results may be inaccurate. The RIN algorithm is extracted from electrophoretic measurements from the Agilent BioAnalyzer. The value obtained ranges between 1 (worst RNA quality) and 10 (best RNA quality). The RNA RIN values are shown in Table 3.4.

Table 3.4. RIN Values for Breast Cancer RNA Samples

Sample	RIN	Sample	RIN	Sample	RIN
11378	2.2	11129	5.9	11216	7.5
12159	2.7	11644	6	11170	7.5
11372	2.7	12418	6.2	11799	7.6
13088	2.9	12078	6.3	13451	7.7
11353	2.9	11882	6.4	11499	7.7
13058	3.3	11815	6.4	10881	7.8
13167	3.5	10850	6.4	11565	7.9
13113	3.7	12375	6.6	13369	8
11208	3.7	10958	6.6	11905	8
11084	3.8	12858	6.8	11817	8.1
11889	4.3	12816	6.9	11108	8.1
11452	4.3	11657	6.9	13412	8.2
12748	4.4	12750	7.1	13269	8.2
11816	4.5	11818	7.1	13123	8.2
13390	4.8	11008	7.1	13337	8.4
11066	5.2	11125	7.2	10832	8.6
12831	5.3	12450	7.3	11556	8.8
12513	5.3	10796	7.3	14377	8.9
11432	5.3	12782	7.4	12694	9.1
11894	5.7	11352	7.4	12483	9.1
11834	5.8	13282	7.5	12511	NA
12926	5.9	11806	7.5		

RIN values ranged from 2.2 – 9.1, with a median of 6.85 and a mean of 6.34. Sixteen of the samples had RIN values less than 5. However, as the cDNA was already prepared, RT-PCR and real-time experiments were conducted on all 65 samples, with the exception of the second testing of IL-17 by real-time PCR.

3.4. Analysis of Cytokine Transcripts in Breast Cancer Tissues by Conventional RT-PCR

IL-6 transcript levels were determined by RT-PCR for the 65 breast tumor samples. Table 3.5. and Figure 3.14A. provide the results obtained for both the 65

samples (all RIN values) and 49 samples ($RIN \geq 5$). Figure 3.14A shows that the data are not normally distributed for all 65 samples. Figure 3.14B shows that exclusion of the RIN values less than 5 does not change the result that the data are not normally distributed. Therefore, for statistical analysis, nonparametric statistical tests were used.

Table 3.5. Descriptive statistics of RT-PCR transcript levels of IL-6

	IL-6 (N=65)	IL-6 (N=49)
Mean	178.9	164.7
Median	149.1	149.5
Range	699.9	699.9

The IL-6 values obtained on the 65 samples were compared to the first set of IL-6 values on the same samples in the initial study, using Spearman's correlation test, $p=0.114$ (N=64) or $p=0.049$ (N=48). There is a significant correlation between the two sets of data obtained when samples with RIN values greater or equal to 5 were used, demonstrating that the results are reproducible.

Relative IL-17 transcript levels were also determined for the 65 breast tumor cDNA samples. These results are summarized in Table 3.6. and Figure 3.15A-B. Once again, the data are not normally distributed; therefore nonparametric statistical tests were used for analysis.

Table 3.6. Descriptive statistics of RT-PCR transcript levels of IL-17

	IL-17 (N=65)	IL-17 (N=49)
Mean	14.22	11.93
Median	8.5	7.8
Range	71.9	71.9

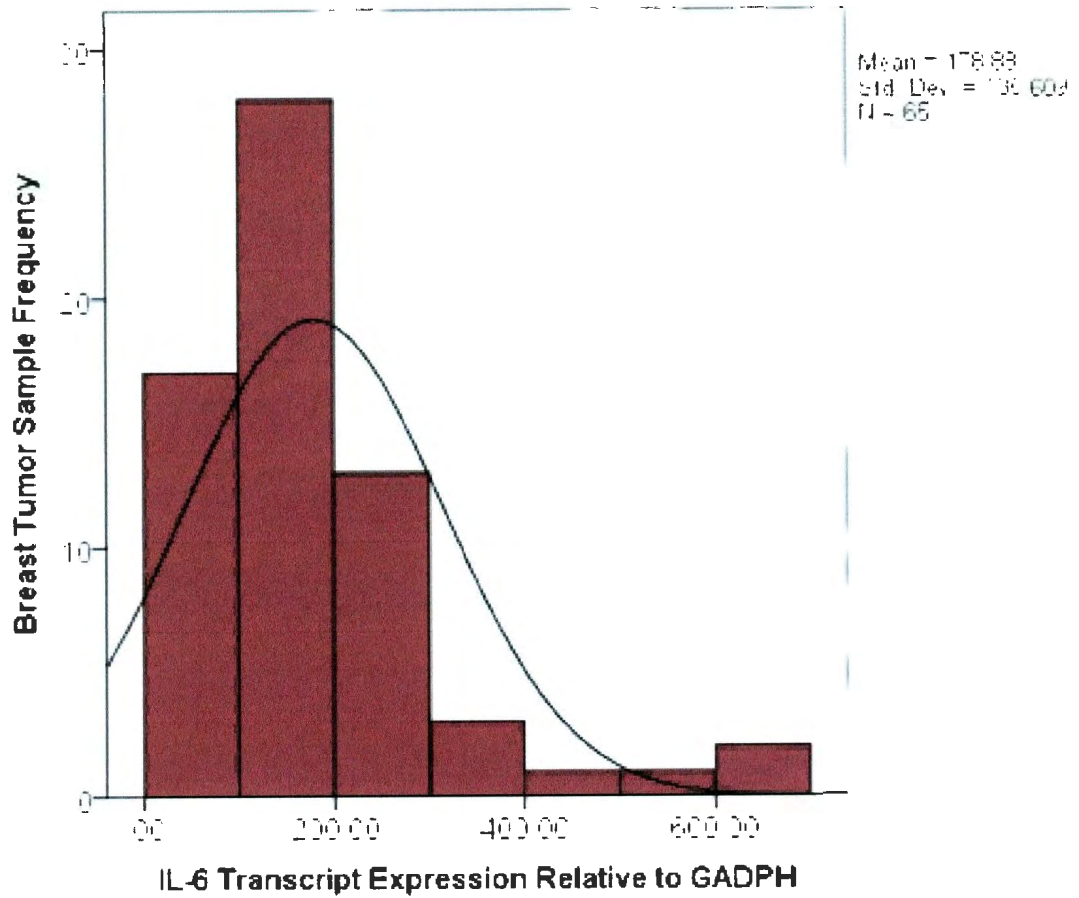


Figure 3.14A. *IL-6 transcript expression in BCT samples.* The figure shows the distribution of IL-6 transcript levels analyzed by conventional RT-PCR in 65 breast tumor samples. The data are not normally distributed.

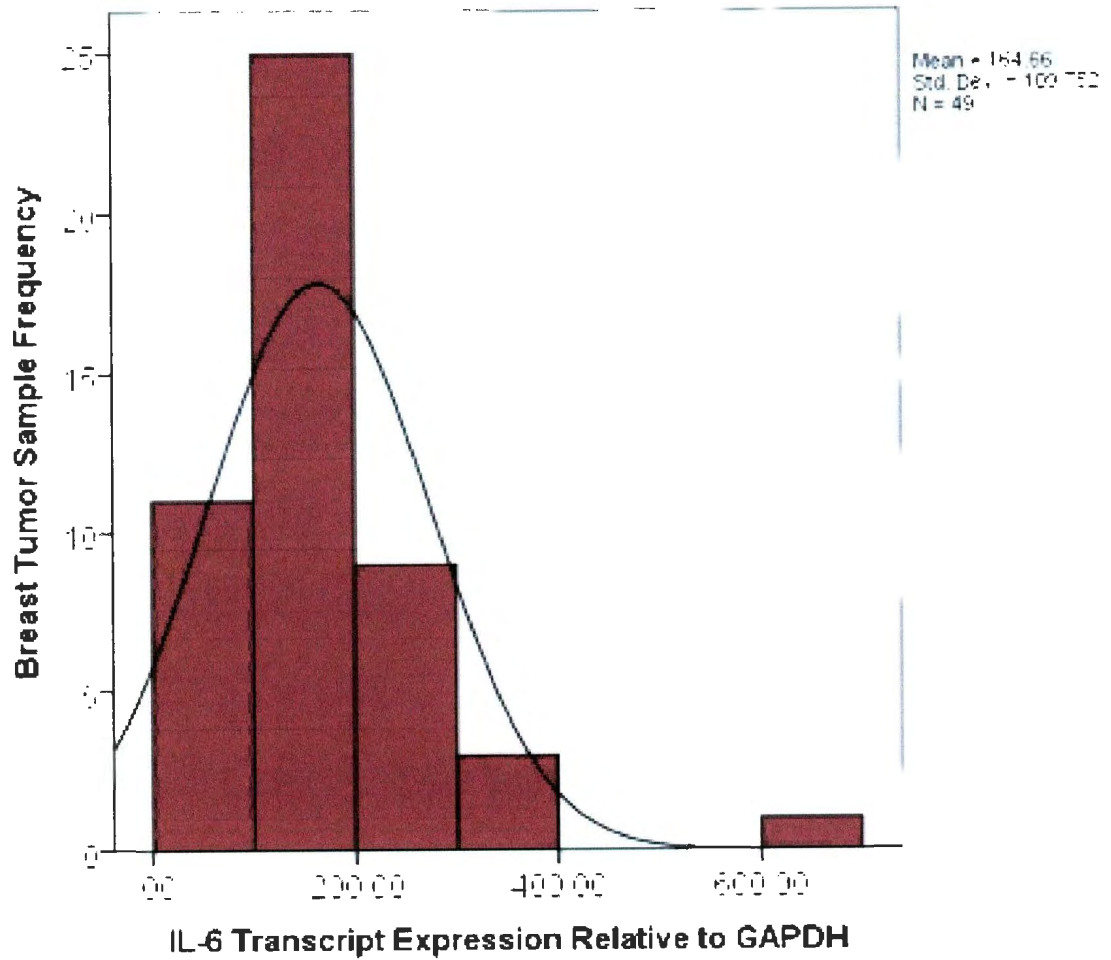


Figure 3.14B. *IL-6 transcript expression in BCT samples.* The figure shows the distribution of IL-6 transcript levels analyzed by real-time PCR in 49 breast tumor samples. The data are not normally distributed.

These values reflect the mRNA levels of IL-17 obtained through conventional RT-PCR experiments and are compared later to the values obtained by real-time PCR in Section 3.7. Table 3.7. summarizes the correlations obtained between IL-17 and IL-6. The IL-6 transcript levels from both subsets associate significantly ($RIN \geq 5$). As a result, we had confidence that the level of IL-6 detected by our RT-PCR experiments was accurate.

Table 3.7. Spearman's rho significance for RT-PCR relative transcripts of IL-6 and IL-17 (N=49)

	IL-6 (original set)		IL-6		IL-17	
	RIN<5	RIN≥5	RIN<5	RIN≥5	RIN<5	RIN≥5
IL-6 (original set)						
IL-6 (T _H 17 subset)	0.114	0.049*				
IL-17	NS	NS	NS	NS		

3.5. Optimization of Real-time PCR Conditions

Real-time PCR kits were obtained from Invitrogen, as previously described in Section 2.5. The denaturation, annealing and extension steps were predetermined for these real-time PCR kits, but the quantity of cDNA required optimization. Section 2.3. describes the process involved in converting 1 µg of RNA into 20 µL of cDNA. Five log fold dilutions (1 µL – 1/10000 µL) of the positive control cDNA were prepared for amplification, which was performed over 40 cycles (see Section 2.5. for the conditions). Figure 3.16A-B contain the amplification plots obtained for IL-17 and RORc2 transcripts in HLA-04, the positive control. An optimal threshold for detection of fluorescence from the FAMTM is selected automatically from regression parameters of the standard curve. A threshold cycle (C_t) for each volume is assigned based upon the intersection of the

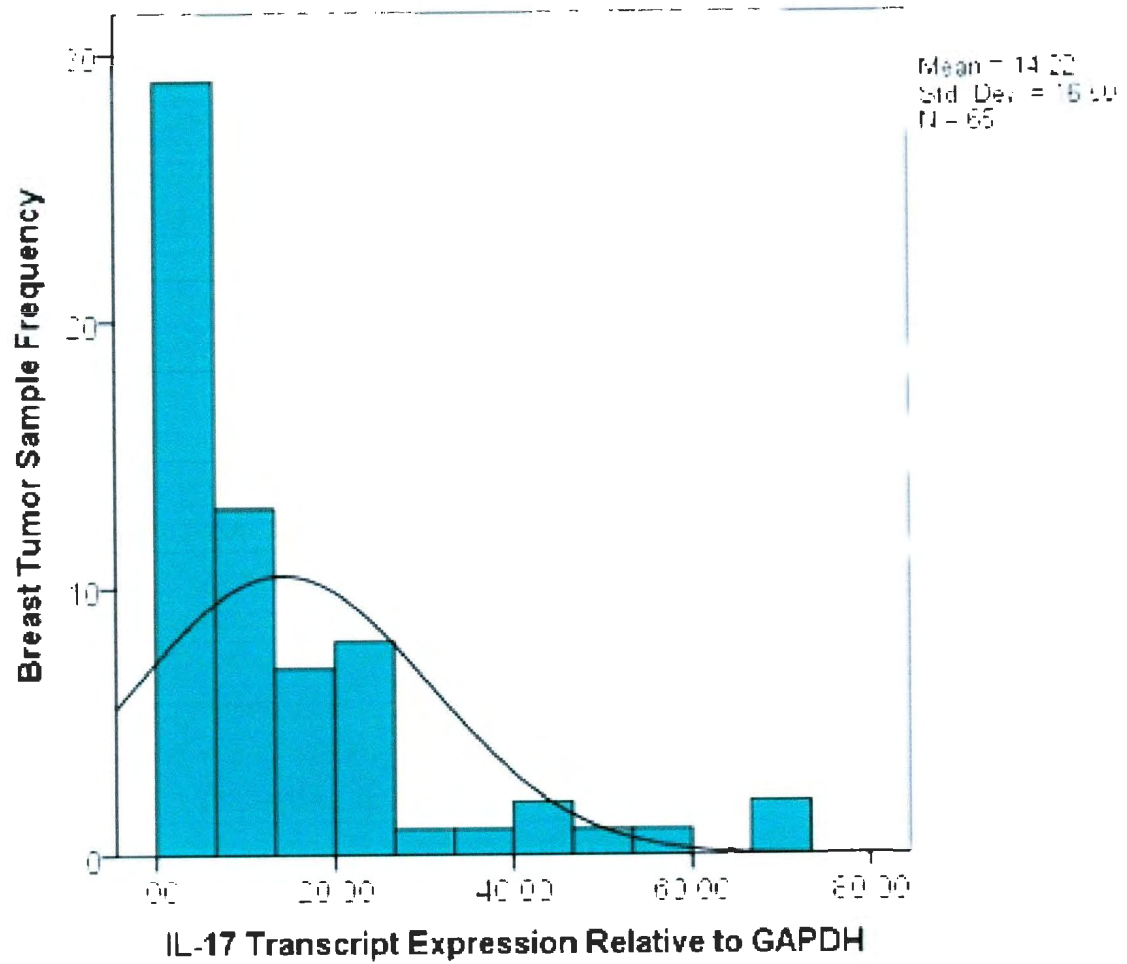


Figure 3.15A. *IL-17 transcript expression in BCT samples.* The figure shows the distribution of IL-17 transcript levels analyzed by conventional RT-PCR in 65 breast tumor samples. The data is not normally distributed.

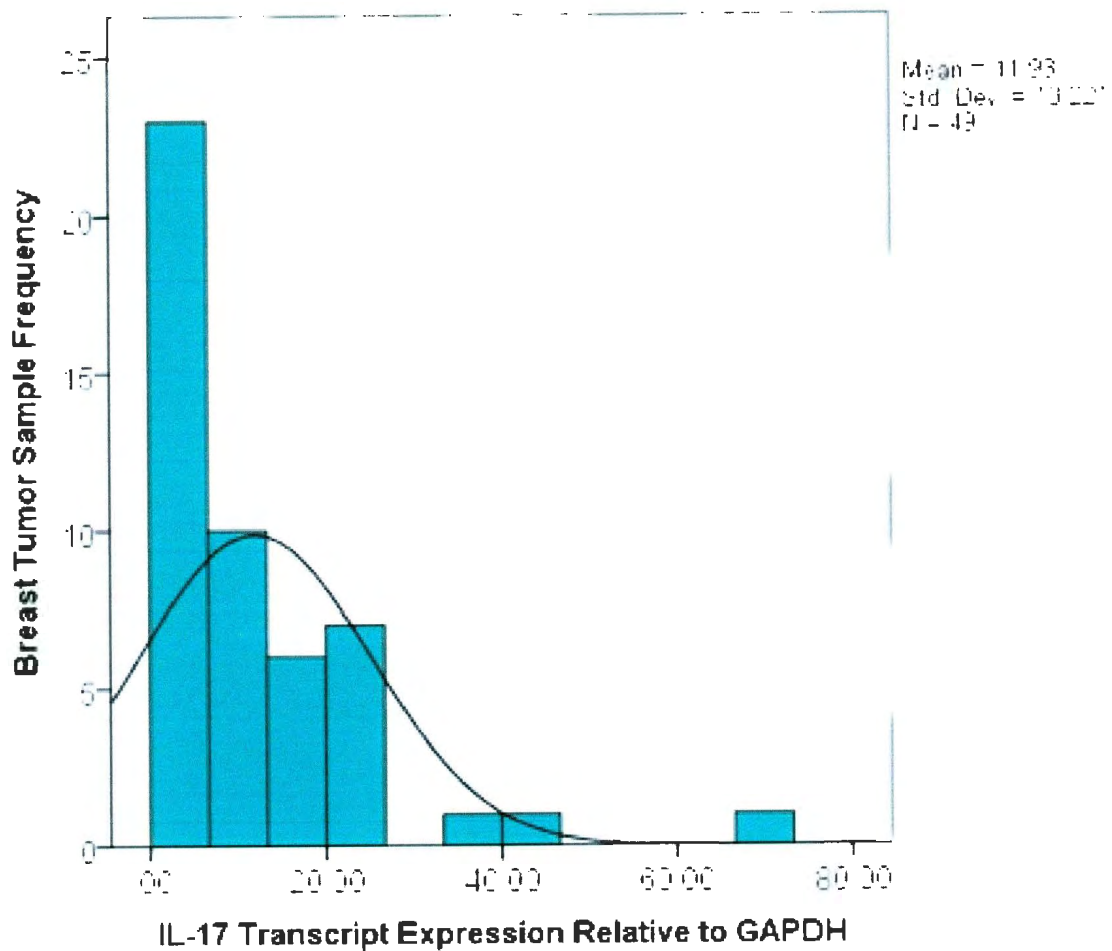


Figure 3.15B. *IL-17 transcript expression in BCT samples.* The figure shows the distribution of IL-17 transcript levels analyzed by real-time PCR in 49 breast tumor samples. The data is not normally distributed.

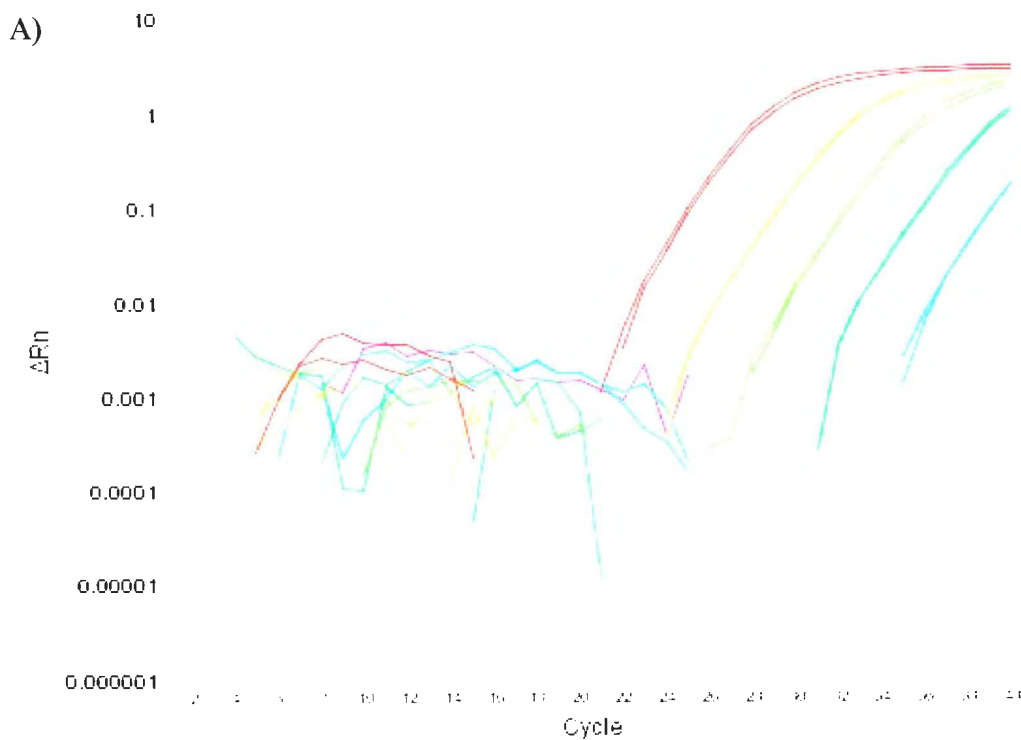


Figure 3.16A. *Determining the optimal dilution of cDNA for real-time assays A) IL-17 amplification.* Log fold dilutions of HLA04 were amplified in the StepOne Real-Time PCR machine over 40 cycles. The red line represents amplification of 1 μ L of cDNA, the yellow lines represents amplification of a 1 fold log dilution of cDNA, the light green line represents amplification of a 2 fold log dilution of cDNA and the dark green lines represents amplification of a 3 fold log dilution of cDNA μ L of cDNA and the blue line represents amplification of a 5 fold log dilution of cDNA. The number of amplifications is represented by the x-axis and ΔR_n is represented by the y-axis. ΔR_n is the fluorescence of the reporter dye (FAM) divided by the fluorescence of the passive dye (ROX). Assays were performed in duplicate.

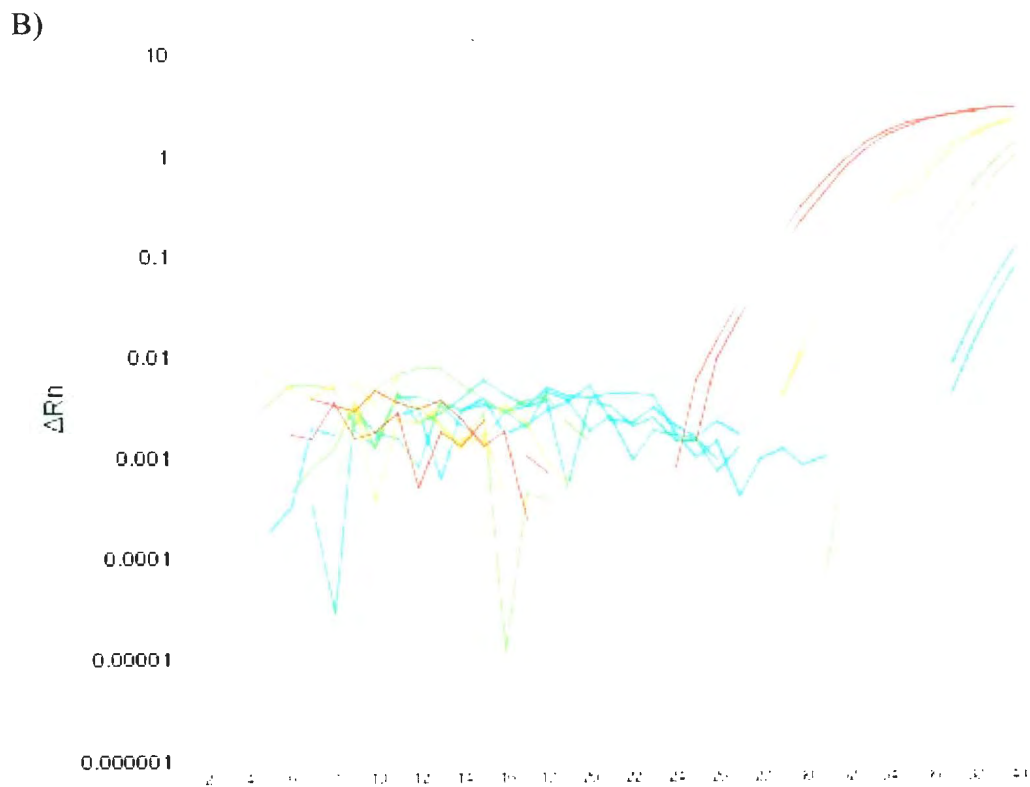


Figure 3.16B. *Determining the optimal dilution of cDNA for real-time assays B) RORc2 amplification.* Log fold dilutions of HLA04 were amplified in the StepOne Real-Time PCR machine over 40 cycles. The red line represents amplification of 1 μ L of cDNA, the yellow lines represents amplification of a 1 fold log dilution of cDNA, the light green line represents amplification of a 2 fold log dilution of cDNA and the dark green lines represents amplification of a 3 fold log dilution of cDNA. The number of amplifications is represented by the x-axis and ΔR_n is represented by the y-axis. ΔR_n is the fluorescence of the reporter dye (FAM) divided by the fluorescence of the passive dye (ROX). Assays were performed in duplicate.

amplification curve and the optimal threshold. Based upon the C_t value, a standard curve is constructed (Figure 3.17A-B). Theoretically, the line constructed from the standard curve should have an R^2 value of greater than 0.80 (Bio-Rad Laboratories, 2006). The results of the R^2 and efficiency values for the transcripts are given in Table 3.8. Please see Appendix B for amplification plots and the standard curve specific for GAPDH.

Table 3.8. R^2 values and efficiencies for real-time PCR standard curves

Transcript	R^2 value	Efficiency (%)
IL-17	0.998	97.232
RORc2	0.981	94.694
GAPDH	0.991	93.117

There was no amplification detected for the 5-fold dilution of HLA-04 for RORc2 and IL-17. The sample was too dilute to detect RORc2 and IL-17, but due to the acceptable R^2 and efficiency values, we continued with HLA-04 as the control. Next, the dilution of cDNA added to the reaction mixture was determined. We chose a dilution of cDNA that contained the least deviation between the duplicates. The cDNA dilution determined was the amount added for both the positive control cDNA and the breast tumor sample cDNA. Table 3.9. shows the volume of stock cDNA, prepared from 1 μ g of RNA required for each specific transcript.

Table 3.9. Transcript specific cDNA volume for real-time PCR assays

Transcript	cDNA volume
IL-17	1/10 μ L
RORc2	1 μ L
GAPDH	1/10 μ L

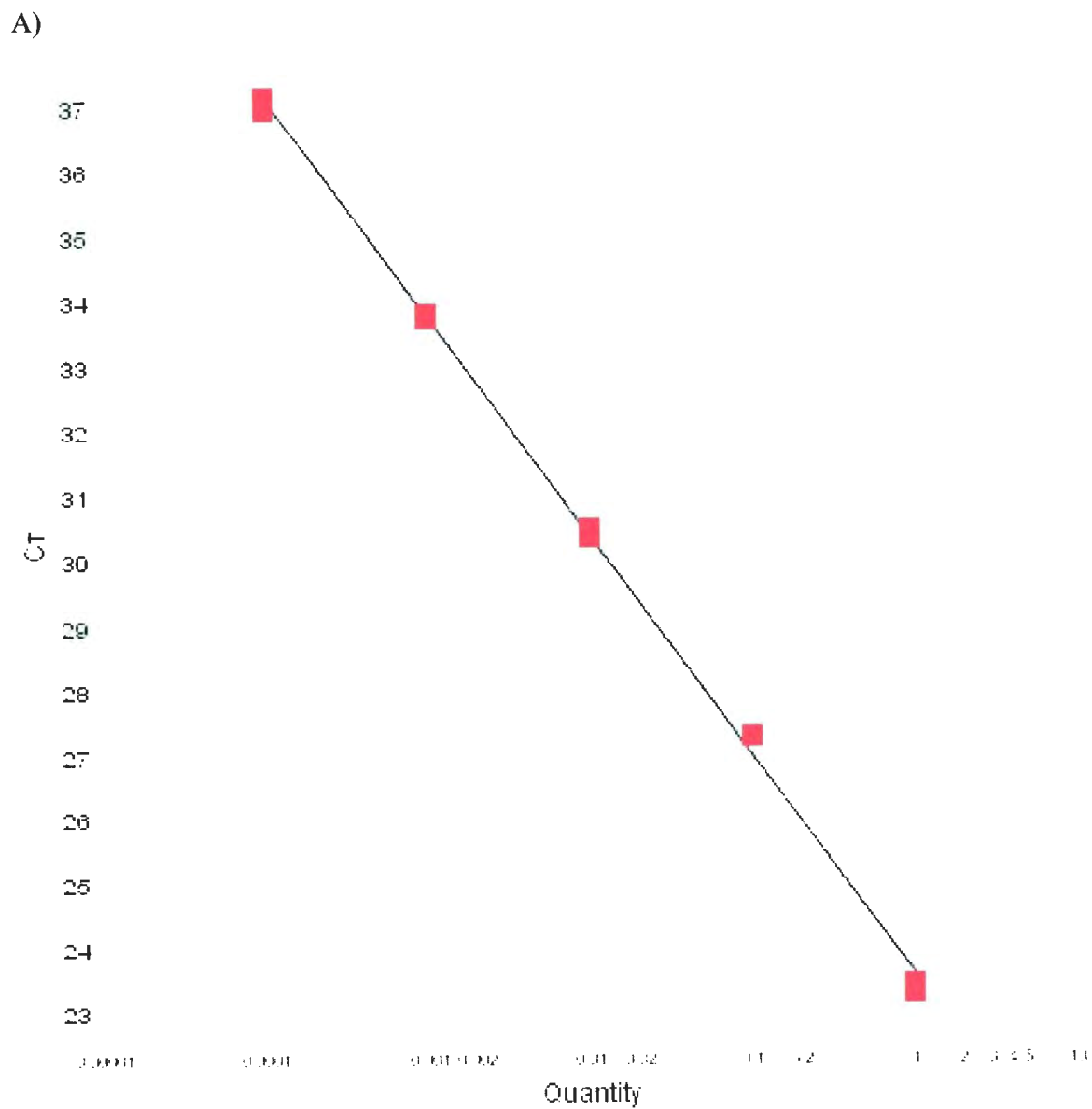


Figure 3.17A. *Standard curve of the threshold cycles (C_t) A) IL-17.* The C_t values obtained from the amplification of log fold diluted HLA04. The slope of this line was -3.39, the Y-intercept was 23.612, R² value was 0.998 and the efficiency was 97.232%.

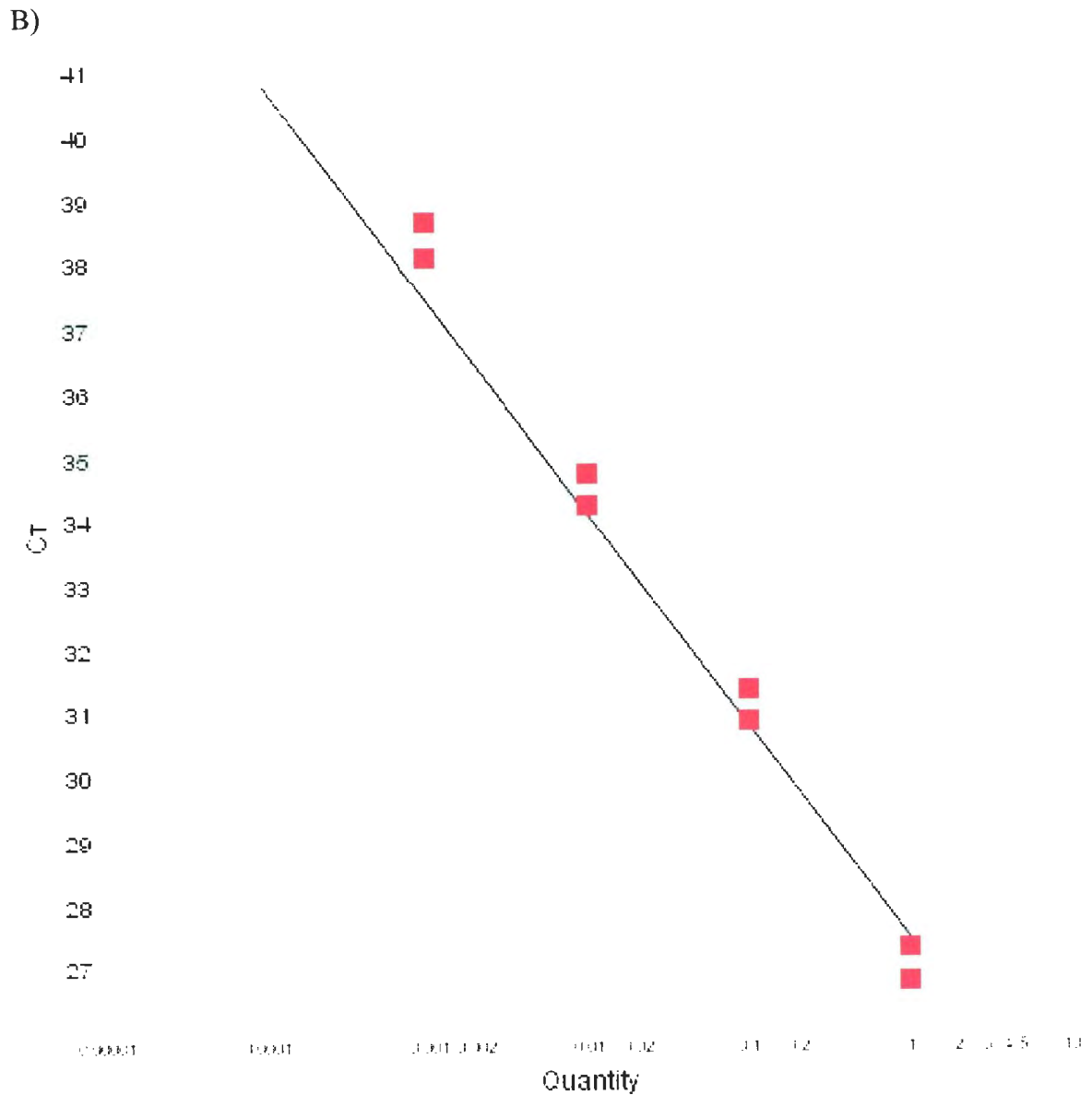


Figure 3.17B. Standard curve of the threshold cycles (C_t) **B)** *RORc2*. The C_t values obtained from the amplification of log fold diluted HLA04. The slope of this line was -3.45, the y-intercept was 28.282, R^2 value was 0.981 and the efficiency was 94.694%. The C_t (y-axis) is plotted against the volume of cDNA added (x-axis).

3.6. Real-time PCR Analysis of IL-17 and RORc2 Transcripts in Breast Cancer Cell Lines

To confirm lack of IL-17 transcripts in BCCL (Figure 3.10) and to determine if RORc2 is expressed in BCCL, we performed real-time PCR assays on cDNA from BCCL described in Section 2.2. As shown in Figure 3.18., we confirmed that IL-17 transcripts were not detected in any of the BCCLs tested. By contrast, RORc2 was expressed at high levels in MDA-MB-435 and SK-BR-3 and at moderate levels in MDA-MB-231 and MDA-MB-468; very low transcripts were detected in BT-474 and none in HS-578. Therefore, RORc2 is not be a reliable lone indicator for T_H17 cells in breast tumor tissue. There was no cDNA available for MCF-7 and T-47D. Future experiments could analyze the levels of RORc2 in both of these cell lines as well as other cancer cell lines.

3.7. Analysis of IL-17 and RORc2 transcripts in Breast Cancer cDNA by Real-Time PCR

As described in Section 2.5, real-time PCR was performed on breast tumor cDNA to determine relative levels of IL-17 and RORc2. The positive control cDNA was PBL HLA-04 and the endogenous control was GAPDH. All 65 breast tumor samples were initially analyzed for both IL-17 and RORc2 as cDNA was prepared at the same time as RIN analysis was done. The results for both sets are presented in Figures 3.19 and 3.20A-B. Spearman's correlation analysis revealed no correlation of IL-17 real-time with IL-17 done by RT-PCR. Therefore, we repeated the real-time PCR experiments for IL-17 on 49 samples with RIN values greater or equal to 5. Since the correlation between the two real-time PCR experiments was significant ($p < 0.000$), we calculated the mean for

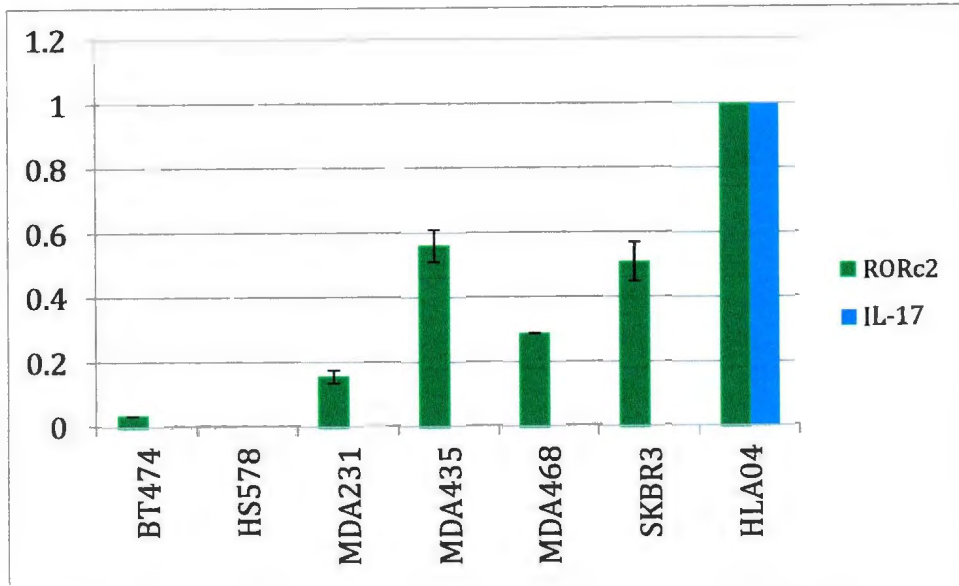


Figure 3.18. *BCCL expression of IL-17 and RORc2 as determined by real-time PCR.* 6 BCCLs (x-axis) were analyzed for transcriptional expression of RORc2 (green bars) and IL-17 (blue bars). MDA-MB-435 and SK-BR-3 expressed higher quantities, whereas MDA 468, MDA-MB-231, and BT-474 expressed lower levels. HS 578 did not express RORc2. No BCCL expressed IL-17. These samples were run in triplicate and the standard deviation is represented by the error bars.

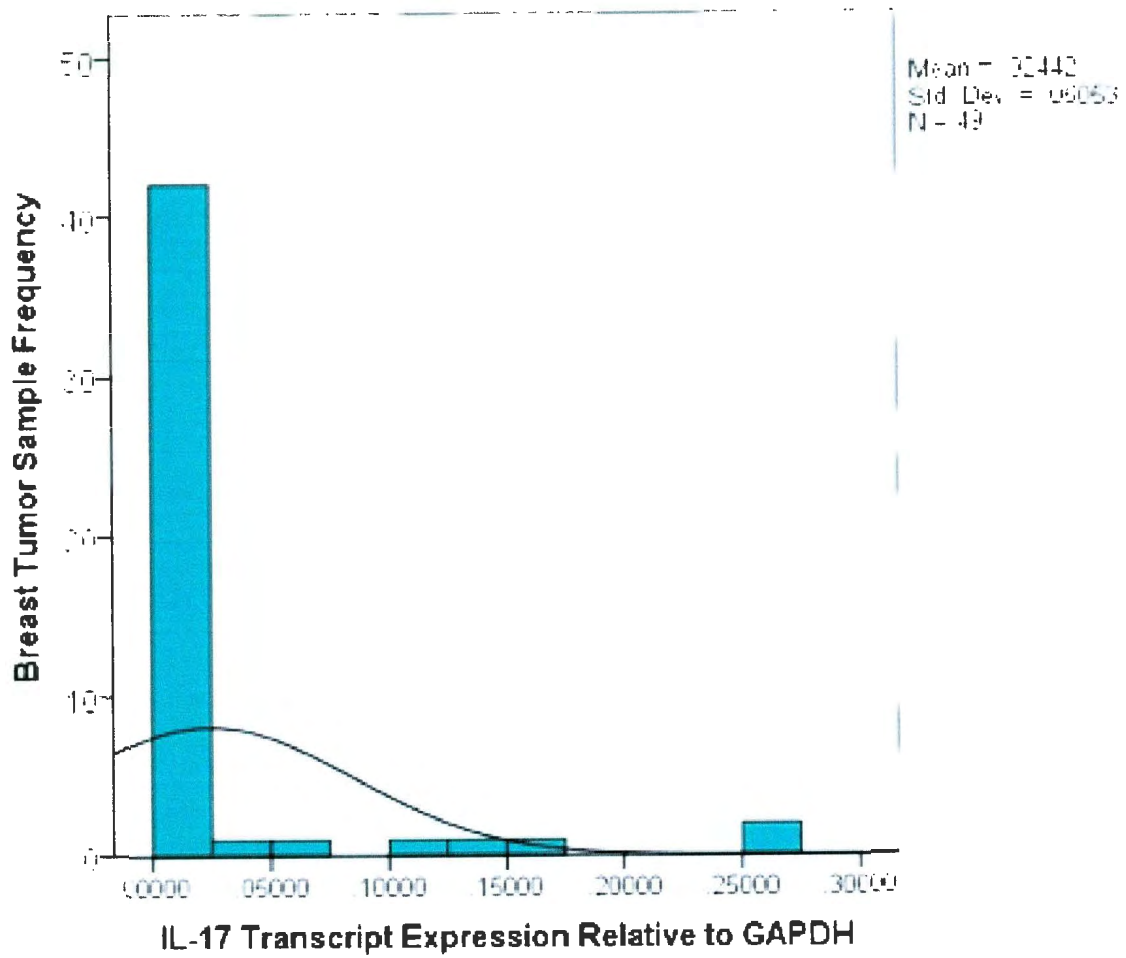


Figure 3.19. *Real-time IL-17 transcript expression in BCT samples.* The figure shows the distribution of IL-17 transcript levels in 49 breast tumor samples. The data are not normally distributed.

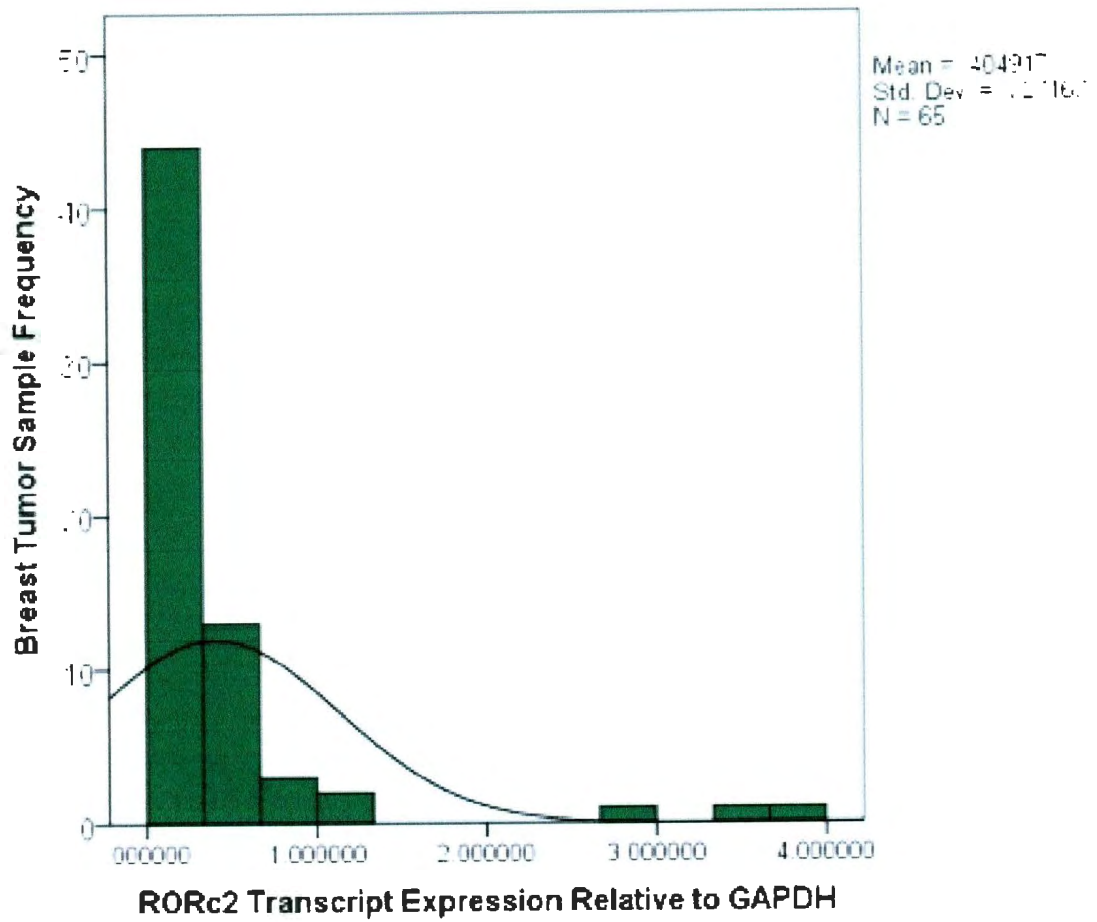


Figure 3.20A. *Real-time RORc2 transcript expression in BCT samples.* The figure shows the distribution of RORc2 transcript levels in 65 breast tumor samples. The data are not normally distributed.

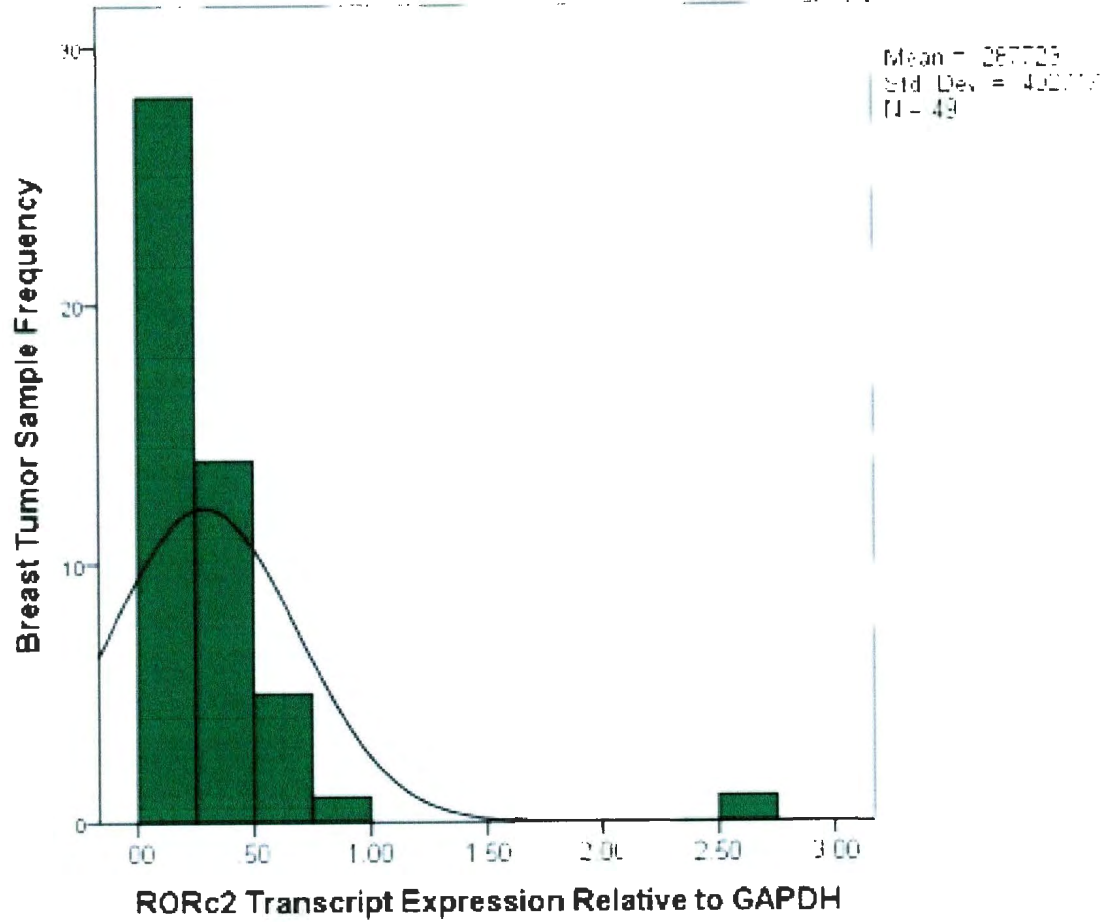


Figure 3.20B. *Real-time RORc2 transcript expression in BCT samples.* The figure shows the distribution of RORc2 transcript levels in 49 breast tumor samples. The data are not normally distributed.

each of the 49 samples and used these values for subsequent analysis (Figure 3.19).

To address the second aim of this project (determine if a correlation exists between intratumoral transcript levels of IL-17, IL-6 and RORc2), we performed a Spearman's correlation analysis among the RT-PCR data collected (IL-17 and IL-6) and the real-time PCR data collected (IL-17 and RORc2). As shown in Table 3.10, there was no significant correlation of IL-17 real-time (mean) with IL-17 RT-PCR, RORc2 (real-time) or IL-6 (RT-PCR). We had expected that the two IL-17 PCRs would correlate, however potential explanations for this poor correlation are discussed in Section 4.3.1. There was no significant correlation between the real-time RORc2 and real-time IL-17 (or RT-PCR IL-17). This is not entirely surprising because RORc2 may be present in breast cancer cells and IL-17 may be absent, as was seen in our analysis of the BCCLs (Figure 3.18). However, real-time levels of RORc2 did significantly correlate with RT-PCR levels of IL-6.

Table 3.10. Spearman's correlation coefficients between IL-17 real-time, IL-17 RT-PCR, RORc2 and IL-6 (N=49)

	IL-17 real-time	IL-17 RT-PCR	RORc2	IL-6
IL-17 real time	1			
IL-17 RT-PCR	0.605	1		
RORc2	0.703	0.644	1	
IL-6	0.334	0.763	0.286*	1

*Real-time RORc2 transcripts correlate with IL-6 RT-PCR (p=0.046)

3.7.1. Derivation of a T_H17 Profile for the Breast Tumor Samples

As T cells, other than CD4⁺ T_H17 cells, are reported to express RORc2, high RORc2 transcripts alone are not good indicators of T_H17 cells. Additionally, 5/6 BCCLs expressed varying levels of RORc2 (Section 3.6). Therefore, RORc2, on its own, is not a

good marker for T_H17 cells. Furthermore, IL-17 can be present in macrophages and therefore, IL-17 is not necessarily indicative of the presence of T_H17 cells. For these reason, levels of RORc2 and IL-17 were analyzed together to identify tumors most likely to have a T_H17 cell profile. Tumors with high frequencies of T_H17 (T_H17^{hi}) should have both RORc2 and IL-17 levels higher than the median (IL-17, median = 0.0029191 (N=49) and RORc2, median = 0.1936 (N=49 or 65)) (see Figure 3.19 and 3.20B for data). Furthermore, tumors were classified as either IL-17^{hi} or RORc2^{hi} if the tumor contained transcript levels higher than the median (ie. A tumor is classified as IL-17^{hi} if IL-17 transcript levels were greater than the median). If the tumor contained transcript levels less than or equal to the median, then the tumor was classified as IL-17^{lo}/RORc2^{lo}. Of the 49 tumors analyzed, 17 tumors were categorized as having a T_H17^{hi} (IL-17^{hi} and RORc2^{hi}) profile, accomplishing our second objective. The T_H17^{hi} profile was not found to correlate with intratumoral transcript levels of IL-6 (data not shown.), accomplishing the first aim of the third objective.

3.7.2. Associations between T_H17 and Tumor Infiltrating Immune Leukocytes

Tumors categorized as IL-17^{hi}, RORc2^{hi}, and T_H17^{hi} were analyzed for associations with T cells using CD3, CD4 and CD8 markers and with macrophages/DCs using CD68 marker, previously obtained by Dr. Sharon Oldford (Section 2.1.) (Oldford et al., 2006). We reasoned that if our derived T_H17 profile was valid (representative of infiltrating CD4⁺ T_H17 cells), the T_H17^{hi} category should positively associate with increased numbers of CD4⁺ T cells in tumor lesions. *Oldford et al.* (2006) had previously characterized immune cell infiltrate using CD3 (total T cells), CD4 (helper, regulatory

and inflammatory T cells), CD8 (cytolytic T cells) and CD68 (macrophages/dendritic cells), we performed a Chi square analysis using the derived IL-17^{hi/lo}, RORc2^{hi/lo} and T_H17^{hi/lo} categories.

Table 3.11A. Chi Square analysis for associations of IL-17 with T cell markers in breast tumor samples

Marker	IL-17 ^{hi}		IL-17 ^{lo}		P-value ^a
	Count (n)	%	Count (n)	%	
<i>CD3</i>					
None-Small	7	29.1	9	52.9	0.124
Moderate-large	17	70.9	8	47.1	
<i>CD4</i>					
None-Small	9	39.1	12	70.6	0.049
Moderate-large	14	60.9	5	29.4	
<i>CD8</i>					
None-Small	13	76.5	12	52.2	0.187
Moderate-large	4	23.5	11	47.8	
<i>CD68</i>					
None-Small	2	8.3	0	0	0.337
Moderate-large	22	91.7	17	100	

a. Pearson Chi Square significance or Fisher's exact test if n<5

b. Significant associations are bolded

Table 3.11B. Chi Square analysis for associations of RORc2 with T cell markers in breast tumor samples

Marker	RORc2 ^{hi}		RORc2 ^{lo}		P-value ^a
	Count (n)	%	Count (n)	%	
<i>CD3</i>					
None-Small	4	22.2	12	52.2	0.063
Moderate-large	14	77.8	11	47.8	
<i>CD4</i>					
None-Small	6	35.3	15	65.2	0.061
Moderate-large	11	64.7	8	34.8	
<i>CD8</i>					
None-Small	8	47.1	17	73.9	0.083
Moderate-large	9	52.9	6	26.1	
<i>CD68</i>					
None-Small	6	33.3	12	52.2	0.228
Moderate-large	12	66.7	11	47.8	

a. Pearson Chi Square significance or Fisher's exact test if n<5

Table 3.11C Chi Square analysis for associations of T_H17 with T cell markers in breast tumor samples

Marker	T _H 17 ^{hi}		T _H 17 ^{lo}		P-value ^a
	Count (n)	%	Count (n)	%	
<i>CD3</i>					
None-Small	1	7.7	15	53.6	0.006
Moderate-large	12	92.3	13	46.4	
<i>CD4</i>					
None-Small	2	16.7	19	67.9	0.005
Moderate-large	10	83.3	9	32.1	
<i>CD8</i>					
None-Small	4	33.3	21	75	0.03
Moderate-large	8	67.7	7	25	
<i>CD68</i>					
None-Small	2	15.4	16	57.1	0.012
Moderate-large	11	84.6	12	42.9	

- a. Pearson Chi Square significance or Fisher's exact test if n<5
- b. Significant associations are bolded

Table 3.11A shows that IL-17^{hi} weakly associates with increased CD4⁺ infiltrating cells. RORc2 (Table 3.10B) does not associate with any of the infiltrating immune cells. There was a trend for high levels of both IL-17 and RORc2 with moderate to large numbers of CD4. However, Table 3.11C shows that the T_H17^{hi} profile significantly associated with increased numbers of T cells (CD3, CD4 and CD8), but not with tumor infiltrating macrophages (CD68). Therefore, these results strongly suggest that the derived T_H17^{hi} profile is a suitable marker for infiltrating CD4⁺ T_H17 cells.

3.7.3. Associations between T_H17 Profiles and HLA-DR Allotypes

In the original study (Oldford et al., 2006), HLA-DR52⁺ tumors were found to associate with decreased RFS and larger tumors. Higher IL-6 transcript levels also associated with decreased RFS and larger tumors. As a result, we predicted that due to the role of IL-6 in the differentiation of T_H17 cells, T_H17 cells may be increased in HLA-

DR52⁺ patients. Following the identification of tumors that were IL-17^{hi}, RORc2^{hi} and T_H17^{hi}, we tested for associations with HLA-DR52 and the associated haplotypes (Tables 3.12A-C)

Table 3.12A. Chi Square analysis for associations of IL-17 with HLA-DR allotypes

HLA-DR allotype	IL-17 ^{hi}		IL-17 ^{lo}		P-value ^a
	Count (n)	%	Count (n)	%	
<i>DR52</i>					0.721
<i>DR52</i> ^{-ve}	13	44.8	10	50	
<i>DR52</i> ^{+ve}	16	55.2	10	50	
<i>DR52DQ7</i>					0.722
<i>DR52DQ7</i> ^{-ve}	23	79.3	15	75	
<i>DR52DQ7</i> ^{+ve}	6	20.7	5	5	
<i>DRB3*01</i>					0.408
<i>DRB3*01</i> ^{-ve}	22	75.9	13	65	
<i>DRB3*01</i> ^{+ve}	7	24.1	7	35	
<i>DRB3*02</i>					0.646
<i>DRB3*02</i> ^{-ve}	20	69	15	75	
<i>DRB3*02</i> ^{+ve}	9	31	5	25	
<i>DRB3*03</i>					0.507
<i>DRB3*03</i> ^{-ve}	20	100	27	93.1	
<i>DRB3*03</i> ^{+ve}	0	0	2	6.9	

a. Pearson Chi Square Significance or Fisher's Exact Test if n<5

Table 3.12B. Chi Square analysis for associations of RORc2 with HLA-DR allotypes

HLA-DR allotype	RORc2 ^{hi}		RORc2 ^{lo}		P-value ^a
	Count (n)	%	Count (n)	%	
<i>DR52</i>					0.879
<i>DR52</i> ^{-ve}	12	48	11	45.8	
<i>DR52</i> ^{+ve}	13	52	13	54.2	
<i>DR57DQ7</i>					0.792
<i>DR52DQ7</i> ^{-ve}	19	76	19	79.2	
<i>DR52DQ7</i> ^{+ve}	6	24	5	20.8	
<i>DRB3*01</i>					0.175
<i>DRB3*01</i> ^{-ve}	20	80	15	62.5	
<i>DRB3*01</i> ^{+ve}	5	20	9	37.5	
<i>DRB3*02</i>					0.588
<i>DRB3*02</i> ^{-ve}	17	68	18	75	
<i>DRB3*02</i> ^{+ve}	8	32	6	25	
<i>DRB3*03</i>					1.0
<i>DRB3*03</i> ^{-ve}	24	96	23	95.8	
<i>DRB3*03</i> ^{+ve}	1	4	1	4.2	

a. Pearson Chi Square Significance or Fisher's Exact Test if n<5

Table 3.12C. Chi Square analysis for associations of T_H17 with HLA-DR allotypes

HLA-DR allotype	T _H 17 ^{hi}		T _H 17 ^{lo}		P-value ^a
	Count (n)	%	Count (n)	%	
<i>DR52</i>					
<i>DR52</i> ^{-ve}	8	47.1	15	46.9	0.990
<i>DR52</i> ^{+ve}	9	52.9	17	53.1	
<i>DR52DQ7</i>					
<i>DR52DQ7</i> ^{-ve}	14	82.4	24	75	0.725
<i>DR52DQ7</i> ^{+ve}	3	17.6	8	25	
<i>DRB3*01</i>					
<i>DRB3*01</i> ^{-ve}	14	82.4	21	65.6	0.323
<i>DRB3*01</i> ^{+ve}	3	17.6	11	34.4	
<i>DRB3*02</i>					
<i>DRB3*02</i> ^{-ve}	11	64.7	24	75	0.448
<i>DRB3*02</i> ^{+ve}	6	35.3	8	25	
<i>DRB3*03</i>					
<i>DRB3*03</i> ^{-ve}	16	94.1	31	96.9	1.0
<i>DRB3*03</i> ^{+ve}	1	5.9	1	3.1	

a. Pearson Chi Square Significance or Fisher's Exact Test if n<5

The data in Tables 3.12A-C, show no significant correlations between HLA-DR allotypes and the presence of high IL-17, RORc2 and T_H17 profiles. Analysis on additional tumors may answer this question more definitively.

3.7.4. Associations between T_H17 Profiles and Prognostic Indicators

A third aim of the third objective was to determine if T_H17 associated with prognostic indicators. Tables 3.13A-D show there are very few associations with the prognostic indicators, such as tumor size, tumor type, tumor grade, clinical lymph node status, estrogen receptor, progesterone receptor, HER2/neu and age of diagnosis, and IL-17, RORc2 and T_H17 profiles.

Table 3.13A. Chi Square analysis for associations of IL-17 with prognostic indicators

Prognostic Factor	IL-17 ^{hi}		IL-17 ^{lo}		P-value ^a
	Count (n)	%	Count (n)	%	
<i>Tumor Size</i>					
≤ 2 cm	9	31	3	15.8	0.316
> 2 cm	20	69	16	84.2	
<i>Tumor Type</i>					
IDC	24	82.8	13	68.4	0.248
Others	5	17.2	6	31.6	
<i>Tumor grade</i>					
Grade I+II	17	60.7	17	89.5	0.046
Grade III	11	39.3	2	10.5	
<i>Clinical Node Status</i>					
Negative	11	39.3	9	45	0.692
Positive	17	60.7	11	55	
<i>Estrogen Receptor</i>					
ER ^{-ve}	7	24.1	6	30	0.648
ER ^{+ve}	22	75.9	14	70	
<i>Progesterone Receptor</i>					
PR ^{-ve}	11	37.9	3	15	0.112
PR ^{+ve}	18	62.1	17	85	
<i>HER2/Neu</i>					
Codes 0-2	16	72.7	15	93.8	0.203
Code 3	6	27.3	1	6.2	

- a. Pearson Chi Square Significance or Fisher's Exact Test if n<5
b. Significant associations are bolded

3.13B. Chi Square analysis for associations of RORc2 with prognostic indicators

Prognostic Factor	RORc2 ^{hi}		RORc2 ^{lo}		P-value ^a
	Count (n)	%	Count (n)	%	
<i>Tumor Size</i>					
≤ 2 cm	5	20	7	30.4	0.404
> 2 cm	20	80	16	69.6	
<i>Tumor Type</i>					
IDC	16	64	21	91.3	0.039
Others	9	36	2	8.7	
<i>Tumor grade</i>					
1&2	19	79.2	16	65.2	0.285
3	5	20.8	8	34.8	
<i>Clinical Node Status</i>					
Negative	12	50	8	33.3	0.242
Positive	12	50	16	66.7	
<i>Estrogen Receptor</i>					
ER ^{-ve}	6	24	7	29.2	0.682
ER ^{+ve}	19	76	17	70.8	
<i>Progesterone Receptor</i>					
PR ^{-ve}	9	36	5	20.8	0.240
PR ^{+ve}	16	64	19	79.2	
<i>HER2/Neu</i>					
Codes 0-2	12	75	19	86.4	0.425
Code 3	4	25	3	13.6	

- a. Pearson Chi-Square significance or Fisher's Exact Test if n<5
- b. Significant associations are bolded

3.13C. Chi Square analysis for associations of T_H17 with prognostic indicators

Prognostic Factor	T _H 17 ^{hi}		T _H 17 ^{lo}		P-value ^a
	Count (n)	%	Count (n)	%	
<i>Tumor Size</i>					
≤ 2 cm	3	17.6	9	29	0.497
> 2 cm	14	82.4	22	71	
<i>Tumor Type</i>					
IDC	12	70.6	25	80.6	0.428
Others	5	29.4	6	19.4	
<i>Tumor grade</i>					
1&2	11	68.8	23	74.2	0.693
3	5	31.2	8	25.8	
<i>Clinical Node Status</i>					
Negative	8	50	12	37.5	0.408
Positive	8	50	20	62.5	
<i>Estrogen Receptor</i>					
ER ^{-ve}	5	29.4	8	25	0.739
ER ^{+ve}	12	70.6	24	75	
<i>Progesterone Receptor</i>					
PR ^{-ve}	7	41.2	7	21.9	0.155
PR ^{+ve}	10	58.8	25	78.1	
<i>HER2/Neu</i>					
Codes 0-2	7	63.6	24	88.9	0.161
Code 3	4	36.4	3	11.1	

a. Pearson Chi-Square significance or Fisher's Exact Test if n<5

3.13D. Associations of IL-17, RORc2 and T_H17 with age of diagnosis

	IL-17		RORc2		T _H 17	
	High	Low	High	Low	High	Low
Count	29	20	25	24	17	32
Mean (age)	57.38	65.26	59.36	61.88	55.71	63.19
Significance ^a	0.037		0.506		0.055	

a. ANOVA

b. Significant associations are bolded

RORc2^{hi} associated with increased frequency of invasive ductal carcinoma. ANOVA analysis also revealed that T_H17^{hi} and IL-17^{hi} profiles trended with a younger age of diagnosis (p = 0.055 and p = 0.037, respectively). As younger age at diagnosis is a

poor prognosis, the presence of IL-17 or T_H17 cells may have a role in promoting breast cancer in younger women (Carlson et al., 2009, McPherson et al. 2000).

3.7.5. Analysis of HLA-DR52 stratified by IL-17 and T_H17 Profiles on Age of Diagnosis

Early age of onset of breast cancer was reported to be associated with an HLA-DR52 subtype (DRB3*02) (Chaudhuri et al., 2005) and we found that reduced age at diagnosis associated with both IL-17^{hi} and T_H17^{hi}. Therefore, we determined the associations of HLA-DR52, stratified by IL-17^{hi/lo} and T_H17^{hi/o}, with the age of diagnosis (Figure 3.21A-B). As shown in Figure 3.21B, HLA-DR52⁺ patients whose tumors had a T_H17 profile were diagnosed at a significantly younger age in comparison to those that are either T_H17^{lo} or HLA-DR52⁻ (p=0.013).

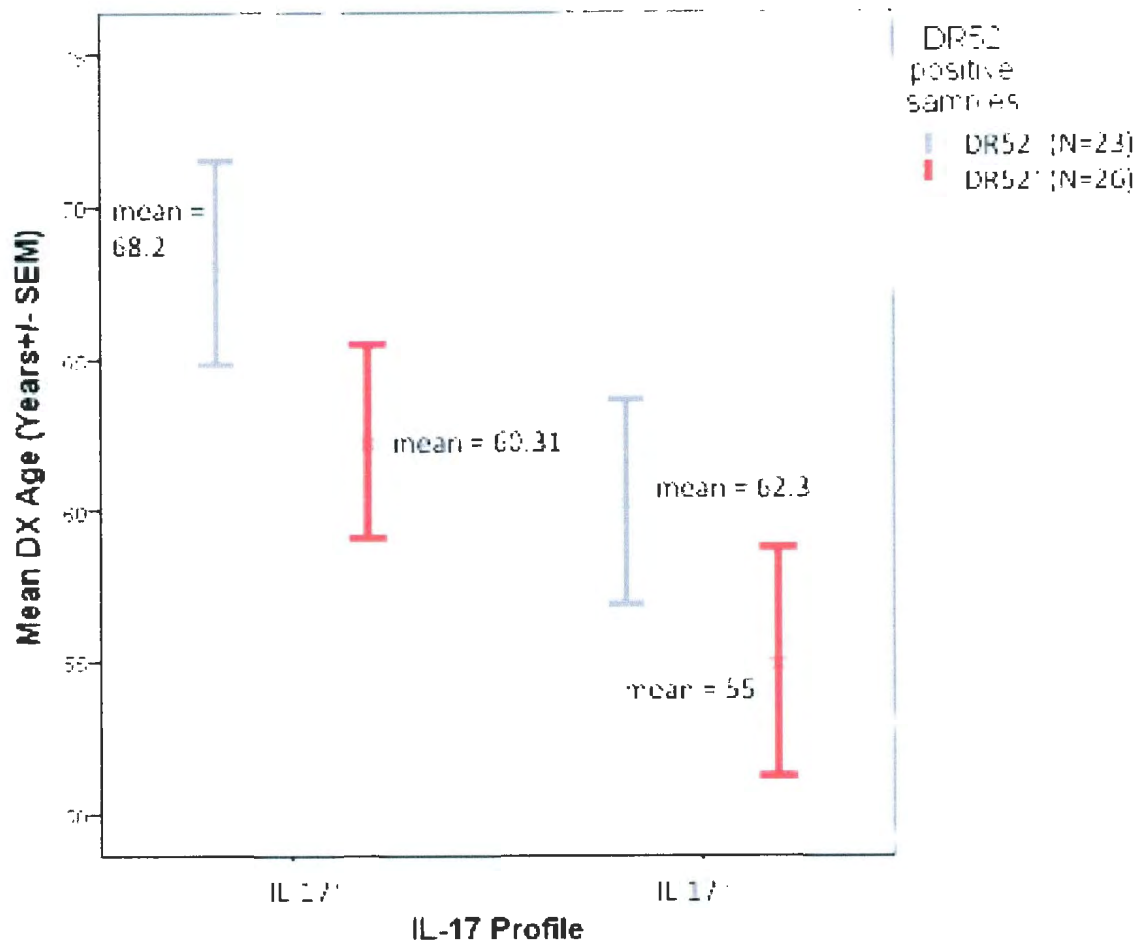


Figure 3.21A. ANOVA analysis of HLA-DR52 stratified by IL-17 profiles on age at diagnosis. The graph has the age at diagnosis on the y-axis and the IL-17 profile categories on the x-axis. The grey bars represent HLA-DR52⁻ and the red bars represent HLA-DR52⁺. The mean age is given adjacent to each error bar. There were no significant associations.

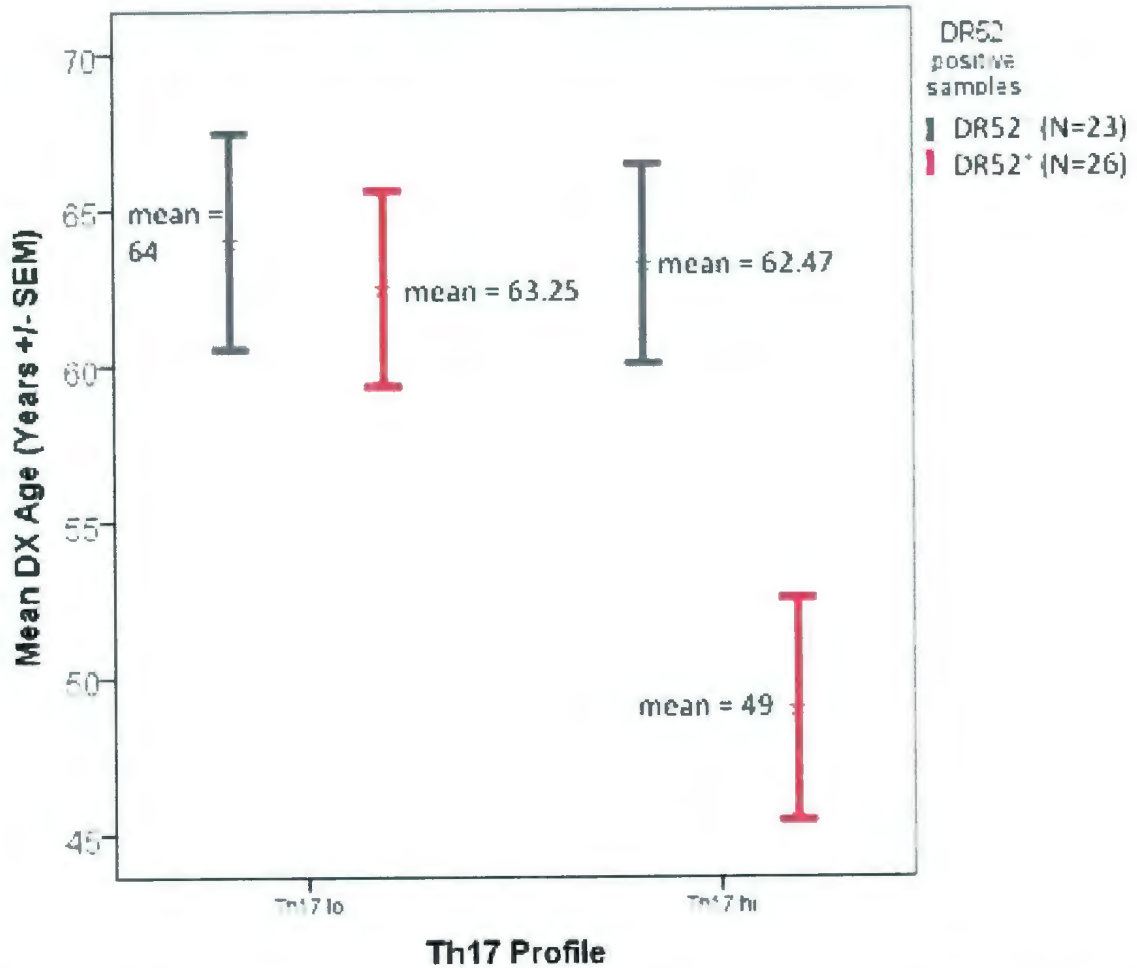


Figure 3.21B. ANOVA analysis of HLA-DR52 stratified by T_H17 profiles on age at diagnosis. The graph has the age at diagnosis on the y-axis and the T_H17 profile categories on the x-axis. The grey bars represent HLA-DR52⁻ and the pink bars represent HLA-DR52⁺. The mean age is given adjacent to each error bar. There was a significant association ($p=0.013$).

3.7.6. Associations between T_H17 Profiles and Overall Survival

The final aim of the final objective was to determine whether breast cancer patients with a IL-17^{hi}, RORc2^{hi} or T_H17^{hi} profile had decreased RFS/OS than patients with a IL-17^{lo}, RORc2^{lo} or T_H17^{lo} profile. To test this hypothesis, we used the Kaplan-Meier statistical test. Patients with IL-17^{hi} patients did not have significantly decreased to time to recurrence (months until distant or regional recurrence) (Figure 3.22A) as compared to patients with IL-17^{lo}. However, there was a trend for IL-17^{hi} and decreased OS (months until death due to disease) (log rank = 3.161, p = 0.075) (Figure 3.22B). Levels of RORc2 were found to neither correlate or trend with RFS and OS (Figure 3.23A-B). Patients with T_H17^{hi} profiles had a decreased RFS (log rank = 1.207 and p = 0.272), shown in Figure 3.24A. Furthermore, tumors with T_H17^{hi} profiles had decreased OS (log rank = 2.488 and p = 0.115), shown in Figure 3.24B. However, both of these trends are not significant.

A)

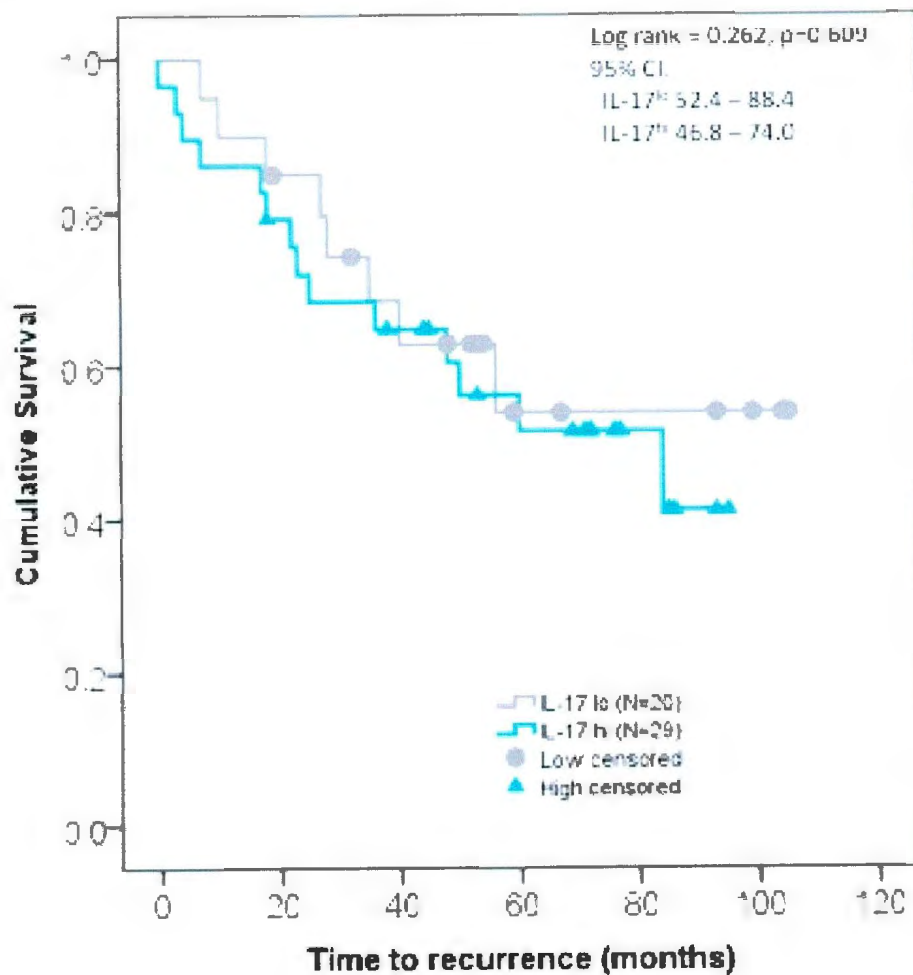


Figure 3.22A. Kaplan-Meier analysis of IL-17 profiles with RFS in breast cancer patients. A) IL-17^h (blue line) is not associated with decreased RFS in comparison to IL-17^{lo} (grey line). The 95% confidence intervals (CI) are listed in the top right, along with log rank and significance.

B)

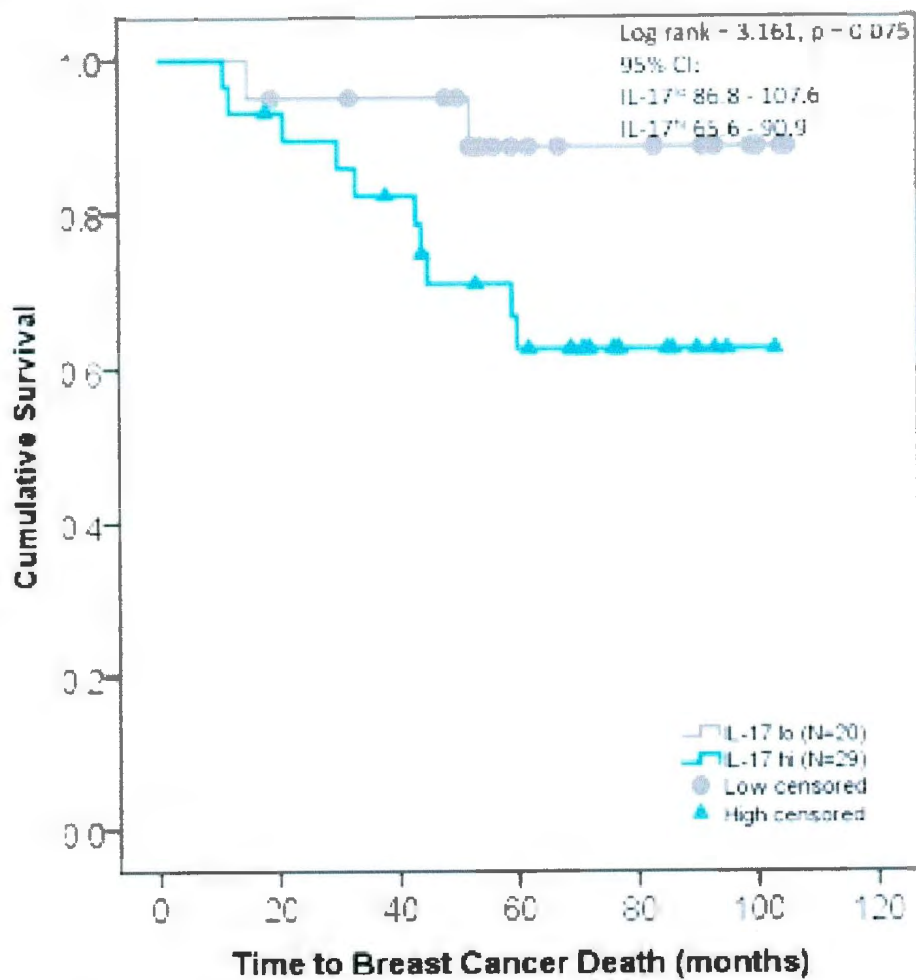


Figure 3.22B. Kaplan-Meier analysis of IL-17 profiles with OS in breast cancer patients. **B)** IL-17^{hi} (blue line) trends with decreased OS in comparison to IL-17^{lo} (grey line). The 95% confidence intervals (CI) are listed in the top right, along with log rank and significance.

A)

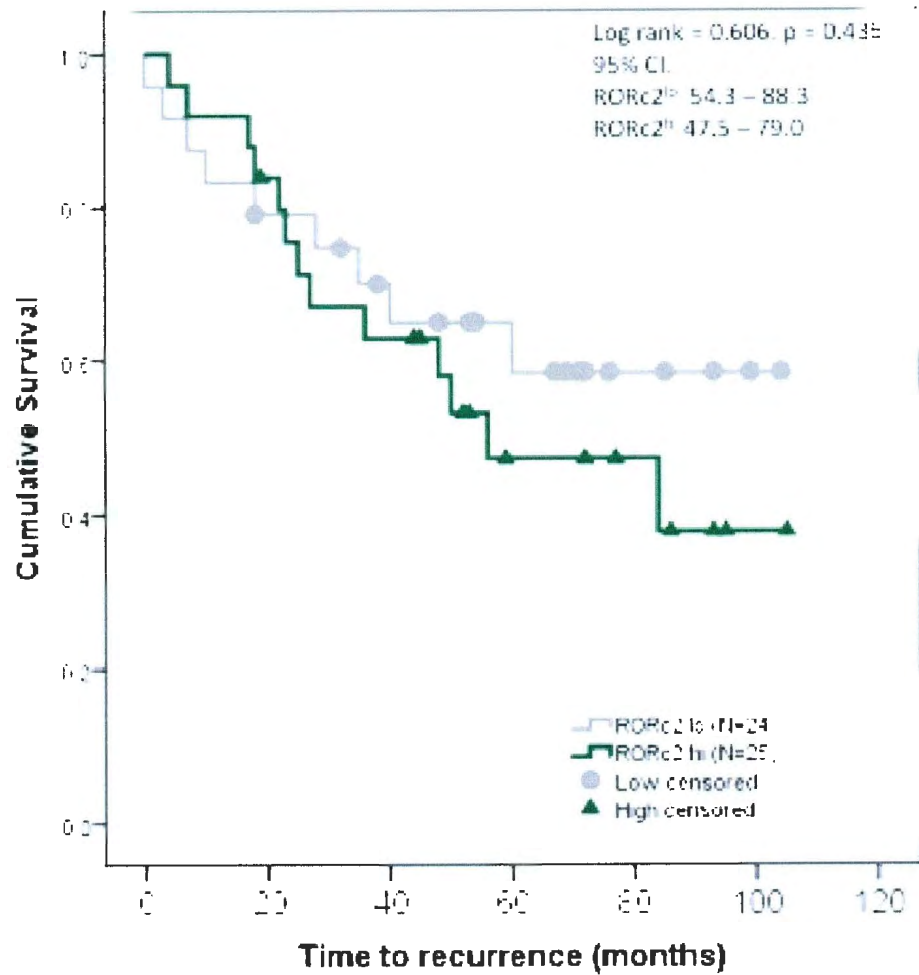


Figure 3.23A. Kaplan-Meier analysis of RORc2 profiles with RFS in breast cancer patients. A) RORc2^{hi} (green line) does not trend or associate with decreased RFS in comparison to RORc2^{lo} (grey line). The 95% confidence intervals (CI) are listed in the top right, along with log rank and significance.

B)

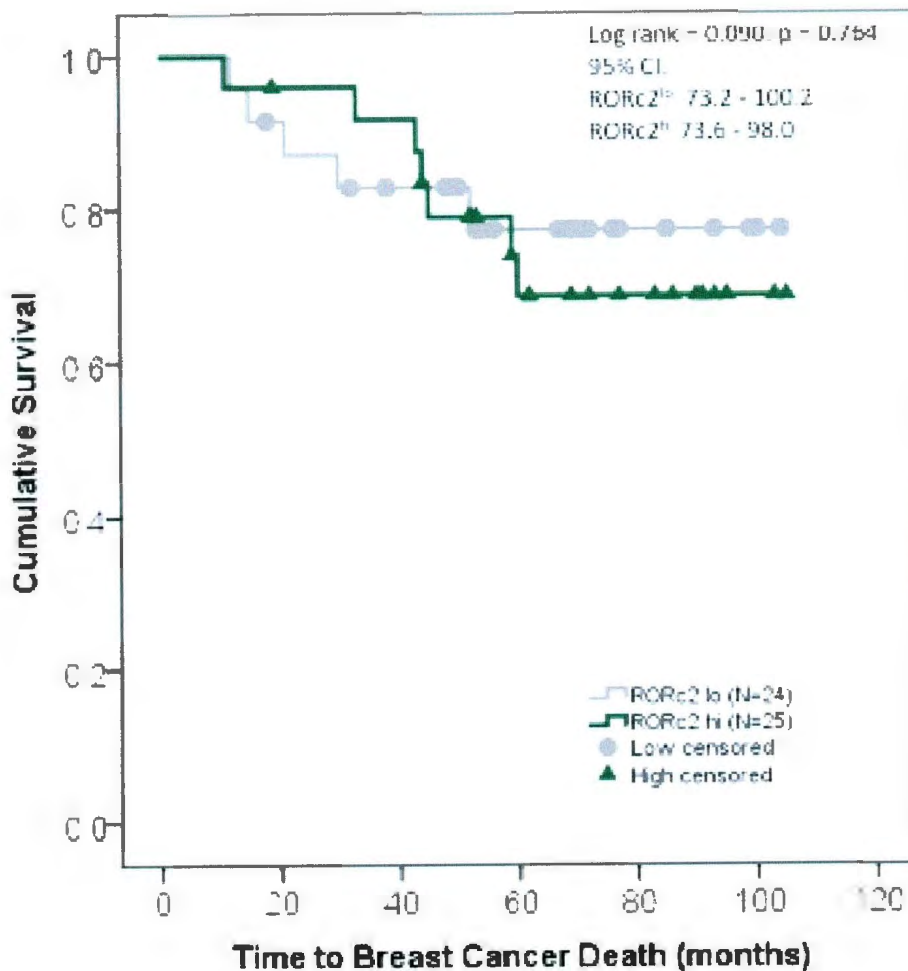


Figure 3.23B. Kaplan-Meier analysis of *fRORc2* profiles with OS in breast cancer patients. **B)** RORc2^{hi} (green line) does not associate or trend with decreased OS in comparison to RORc2^{lo} (grey line). The 95% confidence intervals (CI) are listed in the top right, along with log rank and significance.

A)

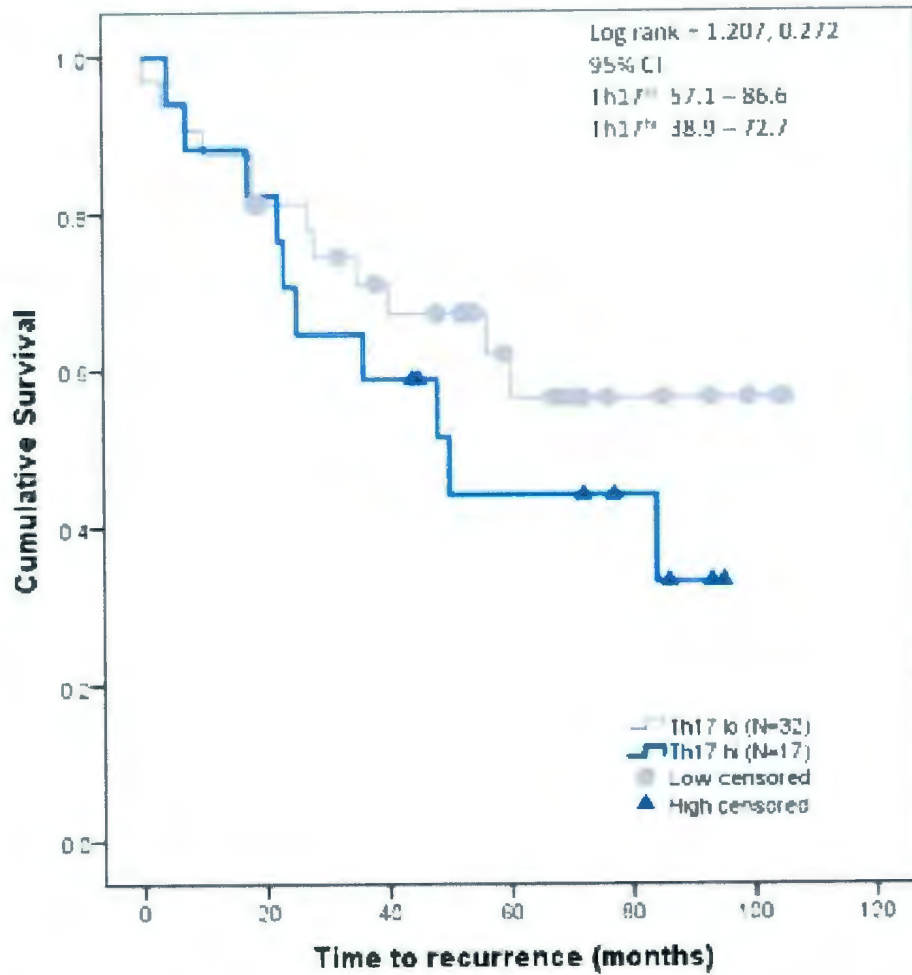


Figure 3.24A. Kaplan-Meier analysis of T_H17 profiles with RFS in breast cancer patients. **A)** T_H17^{hi} (navy line) does not trend or associate with decreased RFS in comparison to T_H17^{lo} (grey line). The 95% confidence intervals (CI) are listed in the top right, along with log rank and significance.

B)

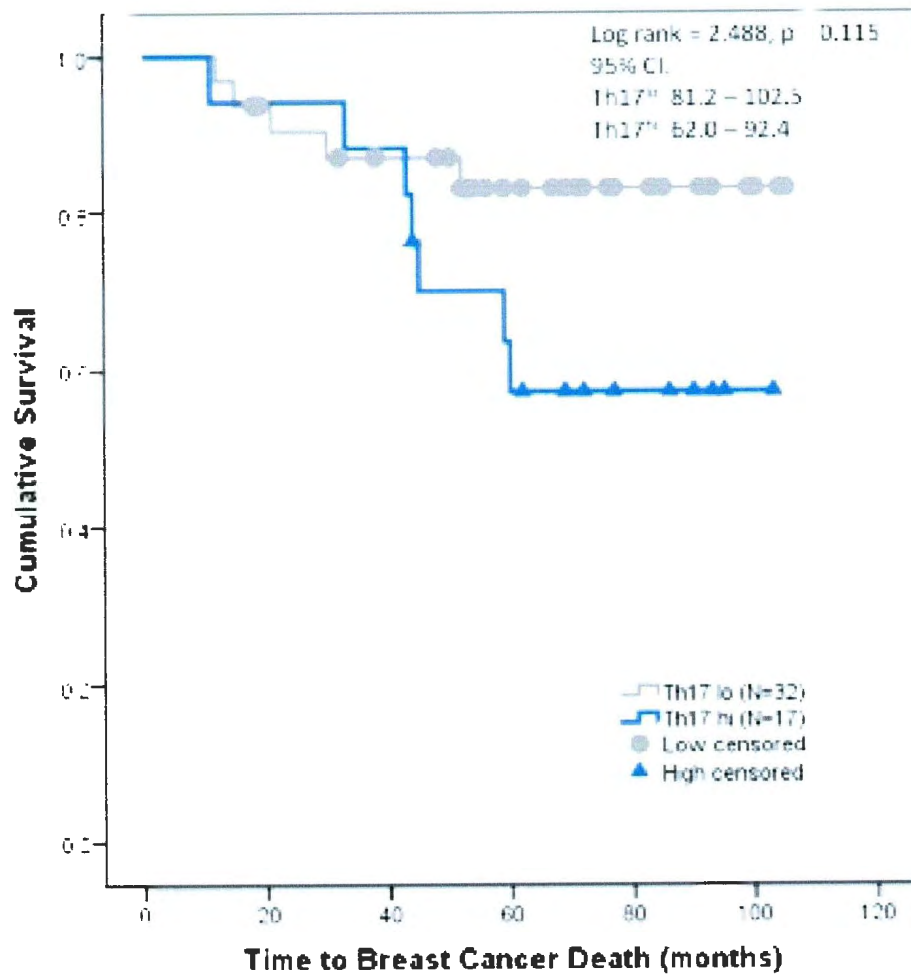


Figure 3.24B. Kaplan-Meier analysis of T_H17 profiles with OS in breast cancer patients. **B)** T_H17^{hi} (navy line) trends with decreased OS in comparison to T_H17^{lo} (grey line). The 95% confidence intervals (CI) are listed in the top right, along with log rank and significance.

3.8. Immunohistochemistry Results

Section 2.6. detailed the procedure for the immunohistochemistry assays. Our initial intent was to dual stain 40 breast tumor slides using antibodies specific for IL-17 (cytoplasm) and RORc (nucleus). In this way, a T_H17 cell could be identified through protein expression if dual staining occurred.

3.8.1. Positive and Negative Controls

Prior to starting this study, the Drover laboratory had successfully developed an IHC technique for doubling staining of CD3 (cytoplasmic) and FOXP3 (nuclear) with antibody binding, optimized as described (Section 2.6). Figure 3.25. is a representative image of dual staining exhibited on a breast cancer lesion (Drover. S, unpublished data). Using the same antibodies, I was able to replicate these results on tonsil tissue and was optimistic that we would have similar success using IL17 and RORc antibodies. While CD3 and FOXP3 were mouse antibodies, IL-17 and RORc were rabbit antibodies. To ensure that procedures involving rabbit antibodies performed equally well we tested a rabbit anti-HER2 and irrelevant rabbit IgG on control slides that were previously prepared in Dr. Drover's laboratory. Sections were from FFPE cell-pellets containing HER2-overexpressing breast cancer cells (SK-BR-3) plus B-and T-cells. The rabbit anti-HER2 antibody bound strongly to cytoplasmic and membrane HER2, but did not bind the other cell types, while the irrelevant antibody did not bind appreciably (data not shown). As these assays were successful, we were confident that the procedures and reagents were performing well and proceeded with optimizing the conditions for IHC using IL-17 and RORc.

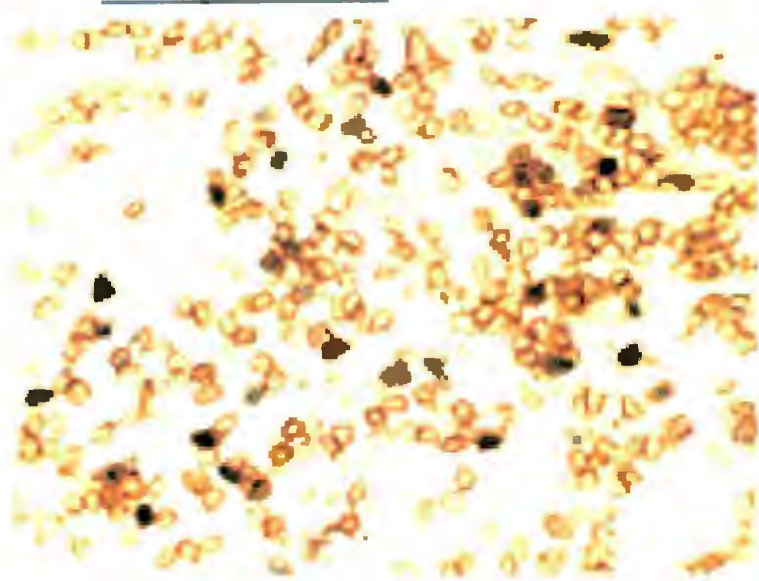


Figure 3.25. *Dual IHC staining of sections from breast cancer lesions using antibodies to FOXP3 and CD3. Co-staining of the section is represented above with FOXP3 (nuclei, dark blue) and the cytoplasm (brown) of CD3⁺ T-cells.*

3.8.2 IL-17 Immunohistochemistry Results

With respect to the IL-17 antibody, we started with the recommended dilutions of the stock IL-17A antibody (200 µg/mL) which was between 1 µL of antibody:50 µL of VAD (4 µg/mL) and 1 µL of antibody:400 µL of VAD (0.5 µg/mL). The concentration of 0.5 µg/mL gave the lowest background staining, with specific cytoplasmic staining. However, regardless of the dilution, the IL-17 antibody stained the nucleus, leading to a high background staining of the tonsil tissue section.

In an attempt to decrease the nuclear staining, we decreased the concentration of the primary antibody, resulting in little to no specific cytoplasmic staining with weak nuclear staining. We also tried reducing the antigen retrieval time to 20 minutes (rather than 60 minutes), tried a different antigen retrieval solution (CC1) and altered the order of addition of the NHS and H₂O₂. Despite our efforts, we could not eliminate the nuclear staining. As the intent was to stain the nucleus as well, high nuclear background staining was problematic. Therefore, although there was positive cytoplasmic staining, the high background nuclear staining was a cause for concern as it would interfere with dual staining.

3.8.3 RORc Immunohistochemistry Results

The two RORc antibodies also produced high background staining, as well as cytoplasmic staining of the thymus slides. To try and eliminate the background staining, we tried similar procedures as we had for IL-17A antibody optimization, but had no success. Furthermore, as mentioned in Section 2.6.5., RORc is specific for both variants of RORc: RORc1 and RORc2 (Medvedev et al., 1997; Villey et al., 1999). The primary

difference between the two isoforms is that RORc2 has a shorter N-terminus (Villey et al., 1999). Although RORc2 is restricted to the thymus and is the transcription factor for T_H17 cells, RORc1 is expressed in many tissues, including the thymus, lung, and skeletal muscle (Hirose et al., 1994; Medvedev et al., 1997; Villey et al., 1999). Therefore, using an antibody specific for both isoforms is problematic as specific staining for RORc2 cannot be determined accurately and RORc1 is widely expressed.

As a result of these problems, the IHC staining was not carried out on the breast tumor slides. Potential future approaches for IHC are described in Section 4.8.

Chapter 4. Discussion

4.1. Summary of Research

As described previously (Sections 1.1 and 1.6) the hypothesis and work described in this thesis stemmed from results of a previous study in the Drover lab (Oldford et al., 2006): As IL-6 is required for the differentiation of a naïve T cell into a T_H17 cell, we hypothesized that higher levels of T_H17 cells would be present in tumors that had higher IL-6 transcripts and HLA-DR52⁺ haplotypes.

To test these research objectives, we determined transcript levels of RORc2 and IL-17 and developed a T_H17 profile for each tumor. T_H17^{hi} tumors were those with IL-17 and RORc2 transcript levels greater or equal to the median (N=17) and all other categories (IL-17<median and RORc2 >median, IL-17>median and RORc2<median) were T_H17^{lo}. We then used to these profiles in statistical tests to determine associations with IL-6, infiltrating T cells, HLA-DR52, prognostic indicators and survival.

Although the necessary experimentation was conducted to answer our objectives, there are several caveats. First, the original samples size of 65 tumor samples from 65 patients was small but was subsequently reduced to 49 tumors/patients due to the RIN values obtained. Secondly, RORc2 PCR analysis was done once, using real-time RT-PCR, in triplicate and ideally should have been repeated to provide the results with confidence and reliability. Although the samples were run in triplicate, due to small sample quantities, these assays were only analyzed once. Thirdly, the IL-17 traditional RT-PCR and real-time PCR data does not correlate. However, we tried to overcome this obstacle by performing the real-time analysis twice and obtained an excellent correlation

($p < 0.000$ between the two real-time PCR assays of IL-17). Lastly, we were only able to carry out analysis on breast tumor mRNA, transcribed into cDNA, through PCR experimentation. Our initial plan was to additionally carry out IHC on paraffin embedded breast tumor samples. However, there was no acceptable antibody available specific for RORc2. Furthermore, it was challenging to optimize the IL-17A antibody we intended to use. Until an antibody becomes available for RORc2, rather than RORc, we felt that we could not obtain an accurate representation of the T_H17 cells present in the tumor samples.

The following chapter will explore our results and discuss the problems that we encountered.

4.2. Breast Cancer Cell Line Preliminary Research

Prior to analysis of the breast tumor samples, we thought it prudent to analyze breast cancer cell lines for IL-17, IL-6, TGF- β , RORc2 and FOXP3 transcripts. FOXP3 is reported to be expressed in several human cancer lines, including BCCLs (Karanikas et al., 2008). As FOXP3 expression is used to determine a T_{reg} phenotype, its expression in breast cancer cells may lead to false positives. As we were developing a T_H17 profile, it was important to know if BCCLs endogenously transcribe IL-17 or RORc2 to have a better understanding of the tumor milieu. Although IL-17 was not detected by conventional or real-time PCR (Figures 3.10 and 3.18), RORc2 was detected at moderate to high levels in 5/6 BCCLs tested by real-time PCR (Figure 3.18). Based on these findings, RORc2 was not considered a reliable indicator for T_H17 alone. However, although IL-17 was not detected in the BCCLs, infiltrating macrophages, which are

abundant in breast cancer (Oldford et al., 2006), produce IL-17 (Zhu et al., 2008). Therefore, IL-17 would also be considered an unreliable sole marker for T_H17 cells. Therefore to develop T_H17 profile, we decided to use both markers.

IL-6 and TGF- β are required to differentiate T_H17 cells and, therefore, the BCCLs mRNA was tested for presence of these cytokines transcripts. In determining the transcript levels of these cytokines in the BCCLs, one could infer if the tumor cells secrete these cytokines, the tumor cells could impact the plasticity of T cells. *Xu et al.* (2007) found that CD4⁺CD25⁺FOXP3⁺GFP⁺ T regulatory cells could differentiate into T_H17 cells in the presence of IL-6 and absence of TGF- β in FOXP3-GFP knock-in C57BL/6 mice (Xu et al., 2007). This study supports the notion that a T_{reg} cell can differentiate into a T_H17 cell, given certain conditions. Therefore, it is possible the same plasticity exists in a tumor environment.

Although IL-6 and TGF- β are required for the commitment and differentiation of the T_H17 lineage, TGF- β alone promotes a regulatory T cell response. MDA-MB-468, MDA-MB-435, T-47D and MCF-7 all contained higher transcript levels of TGF- β . As TGF- β levels influence a T cell's plasticity towards a T_{reg} phenotype (Bettelli et al., 2006; Pan et al., 2011), we thought that there might be a correlation between FOXP3 and TGF- β levels. However, when we analyzed the transcript levels of FOXP3 within the BCCLs, there were minimal amounts of FOXP3 detected in all 8 cell lines, including those with high TGF- β .

Karanikas et al. (2008) analyzed FOXP3 and TGF- β by RT-PCR and real-time RT-PCR, in 25 different human cancer cell lines, including MCF-7, T-47D, BT20, and MDA-MB-231. They found high levels of FOXP3 (relative to β -actin) in the MCF-7 cell

line and low amounts in T-47D, MDA-M31, and BT20. With respect to TGF- β , MCF-7 was found to express the most TGF- β transcript. MDA-MB-231 and BT20 contained less TGF- β transcript than MCF-7. They reported a significant association between levels of FOXP3 and TGF- β in 25 cancer cells studied ($p=0.009$). Interpretation of these results could suggest a relationship between FOXP3 and TGF- β . When comparing findings by *Karanikas et al.* (2008) to my results, there were some discrepancies. Although, there was a trend for MCF-7, MDA-MB-231 and T-47D to contain higher TGF- β transcripts, there were no discernible differences in the transcript levels of FOXP3 in the BCCLs that we analyzed. This may be attributed to a different relative control; our lab used GAPDH whereas their study used β -actin. However, a more likely possibility for the differences in the FOXP3 data could be attributed to the culture of the breast cancer cells in different media. The Karanikas lab supplemented their medium with 17β -estradiol, hydrocortisone, sodium selenite, insulin and transferrin. These supplements may have an effect of transcription of FOXP3. For example, 17β -estradiol has been shown to augment FOXP3 expression in vitro and vivo mice studies (Polanczyk et al., 2004), which could potentially explain why they found increased FOXP3 in cell lines with high TGF- β .

4.3. PCR Analysis of Breast Tumor Samples

Our finding that IL-17 levels obtained by conventional RT-PCR did not correlate with those obtained by conventional real-time RT-PCR was perplexing and there is no clear explanation. Proper optimization of RT-PCR had been done (described in Section 3.1) and the IL-17 real-time primer kit was predesigned from Taqman Gene Expression assays. According to the product specifications for the IL-17 primer set (catalog number:

HS00174383_m1), there was only one reference sequence, NM_002190.2, which corresponds to IL-17A. The amplicon length of the product was 80 base pairs, which is typical for real-time RT-PCR products (less than 100 base pairs). The product size was confirmed using an agarose gel (data not shown). Therefore, as this product was ready made and used in previous publications for identifying the IL-17 transcript, the real-time RT-PCR primers should be more accurate and reliable than conventional RT-PCR.

As well, there are significant limitations to traditional PCR. In particular, the results are obtained from the end point of the reaction. End point detection has poor precision, low sensitivity, low resolution, results are not expressed numerically and ethidium bromide staining is not very quantitative. Bands are quantified through digitization, which varies according to programs and is dependent upon the image quality produced by the equipment. Real-time PCR is able to detect PCR products as the reaction is proceeding. Therefore, the results are obtained linearly as opposed to the end-point. Taking these factors into consideration we choose to proceed to use the real-time values of IL-17 for the development of a T_H17 profile.

Real-time levels of RORc2 were determined for the 65 samples, although, the 49 samples with $RIN \geq 5$ were used for the T_H17 profile. There was no significant correlation noted between the RORc2 and IL-17 transcripts, regardless of whether the IL-17 transcript levels were determined by real-time PCR or RT-PCR. This was somewhat surprising as we expected a positive correlation between the main cytokine (IL-17A) and the transcription factor (RORc2) for T_H17 cells. However, the fact that the RORc2 did not correlate with IL-17 transcript levels is not unique to the T_H17 cell profile as similar findings were described by *Kitamura et al.* (2005) concerning T_H2 cells. This study

reported that the transcription factor, GATA3, did not correspond to mRNA levels of T_H2 cytokines IL-4 and IL-5 (Kitamura et al., 2005).

Additional studies could analyze the transcript or protein levels of STAT3 as STAT3 is a precursor to RORc2. IL-23R levels could also be analyzed as it is required for the stabilization of T_H17 cells. Having a better understanding of these levels with respect to both IL-17 and RORc2 could assist in determining whether the real-time or the RT-PCR method is more reliable.

4.4. The Relationships between IL-6 and the T_H17 Profile within the Breast Tumor Samples

Although IL-6 transcripts had been previously done once on breast cancer samples (Oldford et al., 2006), we chose to repeat it on the samples. The previous assay used β -actin as the endogenous control. As we were using GAPDH as the endogenous control for IL-17 and RORc2 assays, we re-analyzed IL-6 samples to determine the relative quantity present with respect to GAPDH. Furthermore, the gels were analyzed using different imaging and digitalization software. Despite these differences, using Spearman's correlation test, IL-6 transcript levels significantly correlated with values previously collected ($p=0.05$). This significant correlation provides us with confidence that the transcript levels of IL-6 reported in this thesis are valid.

One of the aims for this thesis was to determine if a relationship existed between IL-6 and T_H17 markers and T_H17 cells. Although IL-6 did not correlate with IL-17 or the T_H17^{hi} profile, we found an association between RORc2 and IL-6 ($p=0.046$). As described in Section 1.3.4., IL-6 is required to activate STAT3, which subsequently leads

to RORc2 expression (Xu et al., 2007) and therefore, we would expect a correlation between RORc2 and IL-6. Yet, because there was a lack of correlation between IL-6 and IL-17 and T_H17^{hi}, we suggest that T_H17 cells may be recruited to the tumor site, rather than differentiate within the site. This could be explored by determining if the ligands, CXCL12 and/or CCL20, which bind to the chemokine receptors, CXCR4 and CCR6 that are abundantly expressed on T_H17 cells (Zou et al., 2010; Yamazaki et al., 2008; Boisvert et al., 2010), are secreted by the tumor cells. Their presence would suggest that T_H17 cells migrate to, rather than differentiate in the tumor milieu. Determining if these ligands are present in the tumor milieu may provide us insight into whether T_H17 cells migrate to or differentiate in a tumor.

4.5. T_H17 Profile and Associations with HLA-DR Allotypes

Studies have found that certain HLA alleles associate with the development of cancer, *Chadhuri et al.* (2000) reported that a subtype of HLA-DR52 (DRB3*02) was increased in younger patients with breast cancer in comparison to age-matched healthy controls. Further, the Drover lab found that HLA-DR52 was associated with larger tumors and decreased recurrence free survival in breast cancer patients. Such studies support the concept that certain MHC class II alleles associate with cancer prevalence or poor prognoses in cancer because tumor associated antigens presented in the context of particular MHC class II alleles may promote suppression of the immune system, conferring an advantage to the cancer. We found no association between the relevant HLA-DR subtypes and IL-17, RORc2 and T_H17 (Tables 3.11A-C). Therefore, within the

limitations of this small samples size, it seems that HLA-DR52 alleles may not promote T_H17 development in breast tumor patients.

4.6. T_H17 Profile Associations with Prognostic Indicators

As described in the introduction, breast cancer is a complex disease with many different molecular subtypes, which vary in their prognosis and treatment. We wanted to determine if T_H17 markers and T_H17 cells associated with prognostic indicators, hormone receptors and breast cancer type. If T_H17 cells were found to associate with a poor or a good prognostic indicator, then future experiments to determine if T_H17 cells were mechanistically associated with the outcome could be conducted.

Tumor size, tumor type, tumor grade, clinical lymph node status, ER presence, PR presence, HER2/neu presence and age of diagnosis were all analyzed for associations with IL-17, RORc2 and T_H17 profiles.

IL-17^{lo} was found to associate with low tumor grades ($p=0.030$). As a result, blocking IL-17 and reducing intratumoral levels could hinder tumor development. This may be a reflection on the ability of IL-17 to promote angiogenesis through inducing VEGF and CXCL-8 production (Figure 1.6). Interestingly, a study by *Fialova et al.* (2012) found higher IL-17A levels with limited stage ovarian cancer (Fialova et al., 2012), however, it is difficult to directly compare breast cancer and ovarian cancer.

Although others (Horlock et al., 2009) have suggested an association between HER2⁺ breast cancer and increased levels of T_H17, we found no such association. This could be due to the methodology as we analyzed T_H17 transcripts from breast cancer tissue. Horlock et al. (2009) enumerated CD4⁺IL-17⁺ cells in the peripheral blood of

breast cancer patients and on comparing the numbers of T_H17 cells to healthy controls, they found T_H17 cells to be increased in HER2⁺ patients.

Our finding that IL-17^{hi} correlated to younger ages for diagnosis, a poor prognostic indicator, suggests IL-17 may have a role in promotion of breast cancer in younger women (Carlson et al., 2009, McPherson et al., 2000). However, a mechanistic approach to IL-17 and promotion of breast cancer in younger women has yet to be found. T_H17^{hi}, like IL-17^{hi}, correlated with a younger age at diagnosis. Due to Chaudhuri's findings (2000), which related HLA-DR52 and a younger age of diagnosis, we decided to split our samples into IL-17^{hi/lo} and T_H17^{hi/lo} categories and analyze the data for associations with HLA-DR52 and younger age at diagnosis (Figure 3.21A-B). T_H17^{hi}/HLA-DR52⁺ tumors had the youngest age at diagnosis (mean age at diagnosis (DX) = 49) and this correlation was significant (p=0.013). IL-17^{hi}/HLA-DR52⁺ patients had a lower mean age of diagnosis (mean = 55), but this was not a significant relationship. As HLA-DR52 heterodimers would present breast tumor antigens to T cells, it is possible that in younger individuals, with higher hormone levels, that CD4⁺ T cells are polarized towards the T_H17 profile. Future studies could analyze the effect estrogen has on T_H17 cells *in vitro* or *in vivo*.

With respect to RORc2, there was a significant association between RORc2^{lo} and invasive ductal tumors (p=0.026). . Since the breast cancer cell lines had increased RORc2, it could potentially be a marker for ductal cancer and be able to differentiate it from lobular cancer.

We theorized that T_H17^{hi}/IL-17^{hi} could associate with positive clinical lymph node status because IL-17 could lead to the secretion of VEGF, which could allow the

movement of breast cancer cells into lymph nodes (Murugaiyan et al., 2009). However, this was not the case as we found no association between positive lymph node status and $T_H17^{hi}/IL-17^{hi}$. Furthermore, *Yang et al.* (2012) found that there was a negative association between T_H17 levels and increased numbers of metastatic nodes in breast cancer patients. Future experiments could explore the possibility that T_H17 cells are having an anti-tumor effect (Figure 1.5) by attracting innate cells into the tumor microenvironment. Determining the levels of CXCL9, CXCL10, NK cells and dendritic cells within the tumor environment with respect to T_H17 cells could be an aim of future experiments. Such experiments could clarify the role of T_H17 cells in tumor microenvironments.

4.7. T_H17 Profile Associations with Survival

The last objective was to determine if survival or recurrence was related to IL-17, RORc2 or T_H17 profiles. Stemming back to the research by Oldford, it was noted that IL-6^{hi} associated with decreased survival. Therefore, we thought that T_H17^{hi} would also correlate to decreased survival.

With respect to the T_H17 cell markers, IL-17^{hi} and T_H17^{hi} trended with decreased OS but these were not significant associations. However, expanding the sample size would test more rigorously whether T_H17 cells in promote decreased survival breast cancer. Furthermore, expansion of the sample size would allow additional statistical analysis, such as a multivariate Cox analysis, to test for associations with survival. In contrast to our trend, *Kryczek et al.* (2009) found a relationship between improved patient outcome and T_H17 cells in ovarian cancer. However, it is difficult to compare ovarian

and breast cancer. Expanding the sample size may provide greater insight into the role of T_H17 cells and RFS and OS.

4.8. Concluding Remarks and Future Studies

We had hypothesized that higher levels of T_H17 cells would be present in tumors that had high IL-6 transcripts and HLA-DR52⁺ haplotypes. However, we found that neither IL-6^{hi} nor HLA-DR52 associated with increased T_H17 cells. We also determined that there were few significant associations between T_H17 markers/profile and prognostic indicators. However, we did note that both IL-17^{hi} and T_H17^{hi} associated with younger age of breast cancer at diagnosis. Further, due to the *Chaudhuri et al.* (2000) study, which reported that HLA-DR52 also correlated to a younger age at diagnosis, we determined that tumors with HLA-DR52⁺/T_H17^{hi} profiles had a significantly lower age at diagnosis than the tumors that were either HLA-DR52⁻ or T_H17^{lo}. Lastly, we determined that T_H17^{hi} did trend with decreased overall survival.

Further studies and alternative experiments could be carried out to support our findings. With respect to the PCR samples, future experiments could be conducted through real-time RT-PCR only. We had a number of problems regarding conventional RT-PCR and as real-time RT-PCR is more sensitive and accurate, one could use real-time PCR alone. Additionally, analyzing mRNA levels of additional T_H17 markers in combination with IL-17 and RORc2, such as STAT3 or IL-21, would give more insight into the presence of T_H17 cells in the breast tumor samples.

This study focused on mRNA transcripts levels. Although our initial intent was to analyze protein expression through dual staining IHC, problems were encountered

concerning availability of a specific RORc2 antibody and optimization of IL-17 antibodies. Future studies may be able to use STAT3 as a nuclear marker, rather than RORc2, and try different optimization techniques for IL-17. Further, to gain an accurate representation of the frequency of T_H17 cells in breast tumors, having healthy breast tissue for a comparison would be ideal.

A major caveat of this project was the small number of samples. Expanding the sample size could clarify trends which were observed in this study, provide confidence for significant associations that were calculated and permit the use of additional statistical tests (multivariate Cox analysis). Furthermore, having healthy breast tumor tissue for mRNA and protein analysis would be a useful control. We used stimulated PBLs as the positive control for IL-17 and RORc2 and the expression of both targets were quite high relative to the levels observed in the breast tumor samples. Having samples of healthy breast tissues would allow for a more accurate and in depth analysis of the potential increase or decrease of T_H17 markers/cells that occurs with breast cancer patients. Additionally, analyzing the peripheral blood of breast cancer patients would provide more information on the circulating T cells, the prevalence of T_H17 cells in the PBL population and associations between PBL T_H17 populations and prognostic indicators.

REFERENCES

- Ahmad, N., & Kumar, R. (2011). Steroid hormone receptors in cancer development: A target for cancer therapeutics. *Cancer Letters*, 300(1), 1-9. doi:10.1016/j.canlet.2010.09.008
- Ali, S., Buluwela, L., & Coombes, R. C. (2011). Antiestrogens and their therapeutic applications in breast cancer and other diseases. *Annual Review of Medicine*, 62, 217-232. doi:10.1146/annurev-med-052209-100305
- Alison, M. R., Nicholson, L. J., & Lin, W. R. (2011). Chronic inflammation and hepatocellular carcinoma. *Recent Results in Cancer Research.Fortschritte Der Krebsforschung.Progres Dans Les Recherches Sur Le Cancer*, 185, 135-148. doi:10.1007/978-3-642-03503-6_8
- Allred, D. C. (2008). The utility of conventional and molecular pathology in managing breast cancer. *Breast Cancer Research : BCR*, 10 Suppl 4, S4. doi: 10.1186/bcr2164; 10.1186/bcr2164
- Bai, Z., & Gust, R. (2009). Breast cancer, estrogen receptor and ligands. *Archiv Der Pharmazie*, 342(3), 133-149. doi:10.1002/ardp.200800174
- Bettelli, E., Carrier, Y., Gao, W., Korn, T., Strom, T. B., Oukka, M., . . . Kuchroo, V. K. (2006). Reciprocal developmental pathways for the generation of pathogenic effector TH17 and regulatory T cells. *Nature*, 441(7090), 235-238. doi:10.1038/nature04753
- Bettelli, E., Korn, T., Oukka, M., & Kuchroo, V. K. (2008). Induction and effector functions of T(H)17 cells. *Nature*, 453(7198), 1051-1057. doi:10.1038/nature07036
- Bhat, H. K., Calaf, G., Hei, T. K., Loya, T., & Vadgama, J. V. (2003). Critical role of oxidative stress in estrogen-induced carcinogenesis. *Proceedings of the National Academy of Sciences of the United States of America*, 100(7), 3913-3918. doi:10.1073/pnas.0437929100
- Biorad Laboratories, Inc. (2006) Real-Time PCR Applications Guide. Retrieved from: www.gene-quantification.de/real-time-pcr-guide-bio-rad.pdf
- Bloom, H. J., & Richardson, W. W. (1957). Histological grading and prognosis in breast cancer; a study of 1409 cases of which 359 have been followed for 15 years. *British Journal of Cancer*, 11(3), 359-377.
- Boccardo, E., Lepique, A. P., & Villa, L. L. (2010). The role of inflammation in HPV carcinogenesis. *Carcinogenesis*, 31(11), 1905-1912. doi:10.1093/carcin/bgq176

- Boisvert, M., Chetoui, N., Gendron, S., & Aoudjit, F. (2010). Alpha2beta1 integrin is the major collagen-binding integrin expressed on human Th17 cells. *European Journal of Immunology*, 40(10), 2710-2719. doi:10.1002/eji.201040307
- Bronte, V. (2008). Th17 and cancer: Friends or foes? *Blood*, 112(2), 214. doi:10.1182/blood-2008-04-149260
- Burger, H. G. (1994). Diagnostic role of follicle-stimulating hormone (FSH) measurements during the menopausal transition--an analysis of FSH, oestradiol and inhibin. *European Journal of Endocrinology / European Federation of Endocrine Societies*, 130(1), 38-42.
- Canadian Cancer Statistics 2012. Toronto, ON: Canadian Cancer Society; 2012. May 2012 ISSN 0835-2976
- Campbell, R. D., & Trowsdale, J. (1993). Map of the human MHC. *Immunology Today*, 14(7), 349-352.
- Carlson, R. W., Allred, D. C., Anderson, B. O., Burstein, H. J., Carter, W. B., Edge, S. B., NCCN Breast Cancer Clinical Practice Guidelines Panel. (2009). Breast cancer. clinical practice guidelines in oncology. *Journal of the National Comprehensive Cancer Network : JNCCN*, 7(2), 122-192.
- Chaudhuri, S., Cariappa, A., Tang, M., Bell, D., Haber, D. A., Isselbacher, K. J., Pillai, S. (2000). Genetic susceptibility to breast cancer: HLA DQB*03032 and HLA DRB1*11 may represent protective alleles. *Proceedings of the National Academy of Sciences of the United States of America*, 97(21), 11451-11454. doi:10.1073/pnas.97.21.11451
- Choudhuri, K., Kearney, A., Bakker, T. R., & van der Merwe, P. A. (2005). Immunology: How do T cells recognize antigen? *Current Biology : CB*, 15(10), R382-5. doi:10.1016/j.cub.2005.05.001
- Coquet, J. M., Kyparissoudis, K., Pellicci, D. G., Besra, G., Berzins, S. P., Smyth, M. J., & Godfrey, D. I. (2007). IL-21 is produced by NKT cells and modulates NKT cell activation and cytokine production. *Journal of Immunology (Baltimore, Md.: 1950)*, 178(5), 2827-2834.
- Coussens, L., Yang-Feng, T. L., Liao, Y. C., Chen, E., Gray, A., McGrath, J., . . . Francke, U. (1985). Tyrosine kinase receptor with extensive homology to EGF receptor shares chromosomal location with neu oncogene. *Science (New York, N.Y.)*, 230(4730), 1132-1139.

- Cua, D. J., & Tato, C. M. (2010). Innate IL-17-producing cells: The sentinels of the immune system. *Nature Reviews.Immunology*, 10(7), 479-489. doi:10.1038/nri2800
- Delassus, G. S., Cho, H., & Eliceiri, G. L. (2011). New signaling pathways from cancer progression modulators to mRNA expression of matrix metalloproteinases in breast cancer cells. *Journal of Cellular Physiology*, doi:10.1002/jcp.22694; 10.1002/jcp.22694
- Delozier, T. (2010). Hormonal treatment in breast cancer. [Hormonotherapie du cancer du sein] *Journal De Gynecologie, Obstetrique Et Biologie De La Reproduction*, 39(8 Suppl), F71-8. doi:10.1016/j.jgyn.2010.10.004
- DeNardo, D. G., Barreto, J. B., Andreu, P., Vasquez, L., Tawfik, D., Kolhatkar, N., & Coussens, L. M. (2009). CD4(+) T cells regulate pulmonary metastasis of mammary carcinomas by enhancing pro-tumor properties of macrophages. *Cancer Cell*, 16(2), 91-102. doi:10.1016/j.ccr.2009.06.018
- DeNardo, D. G., & Coussens, L. M. (2007). Inflammation and breast cancer. balancing immune response: Crosstalk between adaptive and innate immune cells during breast cancer progression. *Breast Cancer Research : BCR*, 9(4), 212. doi:10.1186/bcr1746
- Diamond, M. S., Kinder, M., Matsushita, H., Mashayekhi, M., Dunn, G. P., Archambault, J. M., . . . Schreiber, R. D. (2011). Type I interferon is selectively required by dendritic cells for immune rejection of tumors. *The Journal of Experimental Medicine*, 208(10), 1989-2003. doi:10.1084/jem.20101158
- Disis, M. L. (2010). Immune regulation of cancer. *Journal of Clinical Oncology : Official Journal of the American Society of Clinical Oncology*, 28(29), 4531-4538. doi:10.1200/JCO.2009.27.2146
- Dong, C. (2008). TH17 cells in development: An updated view of their molecular identity and genetic programming. *Nature Reviews.Immunology*, 8(5), 337-348. doi:10.1038/nri2295
- Dong, C. (2011). Genetic controls of Th17 cell differentiation and plasticity. *Experimental & Molecular Medicine*, 43(1), 1-6.
- Edgecombe, A.D. (2002) *HLA Class II Expression on Breast Cancer Cells*. Memorial University of Newfoundland and Labrador: St. John's
- Eisenbarth, G. S. (2003). Insulin autoimmunity: Immunogenetics/immunopathogenesis of type 1A diabetes. *Annals of the New York Academy of Sciences*, 1005, 109-118.

- Elston, C. W., & Ellis, I. O. (1991). Pathological prognostic factors in breast cancer. I. the value of histological grade in breast cancer: Experience from a large study with long-term follow-up. *Histopathology*, 19(5), 403-410.
- English, D., & Andersen, B. R. (1974). Single-step separation of red blood cells, granulocytes and mononuclear leukocytes on discontinuous density gradients of ficoll-hypaque. *Journal of Immunological Methods*, 5(3), 249-252.
- Ernster, V. L., Ballard-Barbash, R., Barlow, W. E., Zheng, Y., Weaver, D. L., Cutter, G., . Geller, B. M. (2002). Detection of ductal carcinoma in situ in women undergoing screening mammography. *Journal of the National Cancer Institute*, 94(20), 1546-1554.
- Fleige, S., & Pfaffl, M. W. (2006). RNA integrity and the effect on the real-time qRT-PCR performance. *Molecular Aspects of Medicine*, 27(2-3), 126-139. doi: 10.1016/j.mam.2005.12.003
- Gage, M., Wattendorf, D., & Henry, L. R. (2012). Translational advances regarding hereditary breast cancer syndromes. *Journal of Surgical Oncology*, 105(5), 444-451. doi: 10.1002/jso.21856; 10.1002/jso.21856
- Ghoreschi, K., Laurence, A., Yang, X. P., Tato, C. M., McGeachy, M. J., Konkel, J. E., . . . O'Shea, J. J. (2010). Generation of pathogenic T(H)17 cells in the absence of TGF-beta signalling. *Nature*, 467(7318), 967-971. doi:10.1038/nature09447
- Happel, K. I., Dubin, P. J., Zheng, M., Ghilardi, N., Lockhart, C., Quinton, L. J., . . . Kolls, J. K. (2005). Divergent roles of IL-23 and IL-12 in host defense against klebsiella pneumoniae. *The Journal of Experimental Medicine*, 202(6), 761-769. doi:10.1084/jem.20050193
- Harrington, L. E., Mangan, P. R., & Weaver, C. T. (2006). Expanding the effector CD4 T-cell repertoire: The Th17 lineage. *Current Opinion in Immunology*, 18(3), 349-356. doi:10.1016/j.coi.2006.03.017
- Hirose, T., Smith, R. J., & Jetten, A. M. (1994). ROR gamma: The third member of ROR/RZR orphan receptor subfamily that is highly expressed in skeletal muscle. *Biochemical and Biophysical Research Communications*, 205(3), 1976-1983. doi:10.1006/bbrc.1994.2902
- Hirschhorn, J. N. (2003). Genetic epidemiology of type 1 diabetes. *Pediatric Diabetes*, 4(2), 87-100. doi:10.1034/j.1399-5448.2001.00013.x
- HLA Nomenclature (19 July 2012). *HLA Nomenclature*. Retrieved from: <http://hla.alleles.org/nomenclature/stats.html>

- Horlock, C., Stott, B., Dyson, P. J., Morishita, M., Coombes, R. C., Savage, P., & Stebbing, J. (2009). The effects of trastuzumab on the CD4+CD25+FOXP3+ and CD4+IL17A+ T-cell axis in patients with breast cancer. *British Journal of Cancer*, *100*(7), 1061-1067. doi:10.1038/sj.bjc.6604963
- Hrubisko, M., Sanislo, L., Zuzulova, M., Michalickova, J., Zeleznikova, T., Sedlak, J., & Bella, V. (2010). Immunity profile in breast cancer patients. *Bratislavske Lekarske Listy*, *111*(1), 20-26.
- Hudis, C. A. (2007). Trastuzumab--mechanism of action and use in clinical practice. *The New England Journal of Medicine*, *357*(1), 39-51. doi:10.1056/NEJMra043186
- Irvin, W. J., Jr, & Carey, L. A. (2008). What is triple-negative breast cancer? *European Journal of Cancer (Oxford, England : 1990)*, *44*(18), 2799-2805. doi:10.1016/j.ejca.2008.09.034
- Ito, T., Carson, W. F., 4th, Cavassani, K. A., Connett, J. M., & Kunkel, S. L. (2011). CCR6 as a mediator of immunity in the lung and gut. *Experimental Cell Research*, *317*(5), 613-619. doi:10.1016/j.yexcr.2010.12.018
- Jordan, V. C. (1993). Fourteenth gaddum memorial lecture. A current view of tamoxifen for the treatment and prevention of breast cancer. *British Journal of Pharmacology*, *110*(2), 507-517.
- Jovanovic, D. V., Di Battista, J. A., Martel-Pelletier, J., Jolicoeur, F. C., He, Y., Zhang, M., Pelletier, J. P. (1998). IL-17 stimulates the production and expression of proinflammatory cytokines, IL-beta and TNF-alpha, by human macrophages. *Journal of Immunology (Baltimore, Md.: 1950)*, *160*(7), 3513-3521.
- Karanikas, V., Speletas, M., Zamanakou, M., Kalala, F., Loules, G., Kerenidi, T., Germanis, A. E. (2008). FOXP3 expression in human cancer cells. *Journal of Translational Medicine*, *6*, 19. doi:10.1186/1479-5876-6-19
- Kesselring, R., Thiel, A., Pries, R., & Wollenberg, B. (2011). The number of CD161 positive Th17 cells are decreased in head and neck cancer patients. *Cellular Immunology*, *269*(2), 74-77. doi:10.1016/j.cellimm.2011.03.026
- Kitamura, N., Kaminuma, O., Mori, A., Hashimoto, T., Kitamura, F., Miyagishi, M., Miyatake, S. (2005). Correlation between mRNA expression of Th1/Th2 cytokines and their specific transcription factors in human helper T-cell clones. *Immunology and Cell Biology*, *83*(5), 536-541. doi:10.1111/j.1440-1711.2005.01364.x
- Koyama, K., Kagamu, H., Miura, S., Hiura, T., Miyabayashi, T., Itoh, R., Gejyo, F. (2008). Reciprocal CD4+ T-cell balance of effector CD62Llow CD4+ and

- CD62LhighCD25+ CD4+ regulatory T cells in small cell lung cancer reflects disease stage. *Clinical Cancer Research : An Official Journal of the American Association for Cancer Research*, 14(21), 6770-6779. doi:10.1158/1078-0432.CCR-08-1156
- Krauss, W. C., Park, J. W., Kirpotin, D. B., Hong, K., & Benz, C. C. (2000). Emerging antibody-based HER2 (ErbB-2/neu) therapeutics. *Breast Disease*, 11, 113-124.
- Kryczek, I., Banerjee, M., Cheng, P., Vatan, L., Szeliga, W., Wei, S., Zou, W. (2009). Phenotype, distribution, generation, and functional and clinical relevance of Th17 cells in the human tumor environments. *Blood*, 114(6), 1141-1149. doi:10.1182/blood-2009-03-208249
- Kryczek, I., Wei, S., Keller, E., Liu, R., & Zou, W. (2007). Stroma-derived factor (SDF-1/CXCL12) and human tumor pathogenesis. *American Journal of Physiology. Cell Physiology*, 292(3), C987-95. doi:10.1152/ajpcell.00406.2006
- Kubler, K., Arndt, P. F., Wardelmann, E., Krebs, D., Kuhn, W., & van der Ven, K. (2006). HLA-class II haplotype associations with ovarian cancer. *International Journal of Cancer. Journal International Du Cancer*, 119(12), 2980-2985. doi:10.1002/ijc.22266
- Kwan M, & et al. (2009). Epidemiology of breast cancer subtypes in two prospective cohort studies of breast cancer survivors. *Breast Cancer Research*, 11(3) doi:10.1186/bcr2261
- Lacroix, M., & Leclercq, G. (2004). Relevance of breast cancer cell lines as models for breast tumours: An update. *Breast Cancer Research and Treatment*, 83(3), 249-289. doi:10.1023/B:BREA.0000014042.54925.cc
- Lee, Y. K., Turner, H., Maynard, C. L., Oliver, J. R., Chen, D., Elson, C. O., & Weaver, C. T. (2009). Late developmental plasticity in the T helper 17 lineage. *Immunity*, 30(1), 92-107. doi:10.1016/j.immuni.2008.11.005
- Liang, S. C., Tan, X. Y., Luxenberg, D. P., Karim, R., Dunussi-Joannopoulos, K., Collins, M., & Fouser, L. A. (2006). Interleukin (IL)-22 and IL-17 are coexpressed by Th17 cells and cooperatively enhance expression of antimicrobial peptides. *The Journal of Experimental Medicine*, 203(10), 2271-2279. doi:10.1084/jem.20061308
- Lin, J., & Weiss, A. (2001). T cell receptor signalling. *Journal of Cell Science*, 114(Pt 2), 243-244.
- Liu, F., Lang, R., Zhao, J., Zhang, X., Pringle, G. A., Fan, Y., Fu, L. (2011). CD8(+) cytotoxic T cell and FOXP3(+) regulatory T cell infiltration in relation to breast

- cancer survival and molecular subtypes. *Breast Cancer Research and Treatment*, doi:10.1007/s10549-011-1647-3
- Liu, J., Duan, Y., Cheng, X., Chen, X., Xie, W., Long, H., Zhu, B. (2011). IL-17 is associated with poor prognosis and promotes angiogenesis via stimulating VEGF production of cancer cells in colorectal carcinoma. *Biochemical and Biophysical Research Communications*, 407(2), 348-354. doi:10.1016/j.bbrc.2011.03.021
- Lodish H, Berk A, Zipursky SL, et al. *Molecular Cell Biology*. 4th edition. New York: W. H. Freeman; 2000. Section 24.1, Tumor Cells and the Onset of Cancer.
- Mahmoodi, M., Nahvi, H., Mahmoudi, M., Kasaian, A., Mohagheghi, M. A., Divsalar, K., Amirzargar, A. (2011). HLA-DRB1,-DQA1 and -DQB1 allele and haplotype frequencies in female patients with early onset breast cancer. *Pathology Oncology Research : POR*, doi:10.1007/s12253-011-9415-6
- Mahmoud, S. M., Paish, E. C., Powe, D. G., Macmillan, R. D., Grainge, M. J., Lee, A. H., Green, A. R. (2011). Tumor-infiltrating CD8+ lymphocytes predict clinical outcome in breast cancer. *Journal of Clinical Oncology : Official Journal of the American Society of Clinical Oncology*, 29(15), 1949-1955. doi:10.1200/JCO.2010.30.5037
- Maniati, E., Soper, R., & Hagemann, T. (2010). Up for mischief? IL-17/Th17 in the tumour microenvironment. *Oncogene*, 29(42), 5653-5662. doi:10.1038/onc.2010.367
- Marteau, P., & Chaput, U. (2011). Bacteria as trigger for chronic gastrointestinal disorders. *Digestive Diseases (Basel, Switzerland)*, 29(2), 166-171. doi:10.1159/000323879
- Martin-Orozco, N., Chung, Y., Chang, S. H., Wang, Y. H., & Dong, C. (2009). Th17 cells promote pancreatic inflammation but only induce diabetes efficiently in lymphopenic hosts after conversion into Th1 cells. *European Journal of Immunology*, 39(1), 216-224. doi:10.1002/eji.200838475
- Maruyama, T., Kono, K., Mizukami, Y., Kawaguchi, Y., Mimura, K., Watanabe, M., . . . Fujii, H. (2010). Distribution of Th17 cells and FOXP3(+) regulatory T cells in tumor-infiltrating lymphocytes, tumor-draining lymph nodes and peripheral blood lymphocytes in patients with gastric cancer. *Cancer Science*, 101(9), 1947-1954. doi:10.1111/j.1349-7006.2010.01624.x; 10.1111/j.1349-7006.2010.01624.x
- Matzinger, P. (1994). Tolerance, danger, and the extended family. *Annual Review of Immunology*, 12, 991-1045. doi:10.1146/annurev.iy.12.040194.005015

- McPherson K., Steel C. M., Dixon J.M. (2000). ABC of breast diseases: Breast cancer—epidemiology, risk factors, and genetics. *BMJ*, 321(7261), 624-628. doi:10.1136/bmj.321.7261.624
- McPherson, K., Steel, C. M., & Dixon, J. M. (2000). Breast cancer—epidemiology, risk factors, and genetics. *BMJ*, 321(7261), 624-628. doi:10.1136/bmj.321.7261.624
- Medvedev, A., Chistokhina, A., Hirose, T., & Jetten, A. M. (1997). Genomic structure and chromosomal mapping of the nuclear orphan receptor ROR gamma (RORC) gene. *Genomics*, 46(1), 93-102. doi: 10.1006/geno.1997.4980
- Mesquita Junior, D., Araujo, J. A., Catelan, T. T., Souza, A. W., Cruvinel Wde, M., Andrade, L. E., & Silva, N. P. (2010). Immune system - part II: Basis of the immunological response mediated by T and B lymphocytes. *Revista Brasileira De Reumatologia*, 50(5), 552-580.
- Michaud L, Espirito J, Esteva F. Breast cancer. In: DiPiro J, Talbert R, Yee G, et al, eds. *Pharmacotherapy*. 7th ed. New York, NY: McGraw-Hill; 2008:2121-2153
- Mincheff, M. (2009). Immunosurveillance and immunoediting--can the immune response be made more "immunodemocratic"? *Journal of B.U.ON.: Official Journal of the Balkan Union of Oncology*, 14 Suppl 1, S89-96.
- Miyahara, Y., Odunsi, K., Chen, W., Peng, G., Matsuzaki, J., & Wang, R. F. (2008). Generation and regulation of human CD4+ IL-17-producing T cells in ovarian cancer. *Proceedings of the National Academy of Sciences of the United States of America*, 105(40), 15505-15510. doi:10.1073/pnas.0710686105
- Murugaiyan, G., & Saha, B. (2009). Pro-tumor vs anti-tumor functions of IL-17. *Journal of Immunology (Baltimore, Md.: 1950)*, 183(7), 4169-4175. doi:10.4049/jimmunol.0901017
- Nerup, J., Platz, P., Andersen, O. O., Christy, M., Lyngsoe, J., Poulsen, J. E., Svejgaard, A. (1974). HL-A antigens and diabetes mellitus. *Lancet*, 2(7885), 864-866.
- O'Connor, W., Jr, Zenewicz, L. A., & Flavell, R. A. (2010). The dual nature of T(H)17 cells: Shifting the focus to function. *Nature Immunology*, 11(6), 471-476. doi:10.1038/ni.1882
- Oldford, S. A., Robb, J. D., Codner, D., Gadag, V., Watson, P. H., & Drover, S. (2006). Tumor cell expression of HLA-DM associates with a Th1 profile and predicts improved survival in breast carcinoma patients. *International Immunology*, 18(11), 1591-1602. doi:10.1093/intimm/dx1092

- Oldford, S.A. (2006) *Interrelationships And Clinical Significance of Expression of Immunological Markers in Invasive Breast Carcinoma*. Memorial University of Newfoundland and Labrador: St. John's
- Olivito, B., Simonini, G., Ciullini, S., Moriondo, M., Betti, L., Gambineri, E., Cimaz, R. (2009). Th17 transcription factor RORC2 is inversely correlated with FOXP3 expression in the joints of children with juvenile idiopathic arthritis. *The Journal of Rheumatology*, 36(9), 2017-2024. doi:10.3899/jrheum.090066
- O'Shea, J. J., & Paul, W. E. (2010). Mechanisms underlying lineage commitment and plasticity of helper CD4+ T cells. *Science (New York, N.Y.)*, 327(5969), 1098-1102. doi:10.1126/science.1178334
- Ostrand-Rosenberg, S. (2008). Immune surveillance: A balance between pro-tumor and anti-tumor immunity. *Current Opinion in Genetics & Development*, 18(1), 11-18. doi:10.1016/j.gde.2007.12.007
- Pan, F., Fan, H., Lu, L., Liu, Z., & Jiang, S. (2011). The yin and yang of signaling in tregs and TH17 cells. *Science Signaling*, 4(165), mr4. doi:10.1126/scisignal.2001709
- PCR Amplification (2012). *PCR Amplification*. Promega. Retrieved on June 19, 2012 from: <http://www.promega.com/resources/product-guides-and-selectors/protocols-and-applications-guide/pcr-amplification/#title2>
- Platz, P., Jakobsen, B. K., Morling, N., Ryder, L. P., Svejgaard, A., Thomsen, M., Hauge, M. (1981). HLA-D and -DR antigens in genetic analysis of insulin dependent diabetes mellitus. *Diabetologia*, 21(2), 108-115.
- Polanczyk, M. J., Carson, B. D., Subramanian, S., Afentoulis, M., Vandenbark, A.A., Ziegler, S. F., & Offner, H. (2004). Cutting edge: Estrogen drives expansion of the CD4+CD25+ regulatory T cell compartment. *Journal of Immunology (Baltimore, Md.: 1950)*, 173(4), 2227-2230.
- Polyak, K. (November 2007). Breast cancer: Origins and evolution. *Journal of Clinical Investigation*, 117(11), 3155-3163. doi:10.1172/JCI33295
- Provinciali, M., Cardelli, M., & Marchegiani, F. (2011). Inflammation, chronic obstructive pulmonary disease and aging. *Current Opinion in Pulmonary Medicine*, 17 Suppl 1, S3-10. doi:10.1097/01.mcp.0000410742.90463.1f
- Rastelli, F., Biancanelli, S., Falzetta, A., Martignetti, A., Casi, C., Bascioni, R., Crispino, S. (2010). Triple-negative breast cancer: Current state of the art. *Tumori*, 96(6), 875-888.

- Ravishankaran, P., & Karunanithi, R. (2011). Clinical significance of preoperative serum interleukin-6 and C-reactive protein level in breast cancer patients. *World Journal of Surgical Oncology*, *9*, 18. doi:10.1186/1477-7819-9-18
- Romagnani, S. (2000). T-cell subsets (Th1 versus Th2). *Annals of Allergy, Asthma & Immunology : Official Publication of the American College of Allergy, Asthma, & Immunology*, *85*(1), 9-18; quiz 18, 21. doi:10.1016/S1081-1206(10)62426-X
- Rosen, P. P. (2001). *Rosen's breast pathology* (Second ed.). Philadelphia, PA: Lippincott Williams and Wilkins.
- Sainsbury, J. R. C., Anderson, T. J., & Morgan, D. A. L. (2000). Breast cancer. *BMJ*, *321*(7263), 745-750. doi:10.1136/bmj.321.7263.745
- Schreiber, R. D., Old, L. J., & Smyth, M. J. (2011). Cancer immunoediting: Integrating immunity's roles in cancer suppression and promotion. *Science (New York, N.Y.)*, *331*(6024), 1565-1570. doi:10.1126/science.1203486
- Schroeder, A., Mueller, O., Stocker, S., Salowsky, R., Leiber, M., Gassmann, M., Ragg, T. (2006). The RIN: An RNA integrity number for assigning integrity values to RNA measurements. *BMC Molecular Biology*, *7*, 3. doi:10.1186/1471-2199-7-3
- Sfanos, K. S., Bruno, T. C., Maris, C. H., Xu, L., Thoburn, C. J., DeMarzo, A. M., Drake, C. G. (2008). Phenotypic analysis of prostate-infiltrating lymphocytes reveals TH17 and treg skewing. *Clinical Cancer Research : An Official Journal of the American Association for Cancer Research*, *14*(11), 3254-3261. doi:10.1158/1078-0432.CCR-07-5164
- Sims, G. P., Rowe, D. C., Rietdijk, S. T., Herbst, R., & Coyle, A. J. (2010). HMGB1 and RAGE in inflammation and cancer. *Annual Review of Immunology*, *28*, 367-388. doi:10.1146/annurev.immunol.021908.132603
- Spolski, R., & Leonard, W. J. (2008). Interleukin-21: Basic biology and implications for cancer and autoimmunity. *Annual Review of Immunology*, *26*, 57-79. doi:10.1146/annurev.immunol.26.021607.090316
- Su, X., Ye, J., Hsueh, E. C., Zhang, Y., Hoft, D. F., & Peng, G. (2010). Tumor microenvironments direct the recruitment and expansion of human Th17 cells. *Journal of Immunology (Baltimore, Md.: 1950)*, *184*(3), 1630-1641. doi:10.4049/jimmunol.0902813
- Subik, K., Lee, J. F., Baxter, L., Strzepak, T., Costello, D., Crowley, P., Tang, P. (2010). The expression patterns of ER, PR, HER2, CK5/6, EGFR, ki-67 and AR by

- immunohistochemical analysis in breast cancer cell lines. *Breast Cancer : Basic and Clinical Research*, 4, 35-41.
- Thorsby, E., & Lie, B. A. (2005). HLA associated genetic predisposition to autoimmune diseases: Genes involved and possible mechanisms. *Transplant Immunology*, 14(3-4), 175-182
- Tosolini, M., Kirilovsky, A., Mlecnik, B., Fredriksen, T., Mauger, S., Bindea, G., Galon, J. (2011). Clinical impact of different classes of infiltrating T cytotoxic and helper cells (Th1, th2, treg, th17) in patients with colorectal cancer. *Cancer Research*, 71(4), 1263-1271. doi:10.1158/0008-5472.CAN-10-2907
- Trinchieri, G. (2010). Type I interferon: Friend or foe? *The Journal of Experimental Medicine*, 207(10), 2053-2063. doi: 10.1084/jem.20101664; 10.1084/jem.20101664
- Ullman, T. A., & Itzkowitz, S. H. (2011). Intestinal inflammation and cancer. *Gastroenterology*, 140(6), 1807-1816. doi:10.1053/j.gastro.2011.01.057
- von Boehmer, H. (2005). Unique features of the pre-T-cell receptor alpha-chain: Not just a surrogate. *Nature Reviews.Immunology*, 5(7), 571-577. doi:10.1038/nri1636
- Xu, L., Kitani, A., Fuss, I., & Strober, W. (2007). Cutting edge: Regulatory T cells induce CD4+CD25-FOXP3- T cells or are self-induced to become Th17 cells in the absence of exogenous TGF-beta. *Journal of Immunology (Baltimore, Md.: 1950)*, 178(11), 6725-6729.
- Villey, I., de Chasseval, R., & de Villartay, J. P. (1999). RORgammaT, a thymus-specific isoform of the orphan nuclear receptor RORgamma / TOR, is up-regulated by signaling through the pre-T cell receptor and binds to the TEA promoter. *European Journal of Immunology*, 29(12), 4072-4080.
- Walboomers, J. M., Jacobs, M. V., Manos, M. M., Bosch, F. X., Kummer, J. A., Shah, K. V., Munoz, N. (1999). Human papillomavirus is a necessary cause of invasive cervical cancer worldwide. *The Journal of Pathology*, 189(1), 12-19. doi:2-F
- Wang, J., Cai, D., Ma, B., Wu, G., & Wu, J. (2011). Skewing the balance of regulatory T-cells and T-helper 17 cells in breast cancer patients. *The Journal of International Medical Research*, 39(3), 691-701.
- Wang, W., Edington, H. D., Rao, U. N., Jukic, D. M., Radfar, A., Wang, H., & Kirkwood, J. M. (2008). Effects of high-dose IFNalpha2b on regional lymph node metastases of human melanoma: Modulation of STAT5, FOXP3, and IL-17. *Clinical Cancer Research : An Official Journal of the American Association for Cancer Research*, 14(24), 8314-8320. doi:10.1158/1078-0432.CCR-08-0705

- Watanabe, M. A., Oda, J. M., Amarante, M. K., & Cesar Voltarelli, J. (2010). Regulatory T cells and breast cancer: Implications for immunopathogenesis. *Cancer Metastasis Reviews*, 29(4), 569-579. doi:10.1007/s10555-010-9247-y
- Weaver, C. T., Harrington, L. E., Mangan, P. R., Gavrieli, M., & Murphy, K. M. (2006). Th17: An effector CD4 T cell lineage with regulatory T cell ties. *Immunity*, 24(6), 677-688. doi:10.1016/j.immuni.2006.06.002
- Wingo, P. A., Jamison, P. M., Young, J. L., & Gargiullo, P. (2004). Population-based statistics for women diagnosed with inflammatory breast cancer (united states). *Cancer Causes & Control : CCC*, 15(3), 321-328. doi: 10.1023/B:CACO.0000024222.61114.18
- Wooster, R., Neuhausen, S. L., Mangion, J., Quirk, Y., Ford, D., Collins, N., Averill, D. (1994). Localization of a breast cancer susceptibility gene, BRCA2, to chromosome 13q12-13. *Science (New York, N.Y.)*, 265(5181), 2088-2090.
- Wraith, D. C., Nicolson, K. S., & Whitley, N. T. (2004). Regulatory CD4+ T cells and the control of autoimmune disease. *Current Opinion in Immunology*, 16(6), 695-701. doi: 10.1016/j.coi.2004.09.015
- Yager, J. D., & Davidson, N. E. (2006). Estrogen carcinogenesis in breast cancer. *The New England Journal of Medicine*, 354(3), 270-282. doi:10.1056/NEJMra050776
- Yamazaki, T., Yang, X. O., Chung, Y., Fukunaga, A., Nurieva, R., Pappu, B., Dong, C. (2008). CCR6 regulates the migration of inflammatory and regulatory T cells. *Journal of Immunology (Baltimore, Md.: 1950)*, 181(12), 8391-8401.
- Yang, L., Qi, Y., Hu, J., Tang, L., Zhao, S., & Shan, B. (2012). Expression of Th17 cells in breast cancer tissue and its association with clinical parameters. *Cell Biochemistry and Biophysics*, 62(1), 153-159. doi:10.1007/s12013-011-9276-3
- Yang, X. O., Nurieva, R., Martinez, G. J., Kang, H. S., Chung, Y., Pappu, B. P., Dong, C. (2008). Molecular antagonism and plasticity of regulatory and inflammatory T cell programs. *Immunity*, 29(1), 44-56. doi:10.1016/j.immuni.2008.05.007
- Ye, D., Mendelsohn, J., & Fan, Z. (1999). Augmentation of a humanized anti-HER2 mAb 4D5 induced growth inhibition by a human-mouse chimeric anti-EGF receptor mAb C225. *Oncogene*, 18(3), 731-738. doi:10.1038/sj.onc.1202319
- Yu, P., & Fu, Y. X. (2006). Tumor-infiltrating T lymphocytes: Friends or foes? *Laboratory Investigation; a Journal of Technical Methods and Pathology*, 86(3), 231-245. doi:10.1038/labinvest.3700389

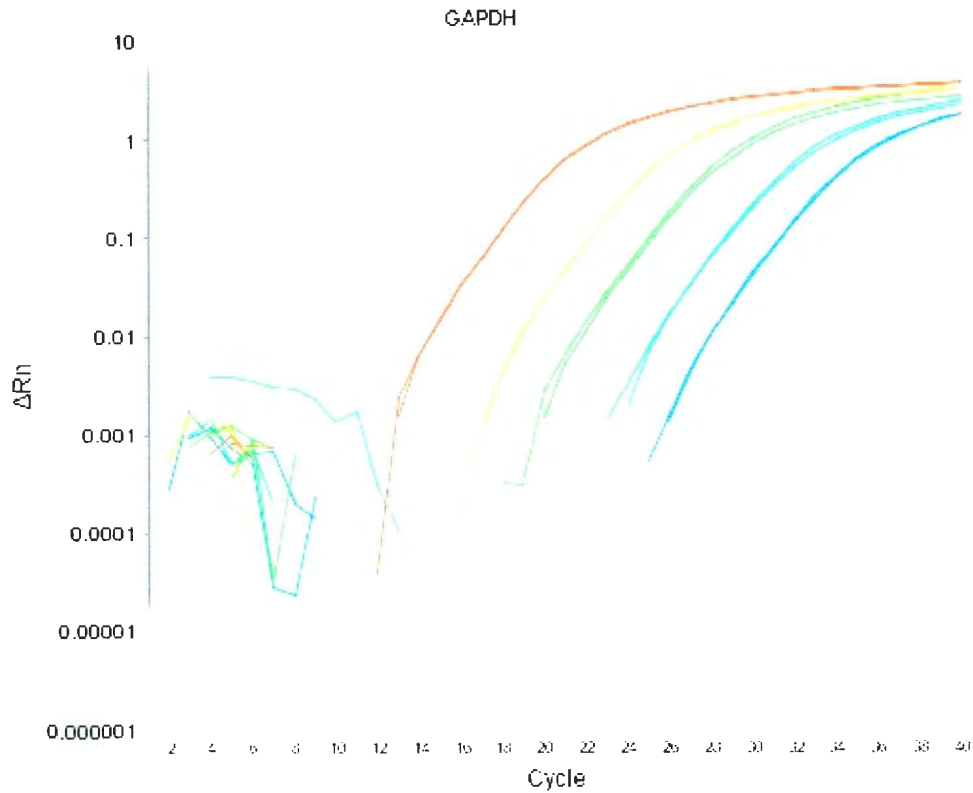
- Zenewicz, L. A., Yancopoulos, G. D., Valenzuela, D. M., Murphy, A. J., Karow, M., & Flavell, R. A. (2007). Interleukin-22 but not interleukin-17 provides protection to hepatocytes during acute liver inflammation. *Immunity*, 27(4), 647-659. doi:10.1016/j.immuni.2007.07.023
- Zhang, B., Rong, G., Wei, H., Zhang, M., Bi, J., Ma, L., Fang, G. (2008). The prevalence of Th17 cells in patients with gastric cancer. *Biochemical and Biophysical Research Communications*, 374(3), 533-537. doi:10.1016/j.bbrc.2008.07.060
- Zhang, J. P., Yan, J., Xu, J., Pang, X. H., Chen, M. S., Li, L., Zheng, L. (2009). Increased intratumoral IL-17-producing cells correlate with poor survival in hepatocellular carcinoma patients. *Journal of Hepatology*, 50(5), 980-989. doi:10.1016/j.jhep.2008.12.033
- Zhang, Y., Ma, D., Zhang, Y., Tian, Y., Wang, X., Qiao, Y., & Cui, B. (2011). The imbalance of Th17/Treg in patients with uterine cervical cancer. *Clinica Chimica Acta; International Journal of Clinical Chemistry*, 412(11-12), 894-900. doi:10.1016/j.cca.2011.01.015
- Zheng, Y., Danilenko, D. M., Valdez, P., Kasman, I., Eastham-Anderson, J., Wu, J., & Ouyang, W. (2007). Interleukin-22, a T(H)17 cytokine, mediates IL-23-induced dermal inflammation and acanthosis. *Nature*, 445(7128), 648-651. doi:10.1038/nature05505
- Zhou, L., Chong, M. M., & Littman, D. R. (2009). Plasticity of CD4+ T cell lineage differentiation. *Immunity*, 30(5), 646-655. doi:10.1016/j.immuni.2009.05.001
- Zhu, X., Mulcahy, L. A., Mohammed, R. A., Lee, A. H., Franks, H. A., Kilpatrick, L., Jackson, A. M. (2008). IL-17 expression by breast-cancer-associated macrophages: IL-17 promotes invasiveness of breast cancer cell lines. *Breast Cancer Research : BCR*, 10(6), R95. doi:10.1186/bcr2195
- Zou, W., & Restifo, N. P. (2010). T(H)17 cells in tumour immunity and immunotherapy. *Nature Reviews.Immunology*, 10(4), 248-256. doi:10.1038/nri2742

Appendix A

Stage	TNM
0	T0 N0 M0
I	T1 N0 M0
II	T0 N1 M0, T1 N1 M0, T2 N0 M0, T2 N1 M0, T3 N0 M0
III	T0 N2 M0, T1 N2 M0, T2 N2 M0, T3 N1-2 M0, T4 N1-3 M0
IV	Any T Any N M1

Appendix B

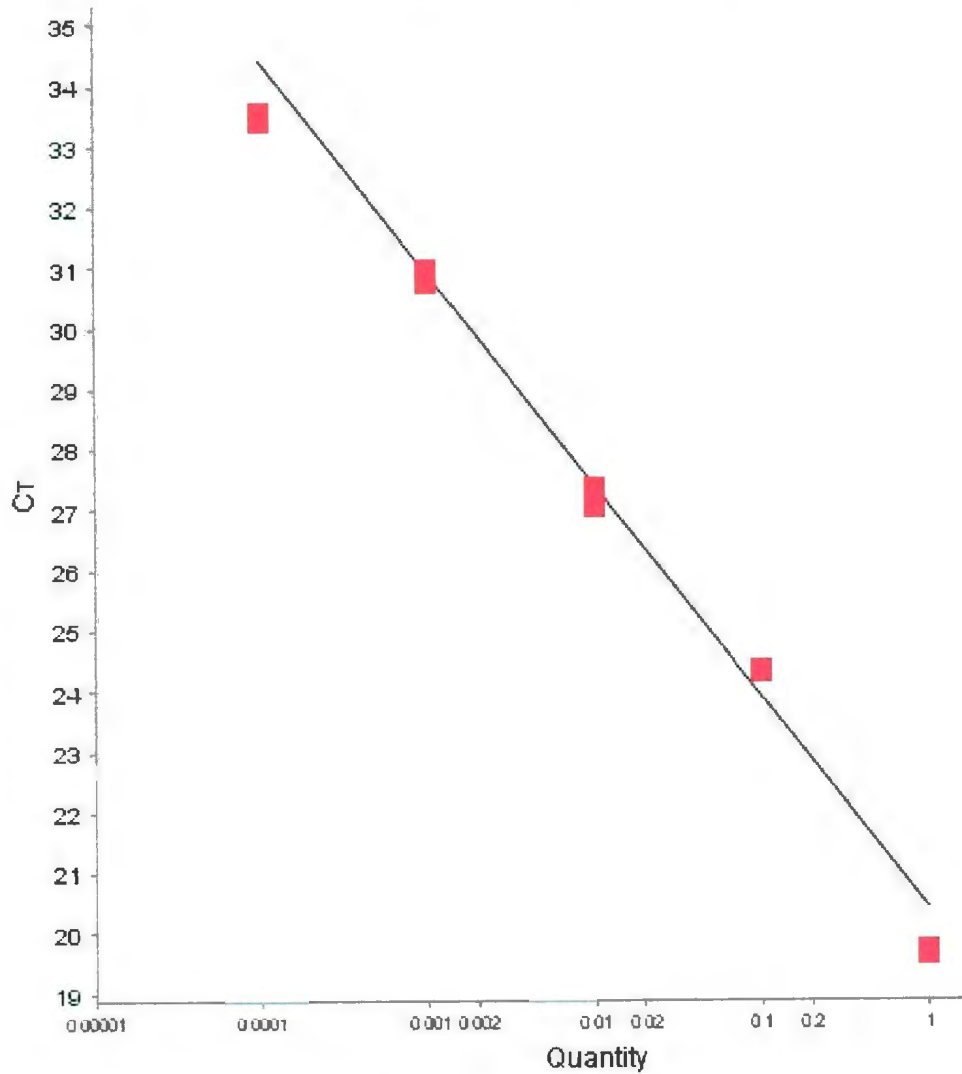
i)



Appendix B. i. *Determining the optimal dilution of cDNA for real-time assays (GAPDH) amplification.* Log fold dilutions of HLA04 were amplified in the StepOne Real-Time PCR machine over 40 cycles. The red line represents amplification of 1 μ L of cDNA, the yellow lines represents amplification of a 1 fold log dilution of cDNA, the light green line represents amplification of a 2 fold log dilution of cDNA and the dark green lines represents amplification of a 3 fold log dilution of cDNA μ L of cDNA and the blue line represents amplification of a 5 fold log dilution of cDNA. The number of amplifications is represented by the x-axis and ΔRn is represented by the y-axis. ΔRn is the fluorescence of the reporter dye (FAM) divided by the fluorescence of the passive dye (ROX). Assays were performed in duplicate.

ii)

Standard Curve



Appendix B. ii. *Standard curve of the threshold cycles (C_t) (GAPDH).* The C_t values obtained from the amplification of log fold diluted HLA04. The slope of this line was -3.499, the y-intercept was 20.423, R^2 value was 0.991 and the efficiency was 93.117%. The C_t (y-axis) is plotted against the volume of cDNA added (x-axis).

